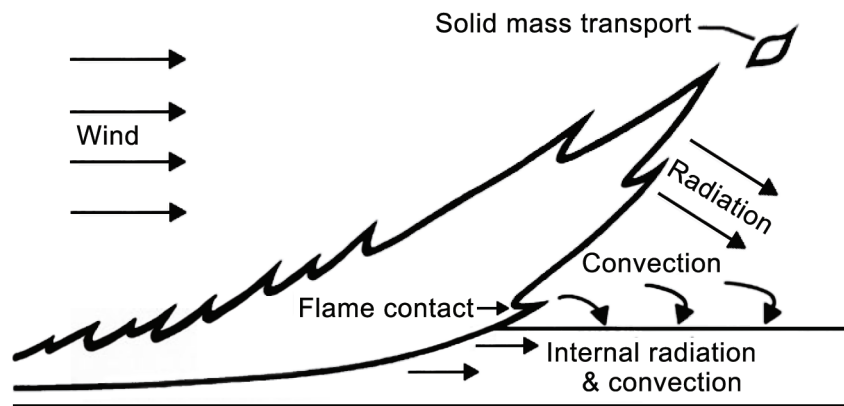


# The Rothermel Surface Fire Spread Model and Associated Developments: A Comprehensive Explanation

Patricia L. Andrews

$$R = \frac{I_R \xi (1 + \phi_w + \phi_s)}{\rho_b \epsilon Q_{ig}}$$



Andrews, Patricia L. 2018. **The Rothermel surface fire spread model and associated developments: A comprehensive explanation**. Gen. Tech. Rep. RMRS-GTR-371. Fort Collins, CO: U.S. Department of Agriculture, Forest Service, Rocky Mountain Research Station. 121 p.

## Abstract

The Rothermel surface fire spread model, with some adjustments by Frank A. Albini in 1976, has been used in fire and fuels management systems since 1972. It is generally used with other models including fireline intensity and flame length. Fuel models are often used to define fuel input parameters. Dynamic fuel models use equations for live fuel curing. Models have been developed for the effect of cross-slope wind and for fire spread in directions other than head fire. Equations for the Rothermel model and associated models are presented for easy reference. The influence of input variables on results is examined. While the spread model is used in the U.S. National Fire Danger Rating System (NFDRS), there are significant differences. The NFDRS equations and fuel models are given. This paper is intended to serve as a reference for those interested in the foundation of wildland fire modeling. System developers will benefit from equations from various sources being in one document. Developers of custom fuel models will find information on the impact of fuel parameters on rate of spread calculations.

---

**Keywords:** wildland fire, rate of spread, flame length, fuel model, fire-danger rating, mathematical model

## The Author

**Patricia Andrews** retired in 2012 as a research scientist with the Rocky Mountain Research Station at the Missoula Fire Sciences Laboratory in Missoula, Montana. She completed a B.A. degree in math and chemistry education at Montana State University-Billings, an M.A. degree in mathematics, and a Ph.D. in forestry at the University of Montana. Her research focus was fire behavior prediction and fire-danger rating. She received the Forest Service, U.S. Department of Agriculture, Research and Development Science Delivery Award in 2012.

## Acknowledgments

I thank Faith Ann Heinsch for recognizing the need for this document and for her significant technical contribution as well as oversight and review. I appreciate the helpful comments provided by Dick Rothermel, Bob Burgan, Bret Butler, and Mark Finney. Bill Chatham reviewed the paper from the point of view of a programmer. Joe Scott reviewed information related to dynamic fuel models. Matt Jolly and Larry Bradshaw reviewed the fire-danger rating section.

## Foreword

Dr. Andrews has produced an outstanding complete description of not only the Rothermel model, but also the modifications and addendums that have evolved for supporting the many systems that use the model. This work shows all the equations, discusses their relevance, and illustrates graphically their response to changes in their inherent variables. The variables required for driving the models referred to as *inputs*, which must be obtained to describe the environment in which the fire is burning, are often misunderstood. Dr. Andrews explains the role of these inputs in a clear and precise way that has not been available previously. This is especially pertinent to the role of living vegetation, a variable poorly understood. Living vegetation cannot only exhibit dramatic moisture changes during a fire season but also can dry to the point of curing and be transferred into another class of fuel. This problem is discussed extensively. The information in this publication has been collected and interpreted from a vast range of publications as evidenced by the large number of references (61). In my opinion, Dr. Andrews is unique in that she is a person who has both the background and range of knowledge necessary to produce a publication such as this.

*R. C. Rothermel, Forest Service scientist, retired*



## Preface

I was given the newly published *A Mathematical Model for Predicting Fire Spread in Wildland Fuels* by Richard C. Rothermel (1972) on my first day of work at the Fire Lab (then the Northern Forest Fire Laboratory) in 1973. I was hired as a temporary employee to work for Bill Frandsen to program HEXAGON, an implementation of the Rothermel model for non-uniform fuel (Frandsen and Andrews 1979). Little did I imagine 43 years later, as a retired fire research scientist, that I would be writing a paper about the fire spread model. I retired in 2012 after 39 years at the Fire Lab (now the Missoula Fire Sciences Laboratory). Much of my work involved application of the fire model for fire behavior prediction and fire-danger rating.

Multiple efforts, including some directed by Rothermel, have aimed to replace or improve the fire model. Significant efforts are currently in progress. New models that overcome weaknesses and limitations of the model will undoubtedly be developed. In the meantime, the Rothermel surface fire spread model continues to be the foundation of many research and management applications. Availability of this document may preclude errors, misinterpretations, and incomplete implementation of the model. For example, this document includes explanation of live fuel moisture of extinction, the impact of Albini's change to the original weighting factors, and a recent recommendation that the wind limit not be imposed.

This document contains no new research. I consolidate equations from various older publications. Related models such as flame length and spread direction are given, as well as National Fire Danger Rating System equations. While relationships between input and output variables are presented, this is not a formal sensitivity analysis.

The audience for this document includes research scientists, both those who use models in their fire and fuel research and those who are working to replace the fire spread model. System developers will appreciate having equations from various sources in one document. Those who use fire modeling systems will benefit from understanding what is "under the hood." Developers of custom fuel models will find information on the impact of fuel parameters on rate of spread calculations. In addition, documentation of a widely used model is worthwhile from an historical perspective. I hope that this paper will serve as a valuable reference for students of wildland fire modeling.



# Contents

1 Introduction.....	1
2 Development and Application.....	3
3 The Surface Fire Spread Model.....	7
3.1 Basic Model.....	8
3.1.1 Input Parameters.....	9
3.1.2 Fuel Bed Calculations.....	12
3.1.3 Heat Source, the Numerator.....	13
3.1.4 Heat Sink, the Denominator.....	15
3.1.5 Model Relationships.....	15
3.2 Final Model.....	16
3.2.1 Input Parameters.....	20
3.2.2 Live Fuel Moisture of Extinction.....	20
3.2.3 Weighting Factors.....	21
3.2.4 Characteristic Live and Dead Values.....	23
3.2.5 Fuel Bed Calculations.....	23
3.2.6 Final Calculations.....	24
3.2.7 Wind Limit.....	25
4 Related Models.....	26
4.1 Effective Wind Speed.....	27
4.2 Residence Time.....	27
4.3 Heat per Unit Area.....	28
4.4 Fireline Intensity.....	28
4.5 Flame Length.....	29
4.6 Fuel Models.....	29
4.6.1 Standard Fuel Models.....	29
4.6.2 Dynamic Fuel Models.....	30
4.6.3 Custom Fuel Models.....	37
4.6.4 Special Case Fuel Models.....	37
5 Fire Model Relationships.....	39
5.1 Fire Model Components.....	39
5.1.1 Propagating Flux Ratio.....	41
5.1.2 Optimum Reaction Velocity.....	42
5.1.3 Reaction Intensity.....	43
5.1.4 Heat of Preignition.....	44
5.1.5 Effective Heating Number.....	45
5.2 Fuel.....	45
5.2.1 Fuel Models.....	46
5.2.2 Weighting Factors.....	48
5.2.3 Fuel Particle Properties.....	53
5.2.3.1 Particle Density.....	53
5.2.3.2 Mineral Content.....	54
5.2.3.3 Heat Content.....	54

5.2.4 Fuel Bed Properties .....	55
5.2.4.1 Surface-Area-to-Volume Ratio .....	55
5.2.4.2 Fuel Bed Depth .....	57
5.2.4.3 Fuel Load .....	59
5.2.4.4 Bulk Density .....	61
5.2.4.5 Packing Ratio .....	62
5.3 Fuel Moisture.....	63
5.3.1 Characteristic Fuel Moisture .....	64
5.3.2 Moisture of Extinction.....	65
5.3.2.1 Dead Fuel Moisture of Extinction .....	66
5.3.2.2 Live Fuel Moisture of Extinction .....	66
5.3.3 Moisture Damping Coefficient.....	67
5.3.4 Fuel Moisture in the Heat Source and Heat Sink Terms .....	70
5.3.5 Live Herbaceous Moisture and Dynamic Fuel Models.....	71
5.3.5.1 Characteristic Live Fuel Moisture for Dynamic Fuel Models ....	72
5.3.5.2 Live Fuel Moisture of Extinction for Dynamic Fuel Models.....	72
5.3.5.3 Moisture Damping Coefficient for Dynamic Fuel Models .....	73
5.3.5.4 Reaction Intensity for Dynamic Fuel Models .....	73
5.3.5.5 Rate of Spread for Dynamic Fuel Models .....	77
5.4 Wind and Slope .....	78
5.4.1 Wind Factor.....	78
5.4.2 Slope Factor.....	80
5.4.3 Effective Wind Speed.....	81
5.4.4 Wind Limit .....	83
6 Fire Spread Directions.....	84
6.1 Fire Behavior in the Direction of Maximum Spread.....	85
6.2 Fire Spread from a Single Ignition Point.....	88
6.3 Fire Spread from Fire Perimeter.....	89
6.4 Fireline Intensity .....	91
7 Rothermel Fire Spread Model in NFDRS .....	93
7.1 Input Variables.....	93
7.2 Fuel Models .....	93
7.3 Fuel Model Adjustments .....	98
7.3.1 Dynamic Herbaceous Fuel Load Transfer .....	98
7.3.2 Dynamic Deciduous Woody Fuel Load Transfer.....	98
7.3.3 Drought Fuel Addition .....	98
7.4 SC, ERC, BI Equations .....	98
7.4.1 Spread Component, SC.....	106
7.4.2 Energy Release Component, ERC .....	106
7.4.3 Burning Index, BI .....	109
7.4.4 Burning Index Compared to Flame Length .....	110
8 References .....	111
Appendix A—Basic Fire Spread Equations in Metric Units .....	116
Appendix B—People Behind the Equations .....	119

# 1. Introduction

Fire modeling is often used to support aspects of fire and fuel management, fire ecology, climate change, suppression, smoke, fuel hazard assessment, and budget planning. A component of the modeling involves a description of the fire environment (fuel, weather, and topography) that is used to calculate fire behavior characteristics (including spread rate) and subsequent fire effects. While there are many models for surface fire spread, the Rothermel surface fire spread model is the most commonly used in U.S. fire management systems, with a significant use outside the United States.

Sullivan (2009a,b,c) did a comprehensive review of wildland surface fire spread models developed during the period 1990–2007, presented as three papers, each covering a broad category of models: physical and quasi-physical models, empirical and quasi-empirical models, and simulation and mathematical analogue models. He defined a physical model as one that attempts to represent both the physics and chemistry of fire spread; a quasi-physical model attempts to represent only the physics; an empirical model is one that contains no physical basis at all and is generally statistical in nature; and a quasi-empirical model is one that uses some form of physical framework on which the statistical modeling is based. Mathematical analogue models are those that utilize a mathematical precept rather than a physical one for the modeling of the spread of wildland fire. Simulation models are those that implement a fire behavior model in a landscape spread application. Of the 14 simulation models discussed in Sullivan (2009c), Rothermel (1972) was listed as the primary spread model for nine of them (origin United States of America, Portugal, Greece, France, New Zealand, and Italy).

Rothermel's model is categorized as quasi-empirical. It is based on a heat balance model developed by Frandsen (1971), data obtained from wind tunnel experiments in artificial fuel beds of varying characteristics (Rothermel and Anderson 1966), and Australian wildfire data in grasses (McArthur 1969). The basic Rothermel model, with minor modifications by Albini (1976a), has been used in the same form for decades. Ongoing research will undoubtedly lead to an improved model that can be effectively incorporated into fire and fuel management systems. But given the likelihood of continued use in the near future and the value of an historical record, there is reason to present a comprehensive documentation of the Rothermel fire spread model.

The fire spread model is based on the conservation of energy described by a heat source divided by a heat sink (Frandsen 1971). It assumes a linear flame front and calculates spread rate of a head fire with or without wind or slope. The model is for fire burning upslope with the wind through uniform fuel. The fuel is a mixture of various size classes of live and dead fuel, with a single representative depth. The model requires the presence of fine dead fuel, which is the most influential fuel component. The model only addresses fire in surface fuel, within about 6 ft of the ground; surface fuel can include brush and small trees. The model is not applicable to crown fire in overstory trees, smoldering ground fire, or post-frontal combustion

of fuels that burn after the front has passed. The fire model was designed to use fuel, moisture, and terrain data that would be available prior to ignition. Associated models (flame length, fuel moisture, fuel, wind, spread direction, etc.) make it useful for a range of applications. While the model has significant assumptions and recognized limitations, knowledgeable users and system developers make it work well for various specific applications. Its strengths are simplicity of input requirements and calculations and the possibility of changing many driving variables. It is useful to be able to change fuel parameters, a feature not possible with statistical models that are developed for specific fuel types based on observed fire behavior in that type.

The model was initially used as a quantitative way to calculate U.S. fire-danger rating indices (Deeming et al. 1972) and later as a tool for fire behavior officers (now called FBAN, Fire Behavior Analysts) to predict the behavior of an ongoing wildfire (Rothermel 1983). Andrews and Queen (2001) describe the implementation of the spread model through the evolving use of technology, from nomographs, to handheld calculators, to early programs run in batch mode on remote computers, to desktop and internet-based systems. The model is now incorporated into many systems including, for example, BehavePlus (Andrews 2014) and FARSITE (Finney 1998).

This report combines material from various sources to aid understanding of the surface fire spread model as well as associated models and developments, putting it in one document for ready reference. Sections 3 and 4 present the equations with required input in a form that would be useful to a system developer. A person who is interested in further understanding of the surface fire spread model would continue reading section 5.

Model development, assumptions, and limitations can be found in referenced papers. While relationships between input and output variables are demonstrated, this isn't a formal sensitivity analysis.

- **Section 2** provides background of development and application of the surface fire spread model.
- **Section 3** gives a description of model equations from Rothermel (1972) with the modifications of Albini (1976a). Equations for the basic model, which includes only one size class of dead fuel, are presented first. Then the final model is given, including weighting factors that allow multiple size classes of dead and live fuel.
- **Section 4** describes models often used with, but not technically part of, the Rothermel surface fire spread model, including fireline intensity, flame length, and fuel models.
- **Section 5** illustrates fire model relationships. The impact of changes of an input parameter on results is demonstrated. Some of the material is based on custom fuel model testing methods in the TSTMDL (test model) program from the old BEHAVE system (Burgan 1987; Burgan and Rothermel 1984).
- **Section 6** describes adaptations that allow for modeling spread when the wind is not blowing upslope and for spread in directions other than head fire.

- **Section 7** gives the equations used in the U.S. National Fire Danger Rating System (NFDRS). Although indices are based on the fire models used for fire behavior modeling, there are some significant differences.
- Units in this paper are those in the source documents, generally English. **Appendix A** gives metric equations for the basic spread model and some of the related models.
- To add a personal touch to this equation-laden document, **Appendix B** includes photographs of some of those involved in the development and application of the surface fire spread model.

## 2. Development and Application

Discussion of development and application of the fire spread model is approached through the liberal use of quotes from historical documents.

Establishment of the Missoula Fire Sciences Laboratory is described by Smith (2012) in a document prepared for the 50<sup>th</sup> anniversary of the Fire Lab. The facilities, dedicated in 1960, included a combustion laboratory and two wind tunnels where researchers could examine rate of spread under various conditions. Lab Chief Jack Barrows “recognized that increased understanding of the basics of fire behavior would require input from physical scientists and engineers” (Wells 2008). He initially hired Richard (Dick) Rothermel and Hal Anderson to bring science and engineering skills to the Lab. Rothermel hired William (Bill) Frandsen in 1967 and Frank Albini in 1973.

The approach to developing the fire model is described by Rothermel (1983) in the preface to *How to Predict the Spread and Intensity of Forest and Range Fires*:

When Hal Anderson and I came to the Northern Forest Fire Laboratory in 1961, it was not yet a year old and there was a feeling that surely this lab was going to contribute. Just what would be accomplished was not entirely clear, but things were going to happen. There was also a sense of being overwhelmed, not only by all the unknowns of wildfire behavior, but also by how to use this brand new facility. There were at least two schools of thought in regard to the wind tunnels: (1) bring in box-car loads of fuel from all over the country for burning in the wind tunnels, and (2) weld the doors shut until a logical plan for use of the facilities was developed.

We did not weld the doors and we did not ship in fuel by the box-car load, but we did work hard at understanding fire spread and adapting concepts of modeling and systems to the problems of forest fire prediction. During the first 10 years a fire behavior model was produced. It took 10 more years to learn how to obtain the inputs and interpret the outputs for use by the ‘man on the ground,’ which culminated in the writing of this manual.

A formal problem analysis, written after a significant amount of work had been done on developing concepts for a fire spread model, showed recognition of the role of and limitations of modeling. Rothermel (1968, page 2):

The ability to predict fire spread is certainly the problem to be solved; however, in attacking this problem the researcher is faced with yet another one. That is to discover, define, and evaluate the physical processes involved in the spread of fire in an unconfined fuel complex. These processes are often referred to as 'the mechanism of fire spread.' In a multielement fuel bed, fire spread is a succession of fuel particle ignitions in the direction at which ignitions are able to occur. For ignition to occur, each particle of potential fuel must receive sufficient heat to raise it to ignition. The mechanism of fire spread is, therefore, interrelated with the mechanism of heat transfer from the existing fire to potential fuel and heat necessary to raise this fuel to ignition.

Unless the complete mechanism can be described we can generate only correlations between the fire spread rate and its dependent variables. Correlations to spread rate have been made previously against variables such as fuel moisture, wind, topography, and, to a lesser extent, against fuel loading, fuel size, and compactness. These are important variables but studying them individually does not predict fire spread as these physical controls are altered or vary so that when one or more are changed their combined effects will be evident upon the rate of spread.

In the real world of wildfires physical laws do not vanish just because the reaction is complex. But the urgency to explain encourages over-simplification. Simple correlations are quickly extrapolated beyond the limits to which they are meant to apply. Spread theories based on the fundamental processes as exemplified by the scientific method, however, will increase in their usefulness as each new parameter is incorporated into the theoretical description of the problem.

When the fundamental processes are found and their relation to fire behavior proven, then simplifications can be made to provide a workable solution to the forest manager. The simplifying process will exclude items known to be trivial or of remote possibility.

The approach to the structure of the fire model is described by Rothermel (1972, pages 1 and 3):

W. R. Fons (1946) was the first to attempt to describe fire spread using a mathematical model. Fons focused his attention on the head of the fire where the fine fuels carry the fire and where there is ample oxygen to support combustion. He pointed out that sufficient heat is needed to bring the adjoining fuel to ignition temperature at the fire front. Therefore, Fons reasoned that fire spread in a fuel bed can be visualized as proceeding by a series of ignitions and that its rate is controlled primarily by the ignition time and the distance between particles.

The model was developed from a strong theoretical base to make its application as wide as possible. This base was supplied by Frandsen (1971) who applied the conservation of energy principle to a unit volume of fuel ahead of an advancing fire in a homogeneous fuel bed.

Experimental burning was done in fuel beds of a single size class. Mathematical relationships were then developed to allow for a fuel bed of various size classes as described in the Rothermel (1972) abstract:

The initial work was done using fuel arrays composed of uniform size particles. These fuel sizes were tested over a wide range of bulk densities. These were 0.026-inch-square cut excelsior, ¼-inch sticks, and ½-inch sticks. The problem of mixed fuel sizes was then resolved by weighting the various particle sizes that compose actual fuel arrays by either surface area or loading, depending upon the feature of the fire being predicted.

In describing the landmark research leading to the surface fire spread model, Albini (1984, page 593) said:

A combination of perceptive idealization, innovative experimental techniques, bold extrapolation, and luck led to this achievement.

The concept of a fuel model aids application of the fire model. Eleven fire behavior fuel models were published with the fire model (Rothermel 1972, pages 34–35):

Choosing input parameters for the model from the infinite variety of fuel and environmental arrangements and combinations seems almost overwhelming. However, patterns in the growth of vegetation exist that can be utilized to greatly simplify the inventory process. It also proves helpful to group the inputs in the following manner: 1. Fuel Particle Properties ... 2. Fuel Array Arrangement ... 3. Environmental Related Values ...

These results can be further refined for use in the mathematical model by assembling them into fuel models that represent typical field situations. Such fuel models contain a complete set of inputs for the mathematical fire spread model.

The initial application of the model was fire-danger rating, which required development to be completed within a strict timeframe. Following is from a study plan (Rothermel 1969, page 1) titled “A Fire Behavior Model for Field Application”:

The Fire Physics Project at the Northern Forest Fire Laboratory has been requested to provide a fire spread model for utilization in the revised National Fire Danger Rating System. Current work in fire behavior research is mostly on an individual problem basis such as the effect of moisture, minerals, fuel geometry, etc. There is a strong need for a unified system that will relate the many parameters known to effect fire behavior into a single set of mathematical relationships. These relationships will then provide the framework for constructing the danger rating indexes of spread and intensity.

This study has been undertaken with the concept of first developing the necessary mathematical relationships, evaluating them with whatever research knowledge is currently available, generating the knowledge that is not available within

the time period allotted and making the best approximations possible where knowledge or time runs out. Finally we will state the possible applications of the model and test its validity against reliable field data.

The potential for applications beyond fire-danger rating was recognized in the problem analysis (Rothermel 1968, page 1):

A mathematical model of fire spread could be directly applied in three areas.

1. The 'nonfire' situation in which operations research techniques can be utilized to study possible fire situations and suppression or prescribed burning tactics in hypothetical situations. This area corresponds to the Forest Administration tactics of presuppression planning, training, organizing, etc.

2. The 'possible fire' situation for which advanced planning is needed such as fire-danger rating. This again corresponds to a similar area in Forest Administration tactics of estimating danger, detection, and initial attack.

3. The 'existing fire' situation where the predictions could take the form of probability forecasts as to whether or not a given fire would be able to move under the forecasted weather conditions. This falls within the familiar area of fire behavior.

Use of the model expanded to fuels beyond the original concept as described in Rothermel (1972) abstract:

The model as originally conceived was for dead fuels in a uniform stratum contiguous to the ground, such as litter or grass. It was found to be useful, however, for fuels ranging from pine needle litter to heavy logging slash and for California brush fields.

The range of potential applications was discussed in Rothermel (1972):

The introduction of this model will permit the use of systems analysis techniques to be applied to land management problems. As a result, a new dimension is offered to land managers for appraising the consequences of proposed programs. Questions can be answered such as: What is the resultant fuel hazard when thinning is done in overstocked areas? Can logging practices be modified to reduce the potential fire hazard of the fuels they produce? How much slash should be left on the ground to produce the desired site treatment for the next crop of trees? How long after cutting can a successful burn still be achieved? What is the hazard buildup in chaparral brush fields of the Los Angeles Basin in years subsequent to the last burn?

### 3. The Surface Fire Spread Model

Rothermel's model is based on a foundation provided by Frandsen (1971) who applied the conservation of energy principle to a unit volume of fuel ahead of a steadily advancing fire in a homogeneous fuel bed. In his analysis, the fuel-reaction zone is viewed as fixed and the unit volume moves as a constant depth toward the interface. The unit volume ignites at the interface. Rate of spread is then a ratio between the heat flux received from the source and the heat required for ignition by the potential fuel. Frandsen's equation could not be solved analytically because it contained heat flux terms for which the mechanisms of heat transfer were not known. To solve the equation, it was necessary to use experimental and analytical methods of evaluation for each term.

If fire is thought of as a series of ignitions, it will reach a steady-state spread through a fuel bed at the rate at which adjacent potential fuel can be heated to ignition temperature. The steady rate of spread equation is the heat received by the potential fuel ahead of the fire divided by the heat required to ignite this fuel. The numerator represents the amount of heat actually transferred to the potential fuel, while the denominator represents the amount of heat required to bring this fuel to ignition temperature.

A basic model was developed for one size class of dead fuel with the no wind, no slope rate of spread adjusted for the effects of wind and slope. The final fire spread model includes weighting factors for live and dead fuel of multiple size classes. The Rothermel surface fire spread model addresses a fire spreading upslope with the wind through surface fuels within about 6 feet of the ground.

Description of elements of the basic spread model, which is based on a single size class of dead fuel, is followed by a description of the final model, which includes additional calculations to allow multiple size classes of dead and live fuel. The fire spread model presented here includes the modifications made by Albini (1976a).

The FIREMOD program for fire behavior prediction was an early implementation of the Rothermel fire spread model. In the publication describing FIREMOD, Albini (1976a, pages 14–17) included a section called "Deviations from Rothermel's Equations." Since that time, those changes have been incorporated into the Rothermel model. Changes involve

- correction for mineral content,
- mineral damping coefficient,
- reaction velocity correlation,
- weighting factors for fuel load,
- moisture of extinction of live fuels, and
- weighting factor on intensity by category.

### 3.1 Basic Model

The final rate of spread equation is heat source divided by heat sink and applies to one size class of dead fuel. A series of equations (the basic fire spread model) is used to reach this relationship.

$$R = \frac{I_R \xi (1 + \phi_w + \phi_s)}{\rho_b \varepsilon Q_{ig}}$$

Four tables and a diagram support discussion of the basic model. Units in the tables apply to variables described in the text unless otherwise noted. The reader should refer to the following for definitions, relationships, and units.

- Table 1 briefly describes components of the final fire spread equation.
- Table 2 provides the input parameters required for the basic model.
- Table 3 gives all of the equations in the basic fire spread model, including modifications by Albini (1976a).
- Table 4 shows which term in the basic equation is affected by each of the input variables.
- Figure 1 is a diagram that shows the flow of the calculations in the basic model.

**Table 1**—Definition of components in the final equation for the Rothermel surface fire spread model.

Component	Name	Explanation
$R$	Rate of spread (ft/min)	Flaming front of a surface fire
$I_R$	Reaction intensity (Btu/ft <sup>2</sup> /min)	Energy release rate per unit area of fire front
$\xi$	Propagating flux ratio	Proportion of the reaction intensity that heats adjacent fuel particles to ignition (no wind)
$\phi_w$	Wind factor	Dimensionless multiplier that accounts for the effect of wind in increasing the propagating flux ratio
$\phi_s$	Slope factor	Dimensionless multiplier that accounts for the effect of slope in increasing the propagating flux ratio
$\rho_b$	Bulk density (lb/ft <sup>3</sup> )	Amount of oven-dry fuel per cubic foot of fuel bed
$\varepsilon$	Effective heating number	Proportion of a fuel particle that is heated to ignition temperature at the time flaming combustion starts
$Q_{ig}$	Heat of preignition (Btu/lb)	Amount of heat required to ignite one pound of fuel
$I_R \xi$	No-wind, no-slope propagating flux (Btu/ft <sup>2</sup> /min)	Heat release rate from a fire to the fuel ahead of the fire, without wind or slope
$(1 + \phi_w + \phi_s)$		Increase to the no-wind, no-slope propagating flux due to wind and slope
$I_R \xi (1 + \phi_w + \phi_s)$	Heat source (Btu/ft <sup>2</sup> /min)	Propagating flux
$\rho_b \varepsilon Q_{ig}$	Heat sink (Btu/ft <sup>3</sup> )	Heat required to ignite the fuel
$\frac{I_R \xi}{\rho_b \varepsilon Q_{ig}}$	No-wind, no-slope rate of spread (ft/min)	

**Table 2**—Input parameters for the basic fire spread model (one size class of dead fuel).

Type	Symbol	Parameter	Notes <sup>a</sup>
Fuel particle	$h$	Low heat content (Btu/lb)	Often 8,000 Btu/lb
	$S_T$	Total mineral content (fraction)	Generally 0.0555 lb minerals / lb wood
	$S_e$	Effective mineral content (fraction)	Generally 0.010 (lb minerals – lb silica) / lb wood
	$\rho_p$	Oven-dry particle density (lb/ft <sup>3</sup> )	Generally 32 lb/ft <sup>3</sup>
Fuel array	$\sigma$	Surface-area-to-volume ratio (ft <sup>2</sup> /ft <sup>3</sup> )	
	$w_o$	Oven-dry fuel load (lb/ft <sup>2</sup> )	
	$\delta$	Fuel bed depth (ft)	Mean fuel array value
	$M_x$	Dead fuel moisture of extinction (fraction)	Live fuel is not included in the basic model. Live fuel moisture of extinction is calculated in the final model.
Environmental	$M_f$	Moisture content (fraction)	Dry weight basis lb moisture / lb wood
	$U$	Wind velocity at midflame height (ft/min)	
	$\tan \phi$	Slope steepness, maximum (fraction)	Vertical rise / horizontal distance

<sup>a</sup>While nominal values are used in most applications, the fire model will accept other values.

### 3.1.1 Input Parameters

The model was designed so that rate of spread can be calculated from conditions that can be known before the fire. The input variables in table 2 are grouped into three categories:

- fuel particle properties—heat content, mineral content, particle density;
- fuel array arrangements—fuel load, surface-area-to-volume ratio (SAV), mean depth of fuel bed, dead fuel moisture of extinction; and
- environmental values—fuel moisture content, wind velocity, slope steepness.

Fuel particle properties are parameters that are intrinsic to the fuel particle: heat content ( $h$ ), mineral (ash) content ( $S_T$  and  $S_e$ ), and particle density ( $\rho_p$ ). Fuel particle properties are often (but not necessarily) held constant. These properties were kept as variables in the model to allow for possible future study. Heat content is the heat released during combustion. A commonly used value is 8,000 Btu/lb. The quantity and type of inorganic material in the fuel affects the rate at which it burns. Total mineral content is generally 0.0555 (5.55 percent), and effective mineral content is generally 0.0100 (one percent). Particle density is generally 32 lb/ft<sup>3</sup>.

**Table 3**—Equations for the basic fire spread model (one size class of dead fuel) and source for the equation.

Element	Equation	Source <sup>a</sup>
Rate of spread (ft/min)	$R = \frac{I_R \xi (1 + \phi_w + \phi_s)}{\rho_b \varepsilon Q_{ig}}$	[1] (eq. 52)
Reaction intensity (Btu/ft <sup>2</sup> -min)	$I_R = \Gamma' w_n h \eta_M \eta_s$	[1] (eq. 27)
Optimum reaction velocity (min <sup>-1</sup> )	$\Gamma' = \Gamma'_{max} (\beta / \beta_{op})^A \exp[A(1 - \beta / \beta_{op})]$ $A = 133\sigma^{-0.7913}$	[1] (eq. 38) [2] (p. 15) Replaced [1] (eq. 39)
Maximum reaction velocity (min <sup>-1</sup> )	$\Gamma'_{max} = \sigma^{1.5} (495 + 0.0594\sigma^{1.5})^{-1}$	[1] (eq. 36)
Optimum packing ratio	$\beta_{op} = 3.348\sigma^{-0.8189}$	[1] (eq. 37)
Packing ratio	$\beta = \rho_b / \rho_p$	[1] (eq. 31)
Oven-dry bulk density (lb/ft <sup>3</sup> )	$\rho_b = w_0 / \delta$	[1] (eq. 40)
Net fuel load (lb/ft <sup>2</sup> )	$w_n = w_0 (1 - S_T)$	[2] (p. 14) Replaced [1] (eq. 24)
Moisture damping coefficient	$\eta_M = 1 - 2.59r_M + 5.11(r_M)^2 - 3.52(r_M)^3$ $r_M = M_f / M_x$ (max = 1.0)	[1] (eq. 29)
Mineral damping coefficient	$\eta_s = 0.174S_e^{-0.19}$ (max = 1.0)	[2] (p. 14) Max added to [1] (eq. 30)
Propagating flux ratio	$\xi = (192 + 0.2595\sigma)^{-1} \exp[(0.792 + 0.681\sigma^{0.5})(\beta + 0.1)]$	[1] (eq. 42)
Wind factor	$\phi_w = CU^B (\beta / \beta_{op})^{-E}$ $C = 7.47 \exp(-0.133\sigma^{0.55})$ $B = 0.02526\sigma^{0.54}$ $E = 0.715 \exp(-3.59 \times 10^{-4} \sigma)$	[1] (eq. 47-50)
Slope factor	$\phi_s = 5.275\beta^{-0.3} (\tan \phi)^2$	[1] (eq. 51)
Effective heating number	$\varepsilon = \exp(-138/\sigma)$	[1] (eq. 14)
Heat of preignition (Btu/lb)	$Q_{ig} = 250 + 1116M_f$	[1] (eq. 12)

<sup>a</sup>Source: [1] = Rothermel (1972); [2] = Albini (1976a).

**Table 4**—Input variables that affect each element of the basic fire spread equation (one size class of dead fuel).

Input variable		Components of the basic fire spread equation						
		$R = \frac{I_R \xi (1 + \phi_w + \phi_s)}{\rho_b \varepsilon Q_{ig}}$						
		Heat source (numerator)				Heat sink (denominator)		
		$I_R$	$\xi$	$\phi_w$	$\phi_s$	$\rho_b$	$\varepsilon$	$Q_{ig}$
Fuel particle	$h$	X						
	$S_T$	X						
	$S_e$	X						
	$\rho_p$	X	X	X	X			
Fuel array	$\sigma$	X	X	X			X	
	$w_0$	X	X	X	X	X		
	$\delta$	X	X	X	X	X		
	$M_x$	X						
Environmental	$M_f$	X						X
	$U$			X				
	$\tan \phi$				X			

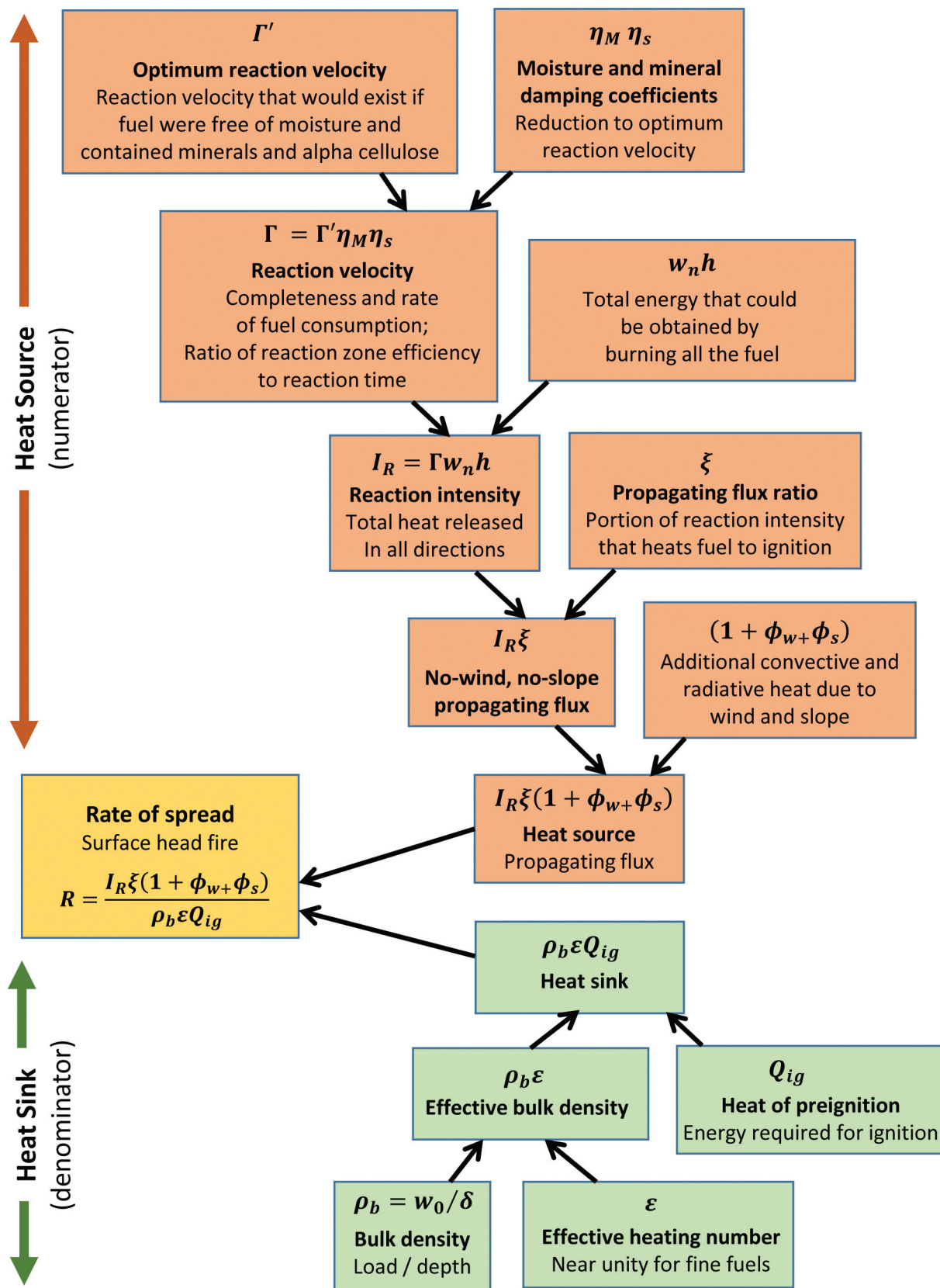


Figure 1—Flow of calculations in the basic fire spread model for one size class of dead fuel.

Fuel array properties related to the fuel bed are fuel surface-area-to-volume ratio ( $\sigma$ ), oven-dry fuel load ( $w_0$ ), fuel bed depth ( $\delta$ ), and dead fuel moisture of extinction ( $M_x$ ). Fuel particle size, which strongly influences fire spread and intensity, is quantified by surface-area-to-volume ratio. The ratio of load to depth indicates the packing of the fuel, another important influencing factor. The dead fuel moisture of extinction is the moisture at which the dead fuel will not sustain a spreading surface fire; this is a user-supplied value.

Environmental values include fuel moisture ( $M_f$ ), midflame wind speed ( $U$ ), and slope steepness ( $\tan \phi$ ). Fuel moisture is specified on a dry weight basis; the fraction of moisture is the weight of water divided by the dry weight of the fuel. Wind speed is at midflame height, the wind that affects surface fire. Slope steepness is specified as a fraction (tangent), vertical rise divided by horizontal distance.

### 3.1.2 Fuel Bed Calculations

Fuel particle and fuel array variables are used to calculate descriptions of the fuel bed as a whole.

The oven-dry fuel load ( $w_0$ ) includes the noncombustible mineral fraction. The load of combustible dry fuel, the net fuel load ( $w_n$ ), includes a reduction by the total mineral content ( $S_T$ ). The Rothermel (1972) equation was changed by Albini (1976a).

$$w_n = w_0 (1 - S_T)$$

The oven-dry bulk density ( $\rho_b$ ) is the oven-dry fuel load ( $w_0$ ) divided by the fuel bed depth ( $\delta$ ).

$$\rho_b = w_0 / \delta$$

Fuel bed compactness and fuel particle size have significant effect upon combustibility, but the effects are not separated and quantified in the model. The compactness of the fuel bed is quantified by the packing ratio ( $\beta$ ), which is defined as the fraction of the fuel array volume that is occupied by fuel. It is the ratio of the fuel array bulk density ( $\rho_b$ ) to the fuel particle density ( $\rho_p$ ).

$$\beta = \rho_b / \rho_p$$

Optimum packing ratio ( $\beta_{op}$ ) is a function of surface-area-to-volume ratio ( $\sigma$ ). Maximum reaction intensity occurs at the optimum packing ratio. It does not optimize rate of spread.

$$\beta_{op} = 3.348 \sigma^{(-0.8189)}$$

Relative packing ratio is packing ratio ( $\beta$ ) divided by the optimum packing ratio ( $\beta_{op}$ ).

$$\beta / \beta_{op}$$

### 3.1.3 Heat Source, the Numerator

The numerator of the basic rate of spread equation is the heat source, or propagating flux ( $I_P$ ), the rate of heat release from a fire to the fuel ahead of the fire. The propagating flux is calculated for a fire burning on flat ground with no wind ( $(I_P)_0$ ) and then multiplied by factors that adjust for the effect of wind ( $\phi_w$ ) and slope ( $\phi_s$ ).

$$\text{Heat source} = I_R \zeta (1 + \phi_w + \phi_s)$$

$$I_P = (I_P)_0 (1 + \phi_w + \phi_s)$$

Reaction intensity ( $I_R$ ) is the total heat release rate per unit area of fire front, and includes heat convected, conducted, and radiated in all directions, not just in the direction of the adjacent potential fuel. The propagating flux ratio ( $\zeta$ ) is the proportion of the total reaction intensity ( $I_R$ ) that actually heats adjacent fuel particles to ignition.

$$\zeta = (192 + 0.2595\sigma)^{-1} \exp[(0.792 + 0.681\sigma^{0.5})(\beta + 0.1)]$$

The no-wind, no-slope propagating flux ( $(I_P)_0$ ) is then

$$(I_P)_0 = I_R \zeta$$

The energy release rate of the fire front is produced by burning gases that have been pyrolyzed from the solid organic matter in the fuels. Therefore, the rate of change in this organic matter from a solid to a gas is a good approximation of the subsequent heat release rate of the fire. Reaction intensity was derived from a series of experiments that recorded the weight loss of a portion of the fuel bed during fire spread. Reaction intensity ( $I_R$ ) is calculated from reaction velocity ( $\Gamma$ ) multiplied by the net fuel load ( $w_n$ ) times the heat content of the fuel ( $h$ ).

$$I_R = \Gamma w_n h$$

The reaction velocity ( $\Gamma$ ) indicates the completeness and rate of fuel consumption. It is defined as the ratio of the reaction zone efficiency to the reaction time. It is a measure of the actual rate of fuel consumption. The fuel parameters considered to have a major effect on the reaction velocity are moisture content, mineral content, particle size, and fuel bed bulk density. The reaction velocity ( $\Gamma$ ) is calculated as optimum reaction velocity ( $\Gamma'$ ) multiplied by the moisture damping coefficient ( $\eta_M$ ) and the mineral damping coefficient ( $\eta_S$ ).

$$\Gamma = \Gamma' \eta_M \eta_S$$

The presence of moisture and minerals reduces the reaction velocity below its potential value. The optimum reaction velocity ( $\Gamma'$ ) is the reaction velocity that would exist if the fuel were free of moisture and contained minerals at the same reaction concentration as alpha cellulose. The equation for  $A$  is an Albini (1976a) change to the equation in Rothermel (1972).

$$\Gamma' = \Gamma'_{max} (\beta/\beta_{op})^A \exp[A(1 - \beta/\beta_{op})]$$

where

$$A = 133\sigma^{-0.7913}$$

The maximum reaction velocity ( $\Gamma'_{max}$ ) is calculated from the surface-area-to-volume ratio ( $\sigma$ ).

$$\Gamma'_{max} = \sigma^{1.5}(495 + 0.0594\sigma^{1.5})^{-1}$$

Moisture damping coefficient ( $\eta_M$ ) is calculated from fuel moisture content ( $M_f$ ) and moisture of extinction ( $M_x$ ).

$$\eta_M = 1 - 2.59r_M + 5.11(r_M)^2 - 3.52(r_M)^3$$

where

$$r_M = M_f/M_x \text{ (max=1.0)}$$

Mineral damping coefficient ( $\eta_s$ ) is a function of the effective mineral content ( $S_e$ ). The maximum of 1.0 is an Albini (1976a) change to the equation in Rothermel (1972).

$$\eta_s = 0.174S_e^{-0.19} \text{ (max = 1.0)}$$

Wind and slope change the no-wind no-slope propagating flux ( $I_R \xi$ ) by exposing the potential fuel to additional convective and radiant heat. The vertical flux is more significant during wind-driven and upslope fires because it was thought that flame tilt over the potential fuel would increase radiation, and more significantly cause direct flame contact and increased convective heat transfer to the potential fuel. The propagating flux occurs at the front of the fire; therefore, the propagating flux is closely related to the fire intensity of the fire front.

Slope factor ( $\phi_s$ ) is based on an evaluation of experimental data, and is a function of slope steepness ( $\tan \phi$ ) and packing ratio ( $\beta$ ).

$$\phi_s = 5.275\beta^{-0.3}(\tan \phi)^2$$

Wind factor ( $\phi_w$ ) was developed from wind tunnel data and wildfire data (McArthur 1969). It is based on midflame wind speed ( $U$ ), relative packing ratio ( $\beta/\beta_{op}$ ), and surface-area-to-volume ratio ( $\sigma$ ).

$$\phi_w = CU^B (\beta/\beta_{op})^{-E}$$

where

$$C = 7.47 \exp(-0.133\sigma^{0.55})$$

$$B = 0.02526\sigma^{0.54}$$

$$E = 0.715 \exp(-3.59 \times 10^{-4}\sigma)$$

### 3.1.4 Heat Sink, the Denominator

The denominator of the rate of spread equation is the heat required for ignition, or heat sink. It is dependent upon the ignition temperature, moisture content of the fuel, and the amount of fuel involved in the ignition process. Heat sink is the product of the heat of preignition ( $Q_{ig}$ ) and the effective bulk density ( $\rho_b \varepsilon$ ).

$$\text{Heat sink} = \rho_b \varepsilon Q_{ig}$$

Heat of preignition ( $Q_{ig}$ ) is the energy per unit mass required for ignition; it is a dosage, not a rate. It was evaluated analytically for cellulosic fuels by considering the change in specific heat from ambient to ignition temperature and the latent heat of vaporization of the fuel moisture ( $M_f$ ).

$$Q_{ig} = 250 + 1,116M_f$$

The amount of fuel involved in the ignition process is the effective bulk density, the bulk density ( $\rho_b$ ) times an effective heating number ( $\varepsilon$ ), which is a dimensionless number that approaches unity for fine fuels and decreases toward 0 as fuel size increases. (Larger values of  $\sigma$  correspond to finer fuels.)

$$\varepsilon = \exp(-138/\sigma)$$

### 3.1.5 Model Relationships

Table 4 shows which of the elements of the basic equation are influenced by each of the input parameters. Note, for example, that heat content ( $h$ ) affects the heat source term through reaction intensity ( $I_R$ ) and does not play a role in heat sink. Surface-area-to-volume ratio ( $\sigma$ ) is used in the calculation of heat source, heat sink, and wind factor.

Figure 1 shows the flow of calculations in the basic fire spread model with a brief description of each component.

### 3.2 Final Model

The equations for the basic fire spread model in table 3 apply to a single size class of dead fuel. In order for the model to be useful for field applications, it was modified to accept fuels composed of heterogeneous mixtures of particle sizes and includes both dead and live fuel. The final model is formulated from the basic equations and a weighting concept. The weighting factors are based on mathematical relationships, not experimental data.

Two tables and a diagram support discussion of the final surface fire spread model. The reader should refer to the following for definitions, relationships, and units.

- Table 5 gives the input parameters, some of which are defined for live and dead category (*i*) and size class (*j*).
- Table 6 is a complete listing of the equations in the final surface fire spread model.
- Figure 2 shows a breakdown of the spread equation, indicating which components apply to the fuel bed, to the dead and live categories, or to each size class.

**Table 5**—Input parameters for the final fire spread model.

Type	Symbol <sup>a</sup>	Parameter
Fuel particle	$h_{ij}$	Heat content (Btu/lb)
	$(S_T)_{ij}$	Total mineral content (fraction)
	$(S_e)_{ij}$	Effective mineral content (fraction)
	$(\rho_p)_{ij}$	Particle density (lb/ft <sup>3</sup> )
Fuel array	$\sigma_{ij}$	Surface-area-to-volume ratio (ft <sup>2</sup> /ft <sup>3</sup> )
	$(w_0)_{ij}$	Oven-dry fuel load (lb/ft <sup>2</sup> )
	$\delta$	Fuel bed depth (ft)
	$(M_x)_1$	Dead fuel moisture of extinction (fraction)
Environmental	$(M_f)_{ij}$	Fuel moisture (fraction)
	$U$	Midflame wind speed (ft/min)
	$\tan \phi$	Slope steepness (fraction)

<sup>a</sup>Category is indicated by *i* = 1 for dead and *i* = 2 for live; size class is indicated by *j*.

**Table 6a**—Final fire spread model equations for heterogeneous fuel and source for the equations.

Element	Equation <sup>a</sup>	Source <sup>b</sup>
<b>Weighting factors</b>		
Mean total surface area per unit fuel cell of each size class within each category	$A_{ij} = (\sigma)_{ij}(w_0)_{ij}/(\rho_p)_{ij}$	[1] (eq. 53)
Mean total surface area of the live and dead categories	$A_i = \sum_j A_{ij}$	[1] (eq. 54)
Mean total surface area of the fuel	$A_T = \sum_i A_i$	[1] (eq. 55)
Weighting factor for characteristic dead and live heat content, effective mineral content, moisture content, and surface-area-to-volume ratio	$f_{ij} = A_{ij}/A_i$	[1] (eq. 56)
Weighting factor for characteristic fuel bed surface-area-to-volume ratio	$f_i = A_i/A_T$	[1] (eq. 57)
Weighting factor for net fuel load	<p>Fuel is partitioned by size into six subclasses:</p> <p><math>\sigma \geq 1,200</math>  <math>1,200 &gt; \sigma \geq 192</math>  <math>192 &gt; \sigma \geq 96</math>  <math>96 &gt; \sigma \geq 48</math>  <math>48 &gt; \sigma \geq 16</math>  <math>16 &gt; \sigma</math></p> <p>Members of each subclass are given the same weighting factor:</p> $g_{ij} = \sum_{\substack{\text{subclass} \\ \text{to which} \\ j \text{ belongs}}} f_{ij}$ <p>For <math>\sigma &lt; 16</math>, <math>g_{ij} = 0</math></p>	[2] (p. 15)
<b>Moisture of extinction</b>		
Live fuel moisture of extinction (fraction)	$(M_x)_2 = 2.9W(1 - M_{f,dead}/(M_x)_1) - 0.226$ (min = $(M_x)_1$ )	[2] (p. 16) replaced [1] (eq. 88)
	<p>Dead-to-live load ratio</p> $W = \frac{\sum_j (w_0)_{1j} \exp(-138/\sigma_{1j})}{\sum_j (w_0)_{2j} \exp(-500/\sigma_{2j})}$ <p>“Fine” dead fuel moisture</p> $M_{f,dead} = \frac{\sum_j (M_f)_{1j} (w_0)_{1j} \exp(-138/\sigma_{1j})}{\sum_j (w_0)_{1j} \exp(-138/\sigma_{1j})}$	

<sup>a</sup>Category is indicated by  $i = 1$  for dead and  $i = 2$  for live; size class is indicated by  $j$ .

<sup>b</sup>Source: [1] = Rothermel (1972); [2] = Albini (1976a).

**Table 6b**—Final fire spread model equations for heterogeneous fuel and source for the equations.

Element	Equation <sup>a</sup>	Source <sup>b</sup>
<b>Characteristic values for live and dead categories</b>		
Net fuel load (lb/ft <sup>2</sup> )	$(w_n)_{ij} = (w_o)_{ij}(1 - (S_T)_{ij})$	[2] (p. 14) replaced [1] (eq. 60)
	$(w_n)_i = \sum_j g_{ij}(w_n)_{ij}$	[2] (p. 15) replaced [1] (eq. 59)
Heat content (Btu/lb)	$h_i = \sum_j f_{ij} h_{ij}$	[1] (eq. 61)
Effective mineral content (fraction)	$(S_e)_i = \sum_j f_{ij}(S_e)_{ij}$	[1] (eq. 63)
Mineral damping coefficient	$(\eta_s)_i = 0.174(S_e)_i^{-0.19}$ (max = 1)	[1] (eq. 62)
Moisture content (fraction)	$(M_f)_i = \sum_j f_{ij}(M_f)_{ij}$	[1] (eq. 66)
Moisture damping coefficient	$(\eta_M)_i = 1 - 2.59(r_M)_i + 5.11(r_M)_i^2 - 3.52(r_M)_i^3$ $(r_M)_i = (M_f)_i / (M_x)_i$ (max = 1)	[1] (eq. 64, 65)
Surface-area-to-volume ratio (ft <sup>2</sup> /ft <sup>3</sup> )	$\sigma_i = \sum_j f_{ij}\sigma_{ij}$	[1] (eq. 72)
<b>Fuel bed characteristic values</b>		
Surface-area-to-volume ratio (ft <sup>2</sup> /ft <sup>3</sup> )	$\sigma = \sum_i f_i\sigma_i$	[1] (eq. 71)
Mean bulk density (lb/ft <sup>3</sup> )	$\rho_b = \frac{1}{\delta} \sum_i \sum_j (w_o)_{ij}$	[1] (eq. 74)
Mean packing ratio	$\beta = \frac{1}{\delta} \sum_i \sum_j (w_o)_{ij} / (\rho_p)_{ij}$ $= \sum_i \sum_j (\rho_b)_{ij} / (\rho_p)_{ij}$	[1] (eq. 73)
Optimum packing ratio	$\beta_{op} = 3.348(\sigma)^{-0.8189}$	[1] (eq. 69)
Relative packing ratio	$\beta / \beta_{op}$	
<b>Wind and slope</b>		
Slope factor	$\phi_s = 5.275\beta^{-0.3}(\tan \phi)^2$	[1] (eq. 80)
Wind factor	$\phi_w = CU^B(\beta / \beta_{op})^{-E}$ $C = 7.47 \exp(-0.133\sigma^{0.55})$ $B = 0.02526\sigma^{0.54}$ $E = 0.715 \exp(-3.59 \times 10^{-4}\sigma)$	[1] (eq. 79, 81, 82, 83, 84)
Wind limit (ft/min)	$U = 0.9I_R$	[1] (eq. 86)

<sup>a</sup>Category is indicated by  $i = 1$  for dead and  $i = 2$  for live; size class is indicated by  $j$ .

<sup>b</sup>Source: [1] = Rothermel (1972); [2] = Albini (1976a).

**Table 6c**—Final fire spread model equations for heterogeneous fuel and source for the equations.

Element	Equation <sup>a</sup>	Source <sup>b</sup>
<b>Heat source</b>		
Maximum reaction velocity (min <sup>-1</sup> )	$\Gamma'_{max} = \sigma^{1.5}(495 + 0.0594\sigma^{1.5})^{-1}$	[1] (eq. 68)
Optimum reaction velocity (min <sup>-1</sup> )	$\Gamma' = \Gamma'_{max}(\beta/\beta_{op})^A \exp[A(1 - \beta/\beta_{op})]$  $A = 133\sigma^{-0.7913}$	[1] (eq. 67)  [2] (p. 15) replaced [1] (eq. 39)
Reaction intensity (Btu/ft <sup>2</sup> -min)	$I_R = \Gamma' \sum_i (w_n)_i h_i (\eta_M)_i (\eta_S)_i$	[2] (p. 17) replaced [1] (eq. 58)
Propagating flux ratio	$\xi = (192 + 0.2595\sigma)^{-1} \exp[(0.792 + 0.681\sigma^{0.5})(\beta + 0.1)]$	[1] (eq. 76)
No-wind, no-slope propagating flux (Btu/ft <sup>2</sup> -min)	$I_R \xi$	
Heat source	$I_R \xi (1 + \phi_w + \phi_s)$	
<b>Heat sink</b>		
Heat of preignition for each size class, live and dead (Btu/lb)	$(Q_{ig})_{ij} = 250 + 1,116(M_f)_{ij}$	[1] (eq. 78)
Heat sink (Btu/ft <sup>3</sup> )	$\rho_b \epsilon Q_{ig} = \rho_b \sum_i f_i \sum_j f_{ij} [\exp(-138/\sigma_{ij})] (Q_{ig})_{ij}$	[1] (eq. 77)
<b>Rate of spread</b>		
Zero-wind, zero-slope rate of spread (ft/min)	$R_0 = \frac{I_R \xi}{\rho_b \epsilon Q_{ig}}$	[1] (eq. 75)
Rate of spread (ft/min)	$R = R_0(1 + \phi_w + \phi_s)$	[1] (eq. 75)

<sup>a</sup>Category is indicated by  $i = 1$  for dead and  $i = 2$  for live; size class is indicated by  $j$ .

<sup>b</sup>Source: [1] = Rothermel (1972), [2] = Albini (1976a).

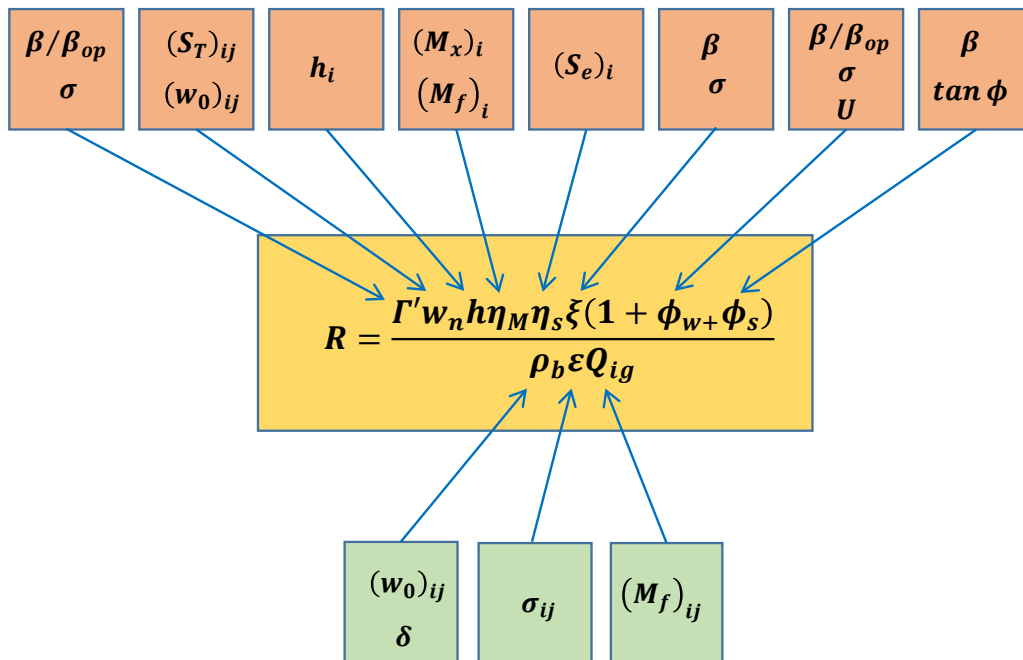


**Figure 2**—Breakdown of the fire spread equation indicating variables that represent the fuel bed (no subscript), live or dead ( $i$ ), and fuel particle ( $ij$ ). See table 6 for variable definitions.

### 3.2.1 Input Parameters

Input values for the final spread model are essentially the same as those for the basic model, for which a single value is assigned to each input parameter (see table 2). Table 5 is a list of the input parameters for the final model. Subscripts  $i$  and  $j$  are used to indicate the category ( $i = 1$  for dead;  $i = 2$  for live) and size class ( $j$ ). Although the fire model imposes no limit on the number of size classes, the standard fire behavior fuel models are limited to three dead and two live size classes (Anderson 1982).

Single values are assigned to midflame wind speed ( $U$ ), slope steepness ( $\tan \phi$ ), fuel bed depth ( $\delta$ ), and dead fuel moisture of extinction ( $(M_x)_1$ ). Surface-area-to-volume ratio ( $\sigma_{ij}$ ) is used to define size classes of both live and dead fuel. For each size class, a value is assigned to fuel load ( $(w_0)_{ij}$ ), heat content ( $(h_{ij})$ ), effective mineral content ( $(S_e)_{ij}$ ), total mineral content ( $(S_T)_{ij}$ ), particle density ( $(\rho_p)_{ij}$ ), and fuel moisture content ( $(M_f)_{ij}$ ).

### 3.2.2 Live Fuel Moisture of Extinction

While dead fuel moisture of extinction ( $(M_x)_1$ ) is an input parameter, live fuel moisture of extinction ( $(M_x)_2$ ) is calculated as described by Rothermel (1972) in the final section “Fuel Models and Application.” He noted that very little research had been done on the burning of living fuels. To obtain reasonable values of reaction intensity for fuel models that contain living fuels, the moisture of extinction for the live fuel is higher than that used for dead fuels. The model assumes that live fuel will burn only if dead fuel is present.

The live fuel moisture of extinction calculation used by Rothermel (1972) was provided by Fosberg and Schroeder (1971). It is based on the ratio of live-to-dead fuels, the moisture content of fine dead fuels, and dead fuel moisture of extinction. Albin (1976a) revised the formulation to reduce the sensitivity of the model output to arbitrary definitions of “fine” by using a method of calculating the relevant load ratio and the “fine” dead fuel moisture content using all size classes. Albin (1976a) also changed the Rothermel (1972) equation to avoid the implicit assumption that dead fuel moisture of extinction is equal to 0.3.

Live fuel moisture of extinction ( $(M_x)_2$ ) is calculated as

$$(M_x)_2 = 2.9W[1 - M_{f,dead}/(M_x)_1] - 0.226, (\min=(M_x)_1)$$

Dead/live load ratio ( $W$ ) is calculated as

$$W = \frac{\sum_j (w_0)_{1j} \exp(-138 / \sigma_{1j})}{\sum_j (w_0)_{2j} \exp(-500 / \sigma_{2j})}$$

“Fine” dead fuel moisture ( $M_{f,dead}$ ) is

$$M_{f,dead} = \frac{\sum_j (M_f)_{1j} (w_0)_{1j} \exp(-138 / \sigma_{1j})}{\sum_j (w_0)_{1j} \exp(-138 / \sigma_{1j})}$$

The above equations for  $W$  and  $M_{f,dead}$  are used only to calculate  $((M_x)_2)$  and are not used elsewhere in the fire spread model.

### 3.2.3 Weighting Factors

The spread model is based on the concept that a singular characteristic parameter can be found by weighting the variations in the parameter across the heterogeneous mixture. The method of weighting gives most of the influence to fine fuels. Model development was based on a consideration of how each fuel parameter in the model exerts its effect on the three characteristic features of a spreading fire: energy source, energy sink, and flow of air or heat within the array.

To aid understanding of fuel distribution, the concept of a unit fuel cell was developed. A unit fuel cell is the smallest volume of fuel within a stratum of mean depth that has sufficient fuel to be statistically representative of the entire fuel complex. This concept aids in mathematically weighting input parameters.

For the fire model, various size fuels are assumed to be uniformly distributed within the fuel array. Larger fuels have a negligible effect on fire spread. The original Rothermel model did not impose a limit on the size of fuel included in the calculations. The Albini adjustment to the weighting factors ignored fuel with  $\sigma < 16 \text{ ft}^2/\text{ft}^3$  (> 3-inch diameter); the weighting factor in this case is set to 0.

The spread model uses the weighting factors  $f_{ij}$  and as  $f_i$  reported in Rothermel (1972) as well as the  $g_{ij}$  weighting factors developed by Albini (1976a).

Weighting factors are based on the surface area of the fuel within each size class and category. The mean total surface area per unit fuel cell of each size class within each category ( $A_{ij}$ ) is determined from the mean load of that size class ( $(w_0)_{ij}$ ), its surface-area-to-volume ratio ( $(\sigma)_{ij}$ ), and particle density ( $(\rho_p)_{ij}$ ).

$$A_{ij} = (\sigma)_{ij} (w_0)_{ij} / (\rho_p)_{ij}$$

The mean total surface area of the dead and live categories per unit fuel cell ( $A_i$ ) is the sum of the areas within the category ( $A_{ij}$ ).

$$A_i = \sum_j A_{ij}$$

The mean total surface area per unit fuel cell ( $A_T$ ) is the sum of the mean total surface area of the dead and live categories ( $A_i$ ).

$$A_T = \sum_i A_i$$

The weighting factor  $f_{ij}$  is calculated as the ratio of the surface area of the  $j^{\text{th}}$  size class ( $A_{ij}$ ) to the total surface area of the dead or live category ( $A_i$ ).

$$f_{ij} = A_{ij} / A_i$$

The weighting factor  $f_i$  is calculated as the ratio of the total surface area of the dead or live category ( $A_i$ ) to total surface area per unit fuel cell ( $A_T$ ).

$$f_i = A_i / A_T$$

The net load of the live and dead fuel categories is calculated by summing the load of each size class in the category, with a weighting factor based on the fraction of that category's fuel surface area contributed by that size class. Rothermel used the  $f$  factors in the 1972 paper. Albini (1976a) developed  $g$  weighting factors for net fuel load because using  $f$  factors suffered the logical flaw that the net load is sensitive to the partitioning of the fuel load among nearly equal size classes. For example, if the load of a size class is split into two halves, the net load is reduced by half, even for the same surface-area-to-volume ratio ( $\sigma$ ). To alleviate this difficulty, fuels are partitioned by size into six subclasses, with all members of each subclass having the same weighting factor. The weighting factor for a subclass ( $g_{ij}$ ) is the fraction of the total fuel surface area contributed by that subclass.

Fuel is partitioned by size into six subclasses:

$$\sigma > 1,200$$

$$1,200 > \sigma \geq 192$$

$$192 > \sigma \geq 96$$

$$96 > \sigma \geq 48$$

$$48 > \sigma \geq 16$$

$$16 > \sigma$$

Members of each subclass are given the same weighting factor:

$$g_{ij} = \sum_{\substack{\text{subclass} \\ \text{to which} \\ \text{j belongs}}} f_j$$

$$g_{ij} = 0 \text{ for } \sigma < 16$$

The  $g_{ij}$  weighting factors are used only for net fuel load. The  $f_{ij}$  weighting factors are used to find the characteristic dead and live heat content, effective mineral content, moisture content, and surface-area-to-volume ratio. The  $f_i$  weighting factors are used to find the characteristic fuel bed surface-area-to-volume ratio.

### 3.2.4 Characteristic Live and Dead Values

Characteristic values are found for the live and dead categories based on values for individual size classes and the weighting factors for that class.

The net fuel load of each size class is reduced by the total mineral content. This is an Albin (1976a) change to the equation in Rothermel (1972).

$$(w_n)_{ij} = (w_0)_{ij} (1 - (S_T)_{ij})$$

Characteristic values for the live and dead categories are as follows:

Net fuel load

$$(w_n)_i = \sum_j g_{ij} (w_n)_{ij}$$

Heat content

$$h_i = \sum_j f_{ij} h_{ij}$$

Effective mineral content

$$(S_e)_i = \sum_j f_{ij} (S_e)_{ij}$$

Mineral damping coefficient, which imposes a maximum value of one, an Albin (1976a) change to the equation in Rothermel (1972)

$$(\eta_s)_i = 0.174(S_e)_i^{-0.19} \text{ (max = 1)}$$

Moisture content

$$(M_f)_i = \sum_j f_{ij} (M_f)_{ij}$$

Moisture damping coefficient

$$(\eta_M)_i = 1 - 2.59(r_M)_i + 5.11(r_M)_i^2 - 3.52(r_M)_i^3$$

$$(r_M)_i = (M_f)_i / (M_x)_i \text{ (max=1)}$$

Surface-area-to-volume ratio

$$\sigma_i = \sum_j f_{ij} \sigma_{ij}$$

### 3.2.5 Fuel Bed Calculations

A single value of reaction velocity ( $\Gamma'$ ) is calculated for the fuel complex, dependent on the packing ratio and fuel particle size. The packing ratio regulates the heat and airflow within the fuel array, and it is a mean value of all particle sizes. However, the surface-area-to-volume ratio is a parameter that characterizes the

particle size of the fuel complex that is regulating the combustion process in the fire front and must be weighted by surface area.

Characteristic surface-area-to-volume ratio ( $\sigma$ ) of the complex is

$$\sigma = \sum_i f_i \sigma_i$$

Mean bulk density ( $\rho_b$ ) is found from the fuel bed depth ( $\delta$ ) and load of each size class ( $(w_o)_{ij}$ ).

$$\rho_b = \frac{1}{\delta} \sum_i \sum_j (w_o)_{ij}$$

Mean packing ratio ( $\beta$ ) is found from fuel bed depth ( $\delta$ ) and from the load ( $(w_o)_{ij}$ ) and particle density ( $(\rho_p)_{ij}$ ) of each size class.

$$\beta = \frac{1}{\delta} \sum_i \sum_j (w_o)_{ij} / (\rho_p)_{ij}$$

### 3.2.6 Final Calculations

Fuel bed values are then used to find the optimum (potential) reaction velocity

$$\Gamma' = \Gamma'_{max} (\beta / \beta_{op})^A \exp[A(1 - \beta / \beta_{op})]$$

where

$$\Gamma'_{max} = \sigma^{1.5} (495 + 0.0594 \sigma^{1.5})^{-1}$$

$$\beta_{op} = 3.348 (\sigma)^{-0.8189}$$

$$A = 133 \sigma^{-0.7913}$$

The equation for A is an Albini (1976a) change to the equation in Rothermel (1972).

Reaction intensity is

$$I_R = \Gamma' \sum_i (w_n)_i h_i (\eta_M)_i (\eta_S)_i$$

While the weighting factor  $f_i$  was part of the original Rothermel (1972) equation for reaction intensity ( $I_R$ ), it was removed at the suggestion of Albini (1976a).

The no-wind no-slope propagating flux ratio ( $\xi$ ) is a function of the mean packing ratio ( $\beta$ ) and characteristic surface-area-to-volume ratio ( $\sigma$ ).

$$\xi = (192 + 0.2595 \sigma)^{-1} \exp[(0.792 + 0.681 \sigma^{0.5})(\beta + 0.1)]$$

In the heat sink term, the bulk density ( $\rho_b$ ) is dependent on bulk properties of the fuel array. The effective heating number ( $\epsilon$ ) and the heat of preignition ( $Q_{ig}$ ) are dependent on fuel surface. Therefore, bulk properties must be separated from the particle properties when summing and weighting.

Heat of preignition for each size class and category is

$$(Q_{ig})_{ij} = 250 + 1116(M\rho)_{ij}$$

Heat sink is

$$\rho_b \epsilon Q_{ig} = \rho_b \sum_i f_i \sum_j f_{ij} [\exp(-138/\sigma_{ij})] (Q_{ig})_{ij}$$

Slope factor ( $\phi_s$ ) and wind factor ( $\phi_w$ ) are calculated from the relative packing ratio ( $\beta/\beta_{op}$ ) and characteristic surface-area-to-volume ratio ( $\sigma$ ) for the fuel bed.

$$\phi_s = 5.275\beta^{-0.3}(\tan \phi)^2$$

$$\phi_w = CU^B(\beta/\beta_{op})^{-E}$$

where

$$C = 7.47\exp(-0.133\sigma^{0.55})$$

$$B = 0.02526\sigma^{0.54}$$

$$E = 0.715\exp(-3.59 \times 10^{-4}\sigma)$$

Final rate of spread for a fuel bed consisting of live and dead fuel of various size classes reduces to the basic equation.

$$R = \frac{I_R \xi (1 + \phi_w + \phi_s)}{\rho_b \epsilon Q_{ig}}$$

### 3.2.7 Wind Limit

Rothermel (1972, page 33) placed an upper limit on the wind factor. What Albini (1976a) called “maximum reliable wind” is a function of reaction intensity ( $I_R$ ). Rate of spread is modeled as constant for wind speeds greater than that value. The wind limit is defined as the point where

$$U/I_R > 0.9$$

The wind limit is then

$$U = 0.9I_R$$

Andrews et al. (2013) corrected an error in an assumption to give the wind limit as

$$U = 96.8I_R^{1/3}$$

The original relationship is included in most fire management systems. In some cases the wind limit is applied to effective wind speed, which is the combined effect of wind and slope. In FIREMOD (Albini 1976a) a footnote indicated if the wind limit was reached but the calculated rate of spread was not changed.

The nomographs (Albini 1976b) used a dashed line to indicate the limit. In those applications, the user had the option of not imposing the limit. BehavePlus5 added the option of either imposing the wind limit or not. Other applications such as the Scott (2007) nomographs, FARSITE (Finney 1998), FlamMap (Finney 2006), and Nexus (Scott 1999) always impose the limit.

The wind limit was included to address fires with low reaction intensity burning under high wind speeds. The wind limit function is based in part on McArthur’s (1969) presentation of and interpretation of fire spread data that decreased with increasing winds. An analysis of conditions driving the 1967 Tasmanian grassland fires indicates that these fires might not have been spreading in fully cured continuous grasslands, as assumed. In addition, more recent grassfire data do not support imposition of a wind limit (Andrews et al. 2013). The authors (including Rothermel) recommend that the wind limit not be imposed. In addition, recent laboratory experiments with winds of 60 mi/h did not indicate a wind limit (Bret W. Butler, Missoula Fire Sciences Laboratory, personal communication, October 2016).

It is conceivable that there is a point at which steady-state spread rate ceases to increase with increasing winds. High spread rates are likely a result of short range spotting and rolling debris, violating the model’s simplifying assumptions. As such, if fires spread faster with increasing winds, by whatever mechanism, then it is not appropriate to impose a wind limit on the model predictions.

## 4. Related Models

To this point in the report, the focus was on the Rothermel surface fire spread model from Rothermel (1972) with the modifications made by Albini (1976a). This section describes some commonly associated mathematical models. Equations as they are implemented in the BehavePlus fire modeling system are given in table 7.

**Table 7—** Related models as implemented in BehavePlus. These models are not technically part of the Rothermel surface fire spread model, but are often used with it. (Variables not defined here are found in tables 1 and 2.)

Element	Equation	Source
Effective midflame wind speed (ft/min)	$U_E = \left[ \phi_E (\beta / \beta_{op})^E / C \right]^{-B}$ <p>where</p> $\phi_E = \phi_w + \phi_s$	Albini (1976b)
Residence time (min)	$t_r = 384 / \sigma$	Anderson (1969)
Heat per unit area (Btu/ft <sup>2</sup> )	$H_A = I_R t_r$	Andrews and Rothermel (1982)
Fireline intensity (Btu/ft/s)	$I_B = H_A R / 60$ $I_B = I_R t_r R / 60$	Albini (1976a) Byram (1959)
Flame length (ft)	$F_B = 0.45 I_B^{0.46}$	Byram (1959)
Dynamic fuel load transfer from live to dead herbaceous (fraction)	$T = -1.11 M + 1.33, 0 \leq T \leq 1.0$ <p>where</p> <p>M is herbaceous fuel moisture (fraction)</p>	Burgan (1979)

This section also addresses fuel models, which are models in that they are a representation of reality, but they are lists of numbers rather than equations.

#### 4.1 Effective Wind Speed

Albini (1976a) used the concept of effective wind speed in designing the nomographs. Effective wind speed represents the combined effect of wind and slope, based on the spread model relationships.

Effective wind factor ( $\phi_E$ ) is the sum of the wind factor and slope factor.

$$\phi_E = \phi_w + \phi_s$$

The wind factor equation is then used to find the effective midflame wind speed ( $U_E$ ) that would result in the calculated effective wind factor ( $\phi_E$ ).

$$\phi_E = CU_E^B (\beta/\beta_{op})^{-E}$$

$$U_E = [\phi_E (\beta/\beta_{op})^E / C]^{-B}$$

#### 4.2 Residence Time

Residence time ( $t_r$ ) is the length of time that it takes the fire front to pass a given point. It does not include the indefinite trailing edge of the fire and assumes no effect of fuel bed packing. Anderson (1969) found that an approximation of the flaming time of fuel particles burning in a uniform fuel array can be calculated from fuel particle size.

$$t_r = 8d$$

where

$$t_r = \text{residence time (min)}$$

$$d = \text{fuel particle diameter (inches)}$$

Rothermel's surface fire spread model uses surface-area-to-volume ratio ( $\sigma$ ) as a measure of fuel particle size. The relationship to diameter is

$$d = 48/\sigma$$

Residence time is then

$$t_r = 384/\sigma$$

### 4.3 Heat per Unit Area

Heat per unit area ( $H_A$ ) is the product of the reaction intensity ( $I_R$ ) and the time that the area is in the flaming zone, as indicated by the residence time ( $t_r$ ). Reaction intensity is the rate of energy release per unit area within the flaming front (Btu/ft<sup>2</sup>/min). Heat per unit area is the amount of heat energy release per unit area within the flaming front (Btu/ft<sup>2</sup>).  $I_R$  is a rate;  $H_A$  is not.

$$H_A = I_R t_r$$

Using the relationship for flame residence time, heat per unit area can be calculated from parameters in the spread model.

$$H_A = 384 I_R / \sigma$$

### 4.4 Fireline Intensity

Byram (1959, page 79) presented a model for fireline intensity as

$$I_B = HwR$$

where

$I_B$  = Byram's fireline intensity (Btu/ft/s)

$H$  = heat yield (Btu/lb of fuel)

$w$  = weight of the available fuel (lb/ft<sup>2</sup>)

$R$  = rate of spread (ft/s)

Albini (1976a) defined relationships to use Rothermel's spread model to find fireline intensity. Heat per unit area ( $H_A$ ) is used to estimate  $Hw$ . Changing the units of  $R$  from ft/s to ft/min gives

$$I_B = H_A R$$

or

$$I_B = (384/\sigma) I_R R$$

Heat per unit area is the heat energy release per unit area within the flaming front. In this relationship "available fuel" therefore includes only the fuel that burns in the flaming front and not the total fuel consumed.

## 4.5 Flame Length

Flame length is calculated from fireline intensity according to Byram's equation (Brown and Davis 1973, page 175).

$$F_B = 0.45I_B^{0.46}$$

where

$F_B$  = Byram's flame length (ft),

$I_B$  = Byram's fireline intensity (Btu/ft/s).

## 4.6 Fuel Models

The input parameters for the surface fire spread model that describe the fuel (see table 5) are fuel bed depth, dead fuel moisture of extinction, and for each live and dead size class: surface-area-to-volume ratio, oven-dry fuel load, heat content, particle density, and total and effective mineral content. There are no restrictions within the Rothermel fire spread model as to the values for these variables. The fire model allows any number of size classes of live and dead fuel.

The common way of defining fuel descriptors for the fire model is through use of a fuel model, which is simply a code such as "2" or "GS3" that is associated with a list of values for the fuel variables required by the fire model. While the *fire model* is a set of equations, a *fuel model* is a list of numbers required by the *fire model*.

There are 53 standard fuel models. Custom fuel models can be developed for conditions not satisfied by the standard models. In addition, some "special case" fuel models involve various relationships to define the fuel parameters and can be quite different from the standard or custom fuel models.

### 4.6.1 Standard Fuel Models

The concept of "fuel model" has proved useful in facilitating application of the fire model. From the preface to Rothermel (1972):

A convenient method of cataloging input parameters is through the concept of fuel models tailored to the vegetation patterns found in the field. The companion fuel models are thus a set of input parameters that describe the inherited characteristics that have been found in certain fuel types in the past. The environmental parameters of wind, slope, and expected moisture changes may be superimposed on the fuel models. This fuel model concept has already been incorporated into the National Fire Danger Rating System (Deeming et al. 1972).

Eleven fire behavior fuel models were published in Rothermel (1972). Two fuel models were added and some changes were made, including changing dead fuel moisture of extinction from a constant 30 percent to various values in Albini (1976b). Anderson (1982) described those 13 standard fire behavior fuel models and

included representative photographs. In order to expand the fuel types beyond what was represented by the 13 fuel models, Scott and Burgan (2005) developed a set of 40 fuel models. While they suggested that the set of 40 could replace the set of 13, there are no duplicates and both sets continue to be used. Therefore there are 53 standard fire behavior fuel models. Table 8 is a list of parameters for the 53 standard fire behavior fuel models. The table also includes characteristic surface-area-to-volume ratio, bulk density, and relative packing ratio, which are intermediate values calculated in the fire model. Some of the fuel parameters are held constant as noted in the table footnote.

Dead fuel components are organized by time lag (1-h, 10-h, and 100-h). Fine dead fuel is 1-hour time lag and has higher surface-area-to-volume ratio than 10-h and 100-h fuel. Moisture of 1-h fuel responds more rapidly to changes in the environment. Live fuels are labeled “herbaceous” (living grasses and forbs, either annual or perennial) or “woody” (foliage and very fine stems of living shrubs). The fire model itself treats live herbaceous and woody fuel the same. The difference is in their role in dynamic fuel models.

#### **4.6.2 Dynamic Fuel Models**

The concept of dynamic fuel models was developed for fire-danger rating to reflect seasonal changes (Burgan 1979a). Fuel load is transferred from the live to the dead category to represent curing. The amount of fuel transferred is generally determined by live herbaceous fuel moisture. Dynamic fuel models were allowed for custom fire behavior fuel models in the old BEHAVE system (Burgan and Rothermel 1984). Seventeen of the set of 40 standard fuel models are dynamic (Scott and Burgan 2005).

The old BEHAVE system and NFDRS transfer load from live herbaceous to the 1-h size class. Scott and Burgan (2005, page 6) changed the model in developing the 40 fire behavior fuel models:

Load transferred to dead is not simply placed in the dead 1-hr time lag class. Instead a new dead herbaceous class is created so that the surface-area-to-volume ratio of the live herbaceous component is preserved.

For the standard fuel models,

$(w_0)_{11}$  = 1-h fuel load (remains constant for the fuel model)

$(w_0)_{12}$  = dead herbaceous fuel load (initially 0)

$(w_0)_{21}$  = live herbaceous fuel load (initial value before load transfer)

$(M_f)_{21}$  = live herbaceous fuel moisture (fraction)

$T$  = fraction of load transferred from live herbaceous to dead herbaceous

**Table 8a**—Standard fuel model parameters<sup>a</sup> with calculated characteristic surface-area-to-volume ratio (SAV), bulk density, and relative packing ratio. Live herbaceous load is the value before dynamic fuel model load transfer to dead herbaceous.

Fuel model code	Fuel model name	Type	Fuel load <sup>b</sup>				Surface-area-to-volume ratio				Dead fuel moist. of extinction	Characteristic SAV	Bulk density	Relative packing ratio				
			1-h	10-h	100-h	Live herbaceous	Live woody	1-h	Live and dead herb.	Live woody					Fuel bed depth	-%	ft <sup>2</sup> /ft <sup>3</sup>	lb/ft <sup>3</sup>
			-----tons/acre-----				-----ft <sup>2</sup> /ft <sup>3</sup> -----				--ft--							
1	Short grass	S	0.74	0	0	0	0	0	0	0	3,500	--	--	1.0	12	3,500	0.03	0.25
2	Timber grass and understory	S	2.0	1.0	0.50	0.50	0	0	0.50	0	3,000	1,500	--	1.0	15	2,784	0.18	1.14
3	Tall grass	S	3.0	0	0	0	0	0	0	1,500	--	--	--	2.5	25	1,500	0.06	0.21
4	Chaparral	S	5.0	4.0	2.0	0	5.0	2,000	0	2,000	--	--	1,500	6.0	20	1,739	0.12	0.52
5	Brush	S	1.0	0.50	0	0	2.0	2,000	0	2,000	--	--	1,500	2.0	20	1,683	0.08	0.33
6	Dormant brush, hardwood slash	S	1.5	2.5	2.0	0	0	1,750	0	1,750	--	--	--	2.5	25	1,564	0.11	0.43
7	Southern rough	S	1.1	1.9	1.5	0	0.37	1,750	0	1,750	--	--	1,500	2.5	40	1,552	0.09	0.34
8	Short needle litter	S	1.5	1.0	2.5	0	0	2,000	0	2,000	--	--	--	0.2	30	1,889	1.15	5.17
9	Long needle or hardwood litter	S	2.9	0.41	0.15	0	0	2,500	0	2,500	--	--	--	0.2	25	2,484	0.80	4.50
10	Timber litter and understory	S	3.0	2.0	5.0	0	2.0	2,000	0	2,000	--	--	1,500	1.0	25	1,764	0.55	2.35
11	Light logging slash	S	1.5	4.5	5.5	0	0	1,500	0	1,500	--	--	--	1.0	15	1,182	0.53	1.62
12	Medium logging slash	S	4.0	14.0	16.5	0	0	1,500	0	1,500	--	--	--	2.3	20	1,145	0.69	2.06
13	Heavy logging slash	S	7.0	23.0	28.0	0	0	1,500	0	1,500	--	--	--	3.0	25	1,159	0.89	2.68

<sup>a</sup>Parameters constant for all fuel models: 10-h SAV 109 ft<sup>2</sup>/ft<sup>3</sup>, 100-h SAV 30 ft<sup>2</sup>/ft<sup>3</sup>, heat content 8,000 Btu/lb, particle density 32 lb/ft<sup>3</sup>, total mineral content 0.0555, effective mineral content 0.010.

<sup>b</sup>Rothermel (1972) expresses load as lb/ft<sup>2</sup>, while this table gives load as tons/acre.

**Table 8b—Standard fuel model parameters<sup>a</sup> with calculated characteristic surface-area-to-volume ratio (SAV), bulk density, and relative packing ratio. Live herbaceous load is the value before dynamic fuel model load transfer to dead herbaceous.**

Fuel model code	Fuel model name	Type	Fuel load <sup>b</sup>					Surface-area-to-volume ratio					Dead fuel moist. of extinction	Characteristic SAV	Bulk density	Relative packing ratio
			1-h	10-h	100-h	Live herbaceous	Live woody	1-h	Live and dead herb.	Live woody	Fuel bed depth	-%				
			-----tons/acre-----					-----ft <sup>2</sup> /ft <sup>3</sup> -----								
GR1	101	Short, sparse, dry climate grass	D	0.1	0	0	0.3	0	2,200	2,000	--	0.4	15	2,054	0.05	0.22
GR2	102	Low load, dry climate grass	D	0.1	0	0	1.0	0	2,000	1,800	--	1.0	15	1,820	0.05	0.22
GR3	103	Low load, very coarse, humid climate grass	D	0.1	0.4	0	1.5	0	1,500	1,300	--	2.0	30	1,290	0.05	0.15
GR4	104	Moderate load, dry climate grass	D	0.25	0	0	1.9	0	2,000	1,800	--	2.0	15	1,826	0.05	0.22
GR5	105	Low load, humid climate grass	D	0.4	0	0	2.5	0	1,800	1,600	--	1.5	40	1,631	0.09	0.35
GR6	106	Moderate load, humid climate grass	D	0.1	0	0	3.4	0	2,200	2,000	--	1.5	40	2,006	0.11	0.51
GR7	107	High load, dry climate grass	D	1.0	0	0	5.4	0	2,000	1,800	--	3.0	15	1,834	0.10	0.43
GR8	108	High load, very coarse, humid climate grass	D	0.5	1.0	0	7.3	0	1,500	1,300	--	4.0	30	1,302	0.10	0.33
GR9	109	Very high load, humid climate grass	D	1.0	1.0	0	9.0	0	1,800	1,600	--	5.0	40	1,612	0.10	0.40
GS1	121	Low load, dry climate grass-shrub	D	0.2	0	0	0.5	0.65	2,000	1,800	1,800	0.9	15	1,832	0.07	0.30

<sup>a</sup>Parameters constant for all fuel models: 10-h SAV 109 ft<sup>2</sup>/ft<sup>3</sup>, 100-h SAV 30 ft<sup>2</sup>/ft<sup>3</sup>, heat content 8,000 Btu/lb, particle density 32 lb/ft<sup>3</sup>, total mineral content 0.0555, effective mineral content 0.010.

<sup>b</sup>Rothermel (1972) expresses load as lb/ft<sup>2</sup>, while this table gives load as tons/acre.

**Table 8c—Standard fuel model parameters<sup>a</sup> with calculated characteristic surface-area-to-volume ratio (SAV), bulk density, and relative packing ratio. Live herbaceous load is the value before dynamic fuel model load transfer to dead herbaceous.**

Fuel model code	Fuel model name	Type	Fuel load <sup>b</sup>							Surface-area-to-volume ratio					Dead fuel moist. of extinction	Characteristic SAV	Bulk density	Relative packing ratio
			1-h	10-h	100-h	Live herbaceous	Live woody	1-h	Live and dead herb.	Live woody	Fuel bed depth	-%	ft <sup>2</sup> /ft <sup>3</sup>	lb/ft <sup>3</sup>				
GS2	Moderate load, dry climate grass-shrub	D	0.5	0.5	0	0.6	1.0	2,000	1,800	1,800	1.5	15	1,827	0.08	0.35			
GS3	Moderate load, humid climate grass-shrub	D	0.3	0.25	0	1.45	1.25	1,800	1,600	1.8	40	1,614	0.08	0.33				
GS4	High load, humid climate grass-shrub	D	1.9	0.3	0.1	3.4	7.1	1,800	1,600	2.1	40	1,631	0.28	1.12				
SH1	Low load, dry climate shrub	D	0.25	0.25	0	0.15	1.3	2,000	1,800	1.0	15	1,674	0.09	0.36				
SH2	Moderate load, dry climate shrub	S	1.35	2.4	0.75	0	3.85	2,000	--	1.0	15	1,672	0.38	1.56				
SH3	Moderate load, humid climate shrub	S	0.45	3.0	0	0	6.2	1,600	--	2.4	40	1,371	0.18	0.64				
SH4	Low load, humid climate timber-shrub	S	0.85	1.15	0.2	0	2.55	2,000	1,800	3.0	30	1,682	0.07	0.30				
SH5	High load, dry climate shrub	S	3.6	2.1	0	0	2.9	750	--	6.0	15	1,252	0.07	0.21				
SH6	Low load, humid climate shrub	S	2.9	1.45	0	0	1.4	750	--	2.0	30	1,144	0.13	0.39				
SH7	Very high load, dry climate shrub	S	3.5	5.3	2.2	0	3.4	750	--	6.0	15	1,233	0.11	0.35				

<sup>a</sup>Parameters constant for all fuel models: 10-h SAV 109 ft<sup>2</sup>/ft<sup>3</sup>, 100-h SAV 30 ft<sup>2</sup>/ft<sup>3</sup>, heat content 8000 Btu/lb, particle density 32 lb/ft<sup>3</sup>, total mineral content 0.0555, effective mineral content 0.010.

<sup>b</sup>Rothermel (1972) expresses load as lb/ft<sup>2</sup>, while this table gives load as tons/acre.

**Table 8d**—Standard fuel model parameters<sup>a</sup> with calculated characteristic surface-area-to-volume ratio (SAV), bulk density, and relative packing ratio. Live herbaceous load is the value before dynamic fuel model load transfer to dead herbaceous.

Fuel model code	Fuel model name	Type	Fuel load <sup>b</sup>					Surface-area-to-volume ratio					Relative packing ratio		
			1-h	10-h	100-h	Live herbaceous	Live woody	1-h	Live and dead herb.	Live woody	Fuel bed depth	Dead fuel moist. of extinction		Characteristic SAV	Bulk density
			-----tons/acre-----	-----ft-----	-----ft <sup>2</sup> /ft <sup>3</sup> -----	-----ft-----	-----%	-----ft <sup>2</sup> /ft <sup>3</sup> -----	-----lb/ft <sup>3</sup> -----						
SH8	148 High load, humid climate shrub	S	2.05	3.4	0.85	0	4.35	750	--	1,600	3.0	40	1,386	0.16	0.57
SH9	149 Very high load, humid climate shrub	D	4.5	2.45	0	1.55	7.0	750	1,800	1,500	4.4	40	1,378	0.16	0.56
TU1	161 Light load, dry climate timber-grass-shrub	D	0.2	0.9	1.5	0.2	0.9	2,000	1,800	1,600	0.6	20	1,606	0.28	1.12
TU2	162 Moderate load, humid climate timber-shrub	S	0.95	1.8	1.25	0	0.2	2,000	--	1,600	1.0	30	1,767	0.19	0.82
TU3	163 Moderate load, humid climate timber-grass-shrub	D	1.1	0.15	0.25	0.65	1.1	1,800	1,600	1,400	1.3	30	1,611	0.11	0.45
TU4	164 Dwarf conifer understory	S	4.5	0	0	0	2.0	2,300	--	2,000	0.5	12	2,216	0.60	3.06
TU5	165 Very high load, dry climate timber-shrub	S	4.0	4.0	3.0	0	3.0	1,500	--	750	1.0	25	1,224	0.64	2.03
TL1	181 Low load, compact conifer litter	S	1.0	2.2	3.6	0	0	2,000	--	--	0.2	30	1,716	1.56	6.49
TL2	182 Low broadleaf litter	S	1.4	2.3	2.2	0	0	2,000	--	--	0.2	25	1,806	1.35	5.87
TL3	183 Moderate load conifer litter	S	0.5	2.2	2.8	0	0	2,000	--	--	0.3	20	1,532	0.84	3.19

<sup>a</sup>Parameters constant for all fuel models: 10-h SAV 109 ft<sup>2</sup>/ft<sup>3</sup>, 100-h SAV 30 ft<sup>2</sup>/ft<sup>3</sup>, heat content 8000 Btu/lb, particle density 32 lb/ft<sup>3</sup>, total mineral content 0.0555, effective mineral content 0.010.

<sup>b</sup>Rothermel (1972) expresses load as lb/ft<sup>2</sup>, while this table gives load as tons/acre.

**Table 8e**—Standard fuel model parameters<sup>a</sup> with calculated characteristic surface-area-to-volume ratio (SAV), bulk density, and relative packing ratio. Live herbaceous load is the value before dynamic fuel model load transfer to dead herbaceous.

Fuel model code	Fuel model name	Type	Fuel load <sup>b</sup>				Surface-area-to-volume ratio				Dead fuel moist. of extinction	Characteristic SAV	Bulk density	Relative packing ratio	
			1-h	10-h	100-h	Live herbaceous	Live woody	1-h	Live and dead herb.	Live woody					Fuel bed depth
		S=Static D=Dynamic	-----tons/acre-----	-----ft-----	-----ft <sup>2</sup> /ft <sup>3</sup> -----	-----ft-----	-----ft-----	-----ft-----	-----ft-----	-----ft-----	-----ft-----	-----ft-----	-----ft-----	-----ft-----	-----ft-----
TL4	184 Small downed logs	S	0.5	1.5	4.2	0	0	2,000	--	--	0.4	25	1,568	0.71	2.75
TL5	185 High load conifer litter	S	1.15	2.5	4.4	0	0	2,000	--	1,600	0.6	25	1,713	0.62	2.56
TL6	186 Moderate load broadleaf litter	S	2.4	1.2	1.2	0	0	2,000	--	--	0.3	25	1,936	0.73	3.37
TL7	187 Large downed logs	S	0.3	1.4	8.1	0	0	2,000	--	--	0.4	25	1,229	1.12	3.56
TL8	188 Long-needle litter	S	5.8	1.4	1.1	0	0	1,800	--	--	0.3	35	1,770	1.27	5.42
TL9	189 Very high load broadleaf litter	S	6.65	3.3	4.15	0	0	1,800	--	1,600	0.6	35	1,733	1.08	4.52
SB1	201 Low load activity fuel	S	1.5	3.0	11.0	0	0	2,000	--	--	1.0	25	1,653	0.71	2.87
SB2	202 Moderate load activity or low load blowdown	S	4.5	4.25	4.0	0	0	2,000	--	--	1.0	25	1,884	0.59	2.63
SB3	203 High load activity fuel or moderate low blowdown	S	5.5	2.75	3.0	0	0	2,000	--	--	1.2	25	1,935	0.43	1.97
SB4	204 High load blowdown	S	5.25	3.5	5.25	0	0	2,000	--	--	2.7	25	1,907	0.24	1.08

<sup>a</sup>Parameters constant for all fuel models: 10-h SAV 109 ft<sup>2</sup>/ft<sup>3</sup>, 100-h SAV 30 ft<sup>2</sup>/ft<sup>3</sup>, heat content 8,000 Btu/lb, particle density 32 lb/ft<sup>3</sup>, total mineral content 0.0555, effective mineral content 0.010.

<sup>b</sup>Rothermel (1972) expresses load as lb/ft<sup>2</sup>, while this table gives load as tons/acre.

The 1-h fuel load remains constant. The live herbaceous fuel load given in table 8 is the value before load is transferred to the dead herbaceous class, which is initially 0 and therefore not listed on the table. The portion (fraction) of fuel load transferred from live herbaceous to dead herbaceous ( $T$ ) is a value between 0 and 1. No live fuel is transferred if live herbaceous fuel moisture is greater than 1.2 (120 percent); all of the live herbaceous fuel is transferred to the dead category when the live herbaceous fuel moisture is 0.3 (30 percent) or less (fig. 3).

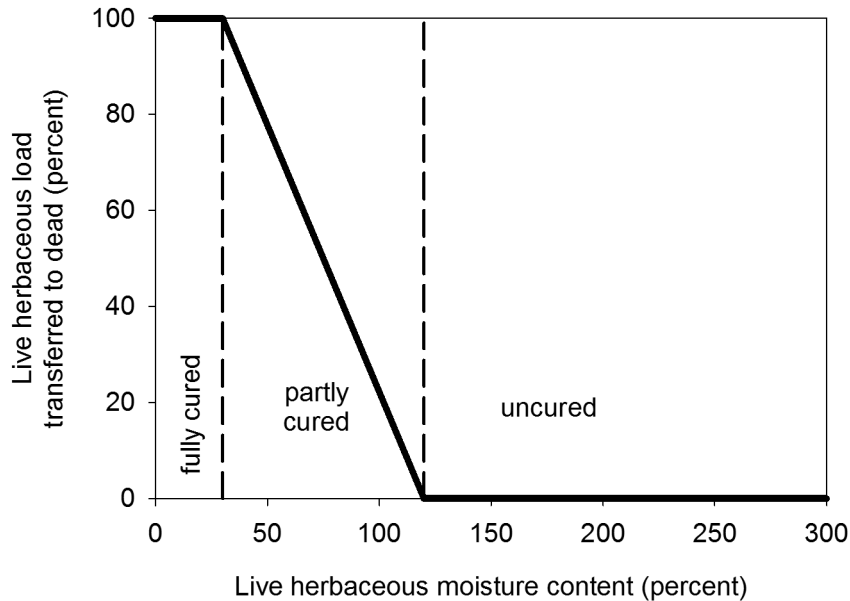


**Figure 3**—Fuel load transfer for dynamic fuel models is a function of live herbaceous fuel moisture.

$$T = -1.11(M_f)_{21} + 1.33, 0 \leq T \leq 1.0$$

The adjusted fuel load values are then

$$(w_0)_{12} = T(w_0)_{21}$$

$$(w_0)_{21, new} = (w_0)_{21} - T(w_0)_{21}$$

This dynamic load transfer model is not part of the fire spread model but is a method of adjusting fuel parameters before the fire model calculations are applied. BehavePlus offers the option of user specification of load transfer portion ( $T$ ) if it is desired not to use live herbaceous fuel moisture to determine the level of curing.

Scott and Burgan (2005, page 4) warn that if the fuel model parameters from table 8 are used in the spread model without applying the load transfer function, all the live herbaceous fuel remains in the live category. They write, “The grass fuel models would therefore predict no (or very little) spread and intensity under any wind or moisture condition.”

### **4.6.3 Custom Fuel Models**

Because the 13 standard fire behavior fuel models did not match some fuel situations, the FUEL subsystem of the old BEHAVE system was developed to help people develop custom fuel models (Burgan 1987; Burgan and Rothermel 1984). The NEWMDL (new model) program was used to construct a “first draft” fuel model from raw field data. The TSTMDL (test model) program was used to test the new fuel model and adjust it until reasonable fire behavior predictions were produced. Now that an additional 40 standard fuel models are available, there is less need to develop custom fuel models (Scott and Burgan 2005).

Developing a custom fuel model is not simply a matter of using data measured in the field. Because a fuel model is a set of values required by the fire spread model, it is critical that the developer understand the internal workings of the fire model. While the FUEL subsystem of the old BEHAVE system is no longer used, the information in the supporting publications is still valid.

### **4.6.4 Special Case Fuel Models**

In addition to standard and custom fuel models, there are “special case” fuel models that provide fuel parameters to the spread model. These fuel models are not limited by the number of size classes or constants used for standard and custom fuel models. In addition, some fuel parameters are calculated.

Rothermel and Philpot (1973) developed the first such special case fuel model for chaparral. Fuel load is calculated as a function of chaparral age, and heat content varies during the season. Brown and Simmerman (1986) developed models for five western aspen types. Curing level is used to calculate fuel load for 1-h, live herbaceous, and live woody fuel, and to find surface-area-to-volume ratio for 1-h and live woody fuel. The curing model is different from that used for dynamic fuel models (Burgan 1979a).

Hough and Albin (1978) developed a special case fuel model for palmetto-gallberry. This model illustrates how a special case fuel model differs from the standard fuel models (tables 9 and 10). Fuel parameters are found for four classes of dead fuel (fine, medium, foliage, and litter) and three classes of live fuel (fine, medium, and foliage). Some fuel parameters are calculated from age of rough, overstory basal area, height of understory, and palmetto coverage. Values for particle density, ash content, and surface-area-to-volume ratio differ from those used for the standard fuel models.

**Table 9**—Fuel model constants for the Hough and Albini (1978) special case palmetto-gallberry fuel model.

<b>Fuel model variable description</b>	<b>Fire model variable</b>	<b>Value</b>
Dead fuel moisture of extinction (fraction)	$(M_x)_{1j}$	0.40
Heat content, live and dead (Btu/lb)	$h_{ij}$	8,300
Particle density, dead fuel (lb/ft <sup>3</sup> )	$(\rho_p)_{1j}$	30
Particle density, live fuel (lb/ft <sup>3</sup> )	$(\rho_p)_{2j}$	46
Total mineral content (fraction)	$(S_T)_{ij}$	0.030
Effective mineral content, dead fuel (fraction)	$(S_e)_{1j}$	0.010
Effective mineral content, live fuel (fraction)	$(S_e)_{2j}$	0.015
Surface-area-to-volume ratio, foliage (ft <sup>2</sup> /ft <sup>3</sup> )	$\sigma_{i1}$	2,000
Surface-area-to-volume ratio, 0–0.25 inch diam. stems (ft <sup>2</sup> /ft <sup>3</sup> )	$\sigma_{i2}$	350
Surface-area-to-volume ratio, 0.25–1.0 inch diam. stems (ft <sup>2</sup> /ft <sup>3</sup> )	$\sigma_{i3}$	140
Surface-area-to-volume ratio, litter (ft <sup>2</sup> /ft <sup>3</sup> )	$\sigma_{14}$	2,000

**Table 10**—Fuel model values calculated for the Hough and Albini (1978) special case palmetto-gallberry fuel model.

<b>Fuel model variable description</b>	<b>Fire model variable</b>	<b>Input used to calculate fuel model variables</b>			
		<b>Age of rough (years)</b>	<b>Overstory basal area (ft<sup>2</sup>/ac)</b>	<b>Height of understory (feet)</b>	<b>Palmetto coverage (percent)</b>
Fuel bed depth (ft)	$\delta$			X	
Dead foliage load (tons/ac)	$(w_0)_{11}$	X			X
Dead 0–0.25 inch diam. load (tons/ac)	$(w_0)_{12}$	X		X	
Dead 0.25–1.0 inch diam. load (tons/ac)	$(w_0)_{13}$	X			X
Litter load (tons/ac)	$(w_0)_{14}$	X	X		
Live foliage load (tons/ac)	$(w_0)_{21}$	X		X	X
Live 0–0.25 inch diam. load (tons/ac)	$(w_0)_{22}$	X		X	
Live 0.25–1.0 inch diam. load (tons/ac)	$(w_0)_{23}$	X		X	

## 5. Fire Model Relationships

Sections 3 and 4 presented equations for the Rothermel surface fire spread model and associated models such as flame length. Fire model relationships are now described in more detail, first looking at some of the important components of the spread model, then examining the role of each input variable. The effect on relationships for dynamic fuel model fuel load transfer as a function of live fuel moisture is included.

The fire spread model includes interactions among input variables. Most relationships are not linear and some are not monotonic. For example, with an increase in fuel bed depth and everything else held constant, rate of spread can increase to a point and then decrease.

The need to examine relationships is pointed out by Rothermel (1972, page 25):

Students of fire behavior can gain a perspective understanding of the effects of various input parameters by computing and crossplotting curve families for reaction velocity, reaction intensity, and other internal variables that govern fire spread.

In describing fuel modeling concepts, Burgan and Rothermel (1984, page 30) say,

Interactions between fuel model, topography, and environmental parameters, and the mathematical fire spread model are so numerous and complex that attempting to present all the possible results would be an unreasonable task. Yet a basic understanding of the relationships provides valuable insight to the fuel modeling process.

The fuel modeling portion of the old BEHAVE system involved exercising the fire model (Burgan and Rothermel 1984). The TSTMDL program provided “a convenient method to examine the effect on fire behavior when individual fuel model parameters are modified.” A subsequent paper (Burgan 1987) goes into more detail on fire model relationships. In addition to Rothermel (1972), those publications are used to guide much of the discussion and some of examples that follow.

The BehavePlus fire modeling system is designed to encourage examining influences through tables and graphs (Heinsch and Andrews 2010). Results can be exported for additional analysis or display by other software. Some of the intermediate values calculated in the surface fire spread model are available as output variables. BehavePlus6 was used to produce values for most of the graphs in this section.

### 5.1 Fire Model Components

Table 4 is repeated here with variable names added to examine the relationships between input variables and components of the basic fire spread equation with one size class of dead fuel (table 11).

**Table 11**—Input variables that affect each element of the basic fire spread equation.

Input variable		Components of the basic fire spread equation						
		$R = \frac{I_R \xi (1 + \phi_w + \phi_s)}{\rho_b \varepsilon Q_{ig}}$						
		Heat source (numerator)				Heat sink (denominator)		
		Reaction intensity ( $I_R$ )	Propagating flux ratio ( $\xi$ )	Wind factor ( $\phi_w$ )	Slope factor ( $\phi_s$ )	Bulk density ( $\rho_b$ )	Effective heating number ( $\varepsilon$ )	Heat of preignition ( $Q_{ig}$ )
Fuel particle	Heat content ( $h$ )	X						
	Total mineral content ( $S_T$ )	X						
	Effective mineral content ( $S_e$ )	X						
	Particle density ( $\rho_p$ )	X	X	X	X			
Fuel array	Surface-area-to-volume ratio ( $\sigma$ )	X	X	X			X	
	Fuel load ( $w_0$ )	X	X	X	X	X		
	Fuel bed depth ( $\delta$ )	X	X	X	X	X		
	Moisture of extinction ( $M_x$ )	X						
Environmental	Moisture content ( $M_f$ )	X						X
	Midflame wind speed ( $U$ )			X				
	Slope steepness ( $\tan \phi$ )				X			

Look across the rows to see which components are affected by each input variable.

- Wind and slope are used only in the wind factor and slope factor.
- Heat content, total and effective mineral content, and dead fuel moisture of extinction affect only reaction intensity.
- Particle density plays a role in the four factors in the heat source term.

- Fuel moisture, surface-area-to-volume ratio, load, and depth are in both the heat source and the heat sink terms.

Now look down the columns to see which inputs affect each component.

- All input variables except wind and slope are used to calculate reaction intensity.
- Propagating flux ratio uses particle density, load, depth, and surface-area-to-volume ratio (SAV).
- In addition to wind and slope, the wind and slope factors use particle density, load, and depth. Wind factor also uses SAV.
- Bulk density is calculated from load and depth.
- Effective heating number function of only SAV.
- Heat of preignition is a function of only fuel moisture.

According to Rothermel (1972, page 3) “rate of spread during the quasi-steady state is a ratio between the heat flux received from the source in the numerator and the heat required for ignition by the potential fuel in the denominator.”

The numerator (heat source; Btu/ft<sup>2</sup>-min) is reaction intensity ( $I_R$ ) times propagating flux ratio ( $\zeta$ ) increased by the influence of wind and slope ( $\phi_w, \phi_s$ ).

$$\text{Heat source} = I_R \zeta (1 + \phi_w + \phi_s)$$

Reaction intensity ( $I_R$ ) is optimum reaction velocity ( $\Gamma'$ ) for the whole fuel bed times the effect of load ( $w_n$ ), heat content ( $h$ ), fuel moisture ( $\eta_M$ ), and mineral content ( $\eta_S$ ) for dead and live fuel.

$$I_R = \Gamma' \sum_i (w_n)_i h_i (\eta_M)_i (\eta_S)_i$$

The denominator (heat sink; Btu/ft<sup>3</sup>) is the heat required for ignition by the potential fuel. Bulk density ( $\rho_b$ ) represents the fuel array. The effective heating number ( $\varepsilon$ ) and the heat of preignition ( $Q_{ig}$ ) are particle properties.

$$\text{Heat sink} = \rho_b \varepsilon Q_{ig} = \rho_b \sum_i f_i \sum_j f_{ij} \varepsilon_{ij} (Q_{ig})_{ij}$$

### 5.1.1 Propagating Flux Ratio

Propagating flux ratio ( $\zeta$ ) indicates the proportion of the total heat produced in the combustion zone that actually preheats adjacent fuel particles to ignition. The no-wind no-slope propagating flux ( $(I_P)_0$ ) is reaction intensity ( $I_R$ ) times the propagating flux ratio ( $\zeta$ ).

Propagating flux ratio is a function of mean packing ratio ( $\beta$ ) and characteristic SAV ( $\sigma$ ). It tends toward 0 as either packing ratio or SAV decreases. Figure 4 shows the increase in propagating flux ratio with an increase in SAV for various packing ratios. Notice that propagating flux ratio increases more rapidly as SAV increases in tightly packed fuel such as litter than in loose fuel beds such as grass.

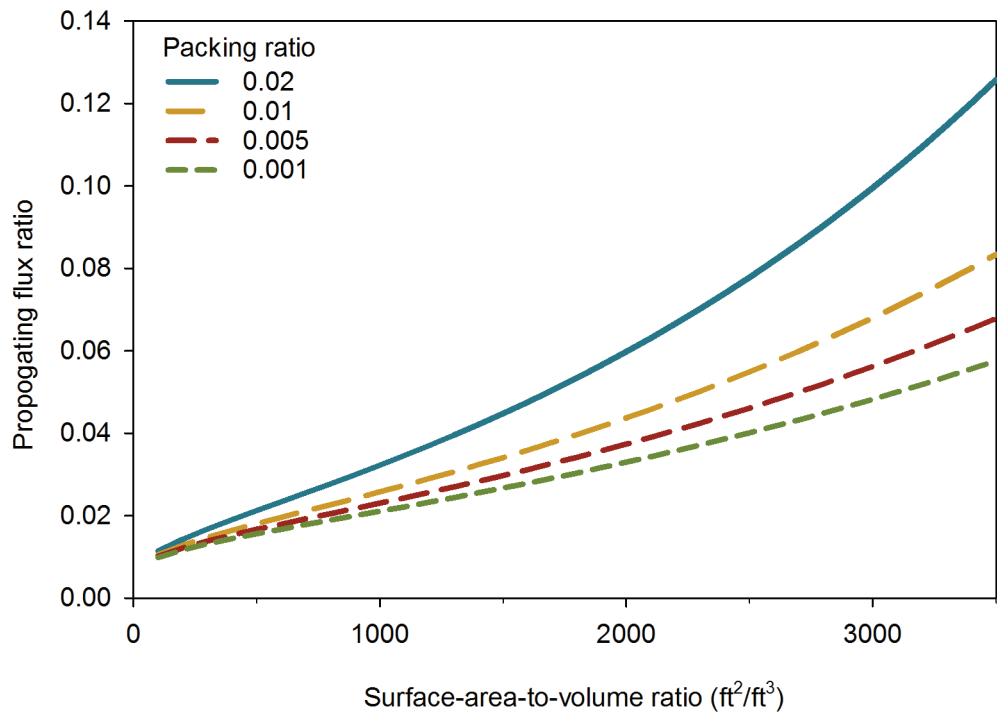


**Figure 4**—Propagating flux ratio is the proportion of heat produced in the combustion zone that actually contributes to fire propagation. It ranges from 0 to 20 percent depending on fuel particle size (SAV) and fuel bed compactness or packing ratio.

### 5.1.2 Optimum Reaction Velocity

Optimum reaction velocity ( $\Gamma'$ ) is a factor in reaction intensity. It is defined as the ratio of the efficiency of the fire to the reaction time. It is a measure of the rate of fuel consumption. It is a function of surface-area-to-volume ratio ( $\sigma$ ) and relative packing ratio ( $\beta/\beta_{op}$ ). A single value of reaction velocity is calculated for the fuel complex.

Packing ratio regulates the heat and airflow within the fuel array, dependent upon whether or not the space is occupied or vacant; ratio is therefore a mean value of all particle sizes. Surface-area-to-volume ratio (SAV) characterizes the particle size of the fuel complex that is regulating the combustion processes in the fire front; SAV is weighted by surface area.

Figure 5 shows that reaction velocity increases as relative packing ratio increases from 0 to 1, at which point reaction velocity is at a maximum. As packing ratio increases above optimum packing ratio (relative packing ratio increases above 1), reaction velocity decreases as the fuel is more tightly packed. Reaction velocity is higher for larger SAV, finer fuels.

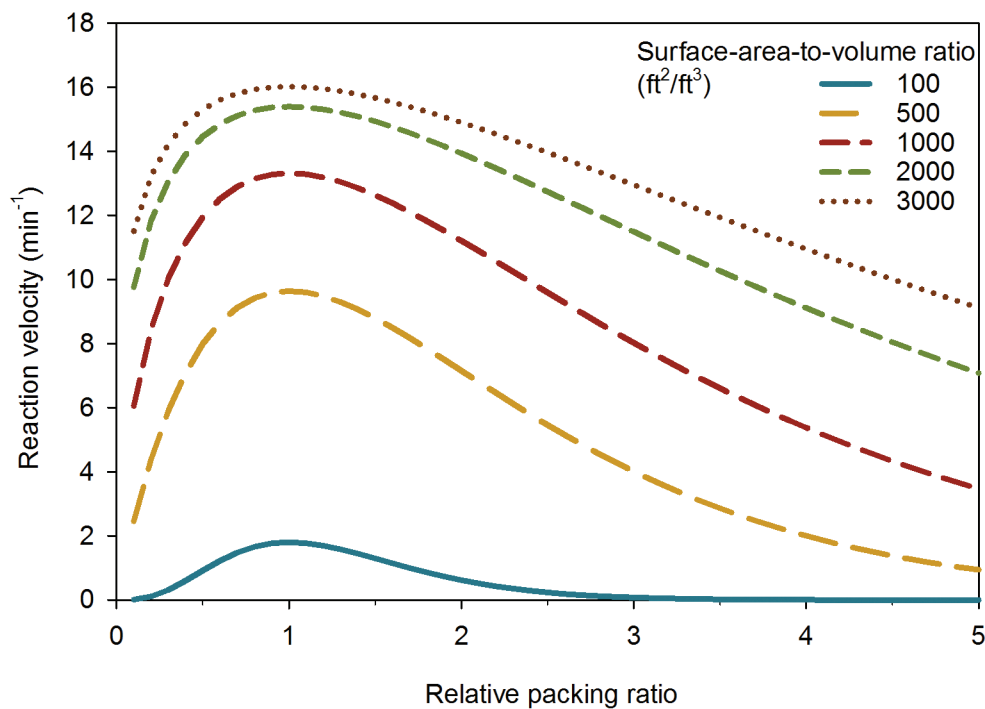


**Figure 5**—Reaction velocity is at a maximum when the fuel bed density is optimized to provide the best fuel-to-air ratio. This occurs when the relative packing ratio is one. Reaction velocity is higher for fine fuel.

### 5.1.3 Reaction Intensity

Reaction intensity ( $I_R$ ) is a measure of the energy release rate per unit area of combustion zone. There is no implication of where this energy is going; it is just a total energy production rate per unit area in the flaming zone.

All of the input variables except wind and slope are used to calculate reaction intensity. Reaction intensity increases with

- Increasing optimum reaction velocity,
- Increasing heat content,
- Decreasing mineral content,
- Decreasing fuel moisture, and
- Increasing moisture of extinction.

An example from Rothermel (1972, pages 37–38) compared reaction intensity and rate of spread for the initial 11 fuel models. “The closed timber litter and the short grass have similar and low reaction intensities. However, the rate of spread differs dramatically for the two models in the presence of wind; the grass has the highest rate of spread, the litter the lowest. This is attributed to the contrast in packing ratio of the two fuels ( $\beta = 0.001$  for grass, and  $\beta = 0.036$  for the litter). This example illustrates the common misconception that rate of spread and reaction intensity are directly related.” Figure 6 shows fuel model 8 (short needle litter) and fuel model 1 (short grass) with moisture of extinction changed to 30 percent to match the 1972 publication. Fuel moisture is 4 percent for rate of spread.

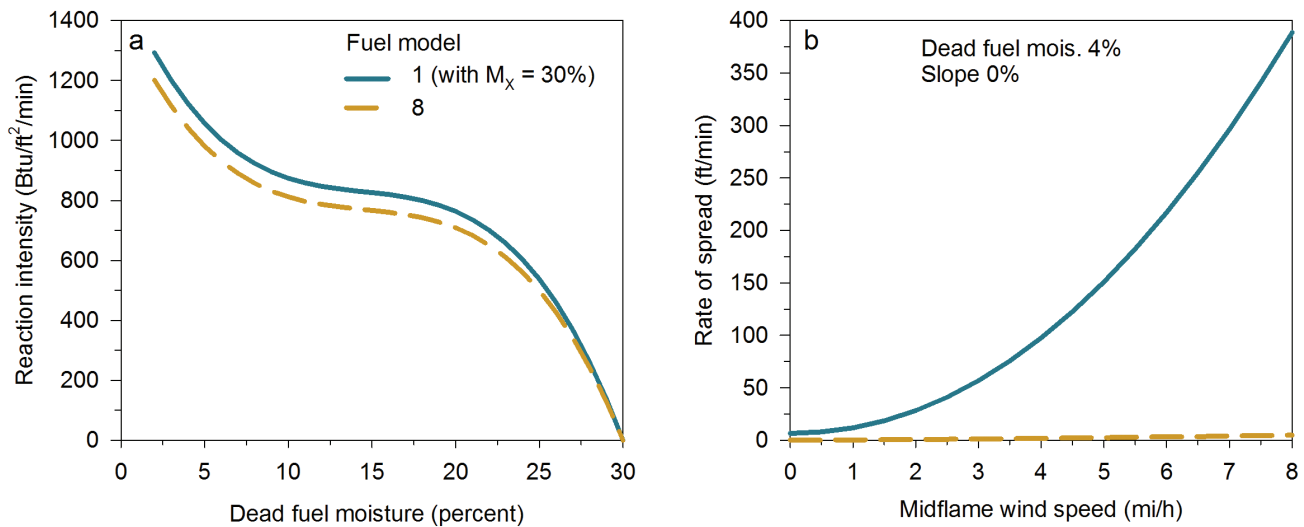


**Figure 6**—While (a) reaction intensity for fuel model 1 (with moisture of extinction 30 percent) and fuel model 8 are similar, there is a large difference in (b) rate of spread (dead fuel moisture 4 percent, 0 percent slope). The difference results from packing ratio, which is much higher for litter than for grass.

“Reaction velocity is the most revealing parameter in the model. If you extend the particle size to smaller and smaller quantities and reduce the packing ratio to describe dust in a silo, the result is explosive.” (Rothermel, Richard C., retired Missoula Fire Sciences Laboratory, personal communication, August 16, 2016).

### 5.1.4 Heat of Preignition

Heat of preignition ( $Q_{ig}$ ) is the heat required to bring a unit weight of fuel to ignition and is a linear function of fuel moisture (fig. 7). A value is calculated for each size class, live and dead. As moisture increases, heat of preignition and heat sink increases so rate of spread decreases.

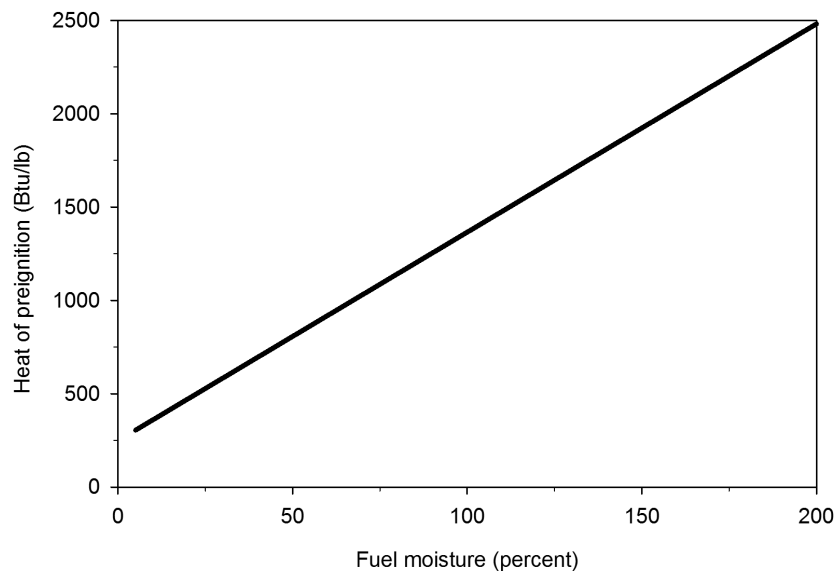


**Figure 7**—Heat of preignition is a function of fuel moisture. It is calculated for each size class, live and dead.

### 5.1.5 Effective Heating Number

Effective heating number ( $\epsilon$ ) is the portion of fuel per unit volume of fuel bed raised to ignition ahead of the advancing fire; it does not depend on heating rate. It is the efficiency of heating as a function of particle size (fig. 8). As SAV increases (finer fuel) effective heating number increases. Fifty percent of fuel with SAV 200  $\text{ft}^2/\text{ft}^3$  must be heated to ignition; 96 percent of fuel with SAV 3,000  $\text{ft}^2/\text{ft}^3$  is heated. As effective heating number increases, heat sink increases.

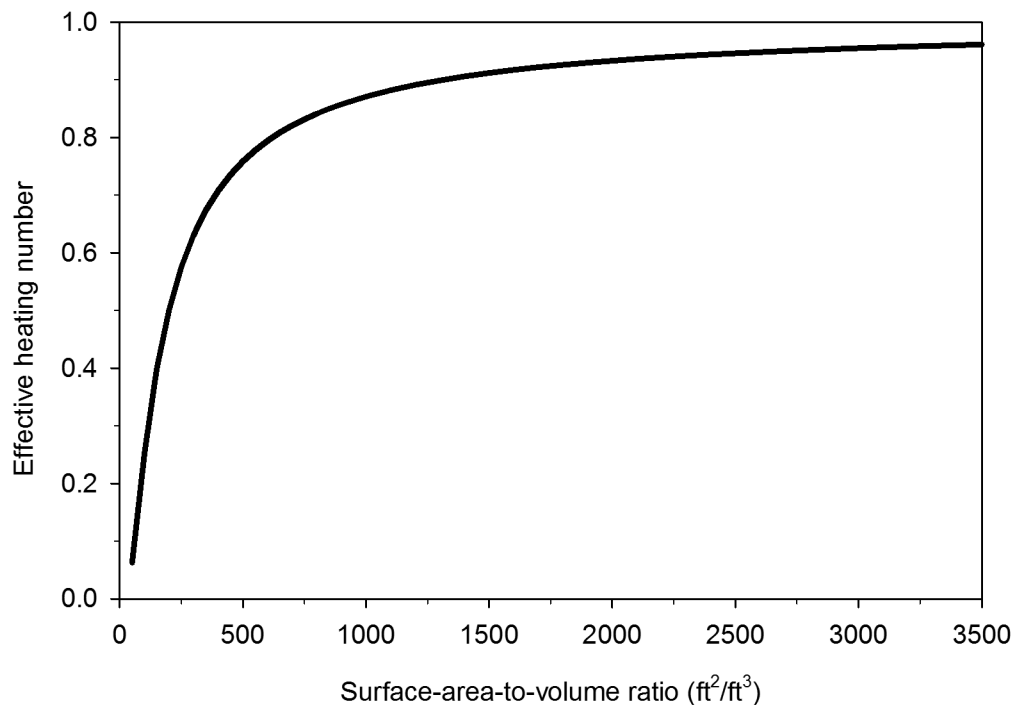


**Figure 8**—Effective heating number is a function of surface-area-to-volume ratio. It is the portion of fuel raised to ignition ahead of the advancing fire.

## 5.2 Fuel

Fuel is described for the Rothermel model by live and dead category and by size class as defined by surface-area-to-volume ratio. The fuel descriptors required by the model can be categorized as fuel particle properties (heat content, mineral content, and particle density) and fuel bed properties (surface-area-to-volume ratio, fuel load, depth, and dead fuel moisture of extinction). Each of these parameters is examined below.

Fuel particle properties are generally treated as constants and the number of size classes is generally limited to 1-h, 10-h, 100-h, live and dead herbaceous, and live herbaceous. These restrictions are due to implementation of the fire model, not the fire model itself. FIREMOD (Albini 1976a) provided full flexibility of the fire model. Developers of the special case fuel models for palmetto-gallberry (Hough and Albini 1978) and western aspen (Brown and Simmerman 1986) used FIREMOD to exercise the fire model and assign fuel model parameters. It is unfortunate that current systems don't provide that flexibility. It might be worthwhile, for example, to define a fuel model with several classes of fine dead fuel.

### **5.2.1 Fuel Models**

Rothermel (1972, page 35) defined a fire behavior fuel model as a “complete set of [fuel] inputs for the mathematical fire spread model.” Fire behavior fuel models are defined specifically for the Rothermel surface fire spread model. U.S. National Fire Danger Rating System equations and fuel models are described in section 7.

The value of fuel models was noted by Rothermel (1972, page 35):

Land managers can be trained to choose the fuel model that is most applicable to the fuels and climate for their areas of interest. If further refinement is desired, internal properties (e.g., fuel loading in logging slash, the ratio of dead-to-living fuel in brush, and the amount and type of understory in timber) for each fuel model could be tailored to permit the model to more closely match specific fuels.

The process of developing a custom fuel model is described by Burgan and Rothermel (1984). It involves collecting field data, exercising the fire model, and comparing results to observed fire behavior. It is not possible to simply use field data. Fuel model development is a modeling process. The need to develop custom fuel models was significantly reduced with the development of 40 additional standard fuel models (Scott and Burgan 2005).

Selecting a standard fuel model can be guided in part by photos (Anderson 1982; Scott and Burgan 2005) and the fuel model name. To avoid using a fuel model only for a specific vegetation or vegetation type, the 40 fuel models refer to fuel types. For example, fuel model 4 is “chaparral” while fuel model SH5 is “high load, dry climate shrub,” SH7 is “very high load, dry climate shrub,” and SH9 is “very high load, humid climate shrub.” A fuel model can be applied to many vegetation types.

Fuel model selection should be guided largely by examining modeled fire behavior. Scott and Burgan (2005, page 17) show rate of spread and flame length for each fuel model under various moisture and wind conditions with the direction to “use the charts to compare the relative behavior of the various models within a fuel type, but be aware that the relative behavior may be different at other moisture contents.”

Fire behavior for several fuel models can be plotted on the same axis for comparison (fig. 9). For fuel moistures 1-h 6 percent, 10-h 7 percent, 100-h 8 percent, and live woody 90 percent, fuel model 4 results in higher rate of spread and flame length than the SH (shrub) fuel models. SH5 has higher spread rate than does SH7 (very high load, dry climate shrub); flame lengths are similar. SH9 has lower spread rate and higher flame length than SH5.

It is especially important to examine fire behavior for a range of conditions for dynamic fuel models, which include a transfer of fuel from the live herbaceous to dead fuel as a representation of curing. The use of live fuel moisture to adjust the fuel model parameters in addition to the influence of live moisture in the model can lead to surprising results (Jolly 2007; Ziel and Jolly 2009).

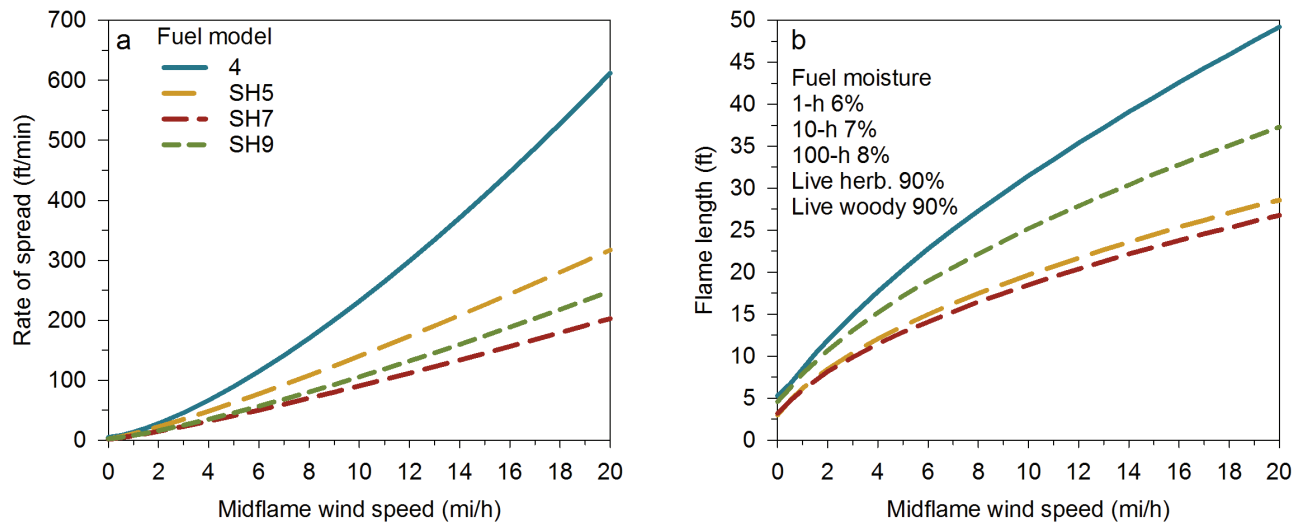


**Figure 9**—Comparison of (a) rate of spread and (b) flame length for fuel models 4, SH5, SH7, and SH9 for fuel moisture 1-hr 6 percent, 10-hr 7 percent, 100-hr 8 percent, live herbaceous 60 percent, and live woody 90 percent.

Consider fuel model GR2 (low load, dry climate grass) with dead fuel moisture 5 percent, midflame wind 6 mi/h, and 0 percent slope. Figure 10 shows rate of spread for live herbaceous fuel moisture 75 to 200 percent. For live herbaceous moisture of 90 percent, rate of spread is 24.1 ft/min. That is 3.7 times faster than for live herbaceous moisture of 100 percent (6.5 ft/min). For live herbaceous moisture greater than 120 percent, there is essentially no fire spread.

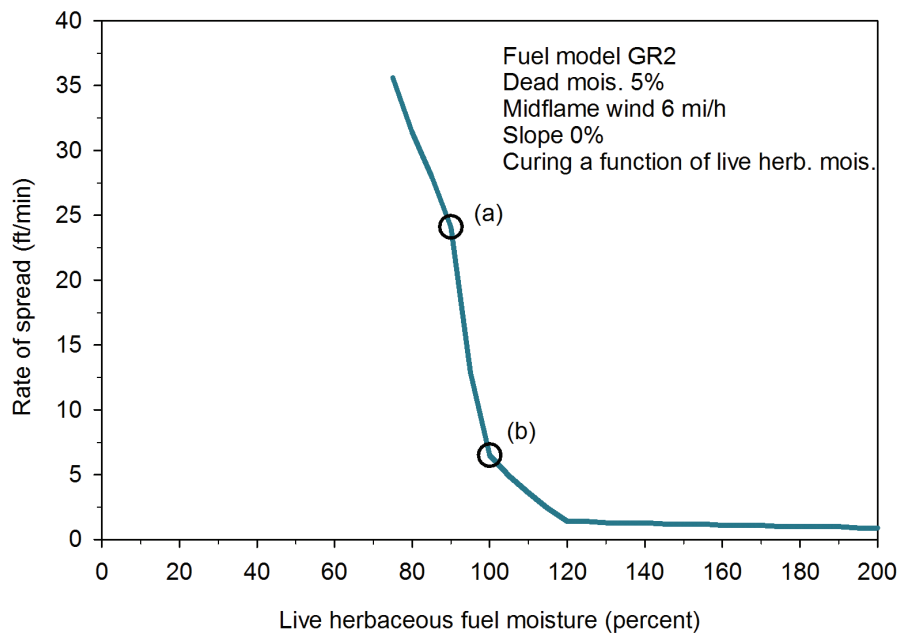


**Figure 10**—For dynamic fuel model GR2 (dead moisture 5 percent, midflame wind 6 mi/h, no slope) when live herbaceous moisture is used to determine curing, rate of spread is (a) 24.1 ft/min for live herbaceous moisture 90 percent and (b) 6.5 ft/min for live herbaceous moisture 100 percent.

The load transfer equation says that 100 percent live herbaceous moisture indicates vegetation is 22 percent cured and 90 percent moisture indicates vegetation is 33 percent cured. Andrews et al. (2006) showed that live fuel moisture may not be an appropriate indicator of curing. BehavePlus offers the option of directly specifying the level of curing rather than calculating it from live herbaceous fuel moisture. Figure 11 shows the results of specifying a curing level of 50 percent. In this case live herbaceous moisture plays a role in the fire model but does not also affect the fuel parameters. An increase in live herbaceous moisture from 90 to 100 percent reduces rate of spread from 31.3 to 29.1 ft/min.

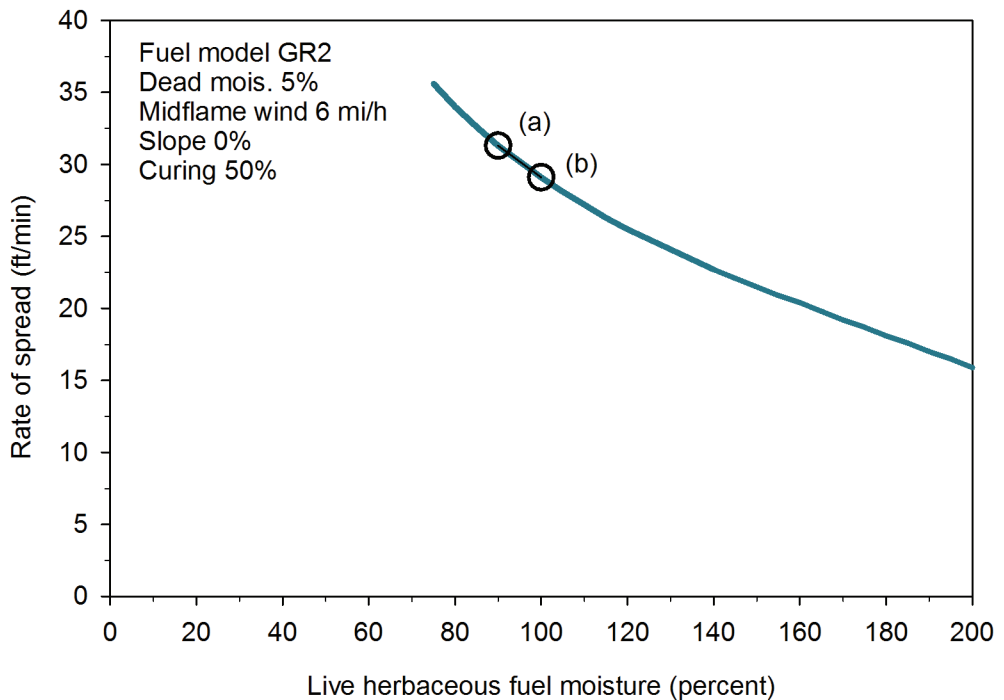


**Figure 11**—For dynamic fuel model GR2 (dead moisture 5 percent, midflame wind 6 mi/h, no slope) with curing set to 50 percent, the effect of live moisture on rate of spread is less than if curing is calculated from live herbaceous moisture (see fig. 10). Rate of spread is (a) 31.3 ft/min for live herbaceous moisture 90 percent and (b) 29.1 ft/min for live herbaceous moisture 100 percent.

### 5.2.2 Weighting Factors

The basic fire spread model is based on one size class of dead fuel. When there are several size classes of dead and live fuel, a method of weighting is used to define characteristic values to be used in the final calculations. The weighting puts most influence on the fine fuels. The model uses the  $f_{ij}$  and  $f_i$  weighting factors defined by Rothermel (1972) for all variables except net fuel load, which uses the  $g_{ij}$  factors defined by Albini (1976a).

The SAV class dividing points for the g-factors are 1,200, 192, 96, 49, and 16 ft<sup>2</sup>/ft<sup>3</sup>. The change from f-factor to g-factor has no effect if the fuel particles fall into those classes. This is the case for all static fuel models including the standard 13 fuel models and 23 of the set of 40 fuel models (table 12). Note the high weighting factors for 1-h fuel.

**Table 12**—Weighting factors for static standard fuel models.

Fuel model	Weighting factors						Fuel model	Weighting factors					
	$f_{ij} = g_{ij}$				$f_i$			$f_{ij} = g_{ij}$				$f_i$	
	1-h	10-h	100-h	Live herb. and woody	Dead	Live		1-h	10-h	100-h	Live herb. and woody	Dead	Live
1	1	0	0	0	1	0	SH7	0.80	0.18	0.02	1	0.38	0.62
2	0.98	0.02	0	1	0.89	0.11	SH8	0.80	0.19	0.01	1	0.22	0.78
3	1	0	0	0	1	0	TU2	0.89	0.09	0.02	1	0.87	0.13
4	0.95	0.04	0.01	1	0.58	0.42	TU4	1	0	0	1	0.72	0.28
5	0.97	0.03	0	1	0.41	0.59	TU5	0.92	0.07	0.01	1	0.74	0.26
6	0.89	0.09	0.02	0	1	0	TL1	0.85	0.10	0.05	0	1	0
7	0.88	0.10	0.02	1	0.80	0.20	TL2	0.90	0.08	0.02	0	1	0
8	0.94	0.03	0.02	0	1	0	TL3	0.76	0.18	0.06	0	1	0
9	0.99	0.01	0	0	1	0	TL4	0.78	0.13	0.10	0	1	0
10	0.94	0.03	0.02	1	0.68	0.32	TL5	0.85	0.10	0.05	0	1	0
11	0.77	0.17	0.06	0	1	0	TL6	0.97	0.03	0.01	0	1	0
12	0.75	0.19	0.06	0	1	0	TL7	0.60	0.15	0.24	0	1	0
13	0.76	0.18	0.06	0	1	0	TL8	0.98	0.01	0	0	1	0
SH2	0.90	0.09	0.01	1	0.33	0.67	TL9	0.96	0.03	0.01	0	1	0
SH3	0.69	0.31	0	1	0.11	0.89	SB1	0.82	0.09	0.09	0	1	0
SH4	0.93	0.07	0	1	0.31	0.69	SB2	0.94	0.05	0.01	0	1	0
SH5	0.92	0.08	0	1	0.39	0.61	SB3	0.97	0.03	0.01	0	1	0
SH6	0.93	0.07	0	1	0.51	0.49	SB4	0.95	0.03	0.01	0	1	0

The g-factors do come into play for dynamic fuel models where live herbaceous fuel is transferred to the dead herbaceous class. There are then two classes of dead fuel with SAV greater than 1,200 for 16 fuel models. Only fuel model SH9 (very high load, humid climate shrub) has 1-h and dead herbaceous fuel in different categories. The g-factors are also needed for the eight fuel models that have both live herbaceous and woody fuel with SAV greater than 1,200. Custom fuel models and special case fuel models may also require use of g-factors.

For the 17 dynamic fuel models in the set of 40, table 13 gives f-factors and g-factors for 100, 50, and 0 percent cured. The f- and g-factors are the same for 10-h and 100-h. For all but SH9, f- and g-factors are the same for dead herbaceous and 1-h fuel.

**Table 13a**—Weighting factors for dynamic standard fuel models for three levels of curing.

Fuel model	Percent cured	Weighting factors													
		$f_{ij}$							$g_{ij}$					$f_i$	
		Dead herb.	1-h	10-h	100-h	Live herb.	Live woody	Dead herb.	1-h	10-h	100-h	Live herb.	Live woody	Dead	Live
GR1	100	0.73	0.27	0	0	1	0	1	1	0	0	0	0	1	0
	50	0.58	0.42	0	0	1	0	1	1	0	0	1	1	0.63	0.37
	0	0	1	0	0	1	0	1	1	0	0	1	1	0.27	0.73
GR2	100	0.90	0.10	0	0	1	0	1	1	0	0	0	0	1	0
	50	0.82	0.18	0	0	1	0	1	1	0	0	1	1	0.55	0.45
	0	0	1	0	0	1	0	1	1	0	0	1	1	0.10	0.90
GR3	100	0.91	0.07	0.02	0	1	0	0.98	0.98	0.02	0	1	1	1	0
	50	0.83	0.13	0.04	0	1	0	0.96	0.96	0.04	0	1	1	0.54	0.46
	0	0	0.77	0.23	0	1	0	0.77	0.77	0.23	0	1	1	0.09	0.91
GR4	100	0.87	0.13	0	0	1	0	1	1	0	0	0	0	1	0
	50	0.77	0.23	0	0	1	0	1	1	0	0	1	1	0.56	0.44
	0	0	1	0	0	1	0	1	1	0	0	1	1	0.13	0.87
GR5	100	0.85	0.15	0	0	1	0	1	1	0	0	0	0	1	0
	50	0.73	0.27	0	0	1	0	1	1	0	0	1	1	0.57	0.43
	0	0	1	0	0	1	0	1	1	0	0	1	1	0.15	0.85
GR6	100	0.97	0.03	0	0	1	0	1	1	0	0	0	0	1	0
	50	0.94	0.06	0	0	1	0	1	1	0	0	1	1	0.51	0.49
	0	0	1	0	0	1	0	1	1	0	0	1	1	0.03	0.97
GR7	100	0.83	0.17	0	0	1	0	1	1	0	0	0	0	1	0
	50	0.71	0.29	0	0	1	0	1	1	0	0	1	1	0.58	0.42
	0	0	1	0	0	1	0	1	1	0	0	1	1	0.17	0.83
GR8	100	0.92	0.07	0.01	0	1	0	0.99	0.99	0.01	0	1	1	1	0
	50	0.85	0.13	0.02	0	1	0	0.98	0.98	0.02	0	1	1	0.54	0.46
	0	0	0.87	0.13	0	1	0	0.87	0.87	0.13	0	1	1	0.08	0.92
GR9	100	0.88	0.11	0.01	0	1	0	0.99	0.99	0.01	0	1	1	1	0
	50	0.79	0.20	0.01	0	1	0	0.99	0.99	0.01	0	1	1	0.56	0.44
	0	0	0.94	0.06	0	1	0	0.94	0.94	0.06	0	1	1	0.12	0.88

**Table 13b**—Weighting factors for dynamic standard fuel models for three levels of curing.

Fuel model	Percent cured	Weighting factors														
		$f_{ij}$						$g_{ij}$					$f_i$			
		Dead herb.	1-h	10-h	100-h	Live herb.	Live woody	Dead herb.	1-h	10-h	100-h	Live herb.	Live woody	Dead	Live	
GS1	100	0.69	0.31	0	0	0	1	1	1	0	0	0	0	0	0.53	0.47
	50	0.53	0.47	0	0	0.28	0.72	1	1	0	0	1	1	0.34	0.66	
	0	0	1	0	0	0.43	0.57	1	1	0	0	1	1	0.16	0.84	
GS2	100	0.51	0.47	0.03	0	0	1	0.97	0.97	0.03	0	0	0	0.54	0.46	
	50	0.34	0.63	0.03	0	0.23	0.77	0.97	0.97	0.03	0	1	1	0.40	0.60	
	0	0	0.95	0.05	0	0.38	0.63	0.95	0.95	0.05	0	1	1	0.27	0.73	
GS3	100	0.80	0.19	0.01	0	0	1	0.99	0.99	0.01	0	0	0	0.59	0.41	
	50	0.67	0.31	0.02	0	0.37	0.63	0.98	0.98	0.02	0	1	1	0.35	0.65	
	0	0	0.95	0.05	0	0.54	0.46	0.95	0.95	0.05	0	1	1	0.12	0.88	
GS4	100	0.61	0.39	0	0	0	1	1	1	0	0	0	0	0.44	0.56	
	50	0.44	0.56	0.01	0	0.19	0.81	0.99	0.99	0.01	0	1	1	0.30	0.70	
	0	0	0.99	0.01	0	0.32	0.68	0.99	0.99	0.01	0	1	1	0.17	0.83	
SH1	100	0.34	0.63	0.03	0	0	1	0.97	0.97	0.03	0	0	0	0.28	0.72	
	50	0.20	0.76	0.04	0	0.06	0.94	0.96	0.96	0.04	0	1	1	0.23	0.77	
	0	0	0.95	0.05	0	0.11	0.89	0.95	0.95	0.05	0	1	1	0.18	0.82	
SH9	100	0.43	0.53	0.04	0	0	1	0.53	0.43	0.04	0	0	0	0.38	0.62	
	50	0.28	0.67	0.05	0	0.12	0.88	0.67	0.28	0.05	0	1	1	0.30	0.70	
	0	0	0.93	0.07	0	0.21	0.79	0.93	0	0.07	0	1	1	0.22	0.78	
TU1	100	0.40	0.44	0.11	0.05	0	1	0.84	0.84	0.11	0.05	0	0	0.38	0.62	
	50	0.25	0.55	0.14	0.06	0.11	0.89	0.80	0.80	0.14	0.06	1	1	0.31	0.69	
	0	0	0.74	0.18	0.08	0.20	0.80	0.74	0.74	0.18	0.08	1	1	0.23	0.77	
TU3	100	0.34	0.65	0.01	0	0	1	0.99	0.99	0.01	0	0	0	0.66	0.34	
	50	0.21	0.79	0.01	0	0.25	0.75	0.99	0.99	0.01	0	1	1	0.55	0.45	
	0	0	0.99	0.01	0	0.40	0.60	0.99	0.99	0.01	0	1	1	0.44	0.56	

As an illustration of the difference between f- and g-factors, consider the effect on net fuel load for dynamic fuel model SH1 (low load, dry climate shrub), 50 percent cured (table 14). For simplification of this example, SAV for live woody is changed from 1,600 to 1,800 ft<sup>2</sup>/ft<sup>3</sup> and 1-h from 2,000 to 1,800 ft<sup>2</sup>/ft<sup>3</sup> so that all fine fuels have the same SAV. (Results are nearly the same for the unchanged SAV.) For fine dead fuels (1-h and dead herbaceous), the original calculation of net load uses  $f_{ij}$  for each, while the  $g_{ij}$  combines the  $f_{ij}$  (0.74 + 0.22 = 0.96). Similarly for live herbaceous and woody fuels (0.05 + 0.95 = 1.00). Oven-dry load is a fuel model parameter. Total net load is calculated in the model using the weighting factors. Note that total net load is higher with the g-factors (1.60 ton/ac) than it would have been with the f-factors (1.36 ton/ac).

**Table 14**—Comparison of *f* and *g* factors and resulting net fuel load for fuel model SH1 (50 percent cured) adjusted so all fine fuels have SAV 1,800 ft<sup>2</sup>/ft<sup>3</sup> to simplify calculations for illustration.

Fuel class	SAV	Oven-dry	<i>f<sub>ij</sub></i>	Net	<i>g<sub>ij</sub></i>	Net
	----ft <sup>2</sup> /ft <sup>3</sup> ----	load		load		load
1-h	1,800	0.25	0.74	0.17	0.96	0.23
10-h	109	0.25	0.04	0.01	0.04	0.01
100-h	--	0	0	0	0	0
Dead herb	1,800	0.07	0.22	0.02	0.96	0.07
Live herb	1,800	0.08	0.05	0.00	1.00	0.07
Live woody	1,800	1.30	0.95	1.15	1.00	1.23
Dead		0.57		0.20		0.30
Live		1.38		1.16		1.30
Total		1.95		1.36		1.60

While the *g*-factors resolve some problems, there remain issues resulting from discrete classes for the *g*-factors. There is a step change when moving from one class to another. This problem can be avoided with proper development of custom and special case fuel models by assuring that the SAV of 1-h and herbaceous fuels are in the same *g*-factor class.

Consider two classes of fine fuel with the same SAV compared with SAV almost the same but in different *g*-factor classes. Again start with fuel model SH1, changing live and dead herbaceous fuel SAV to 1,199 ft<sup>2</sup>/ft<sup>3</sup>. Figure 12a shows a range of 1-h SAV from 700 to 2,000 ft<sup>2</sup>/ft<sup>3</sup> and calculated rate of spread for dead fuel moisture 5 percent, live moisture 60 percent, midflame wind 6 mi/h, and slope 20 percent. When 1-h SAV crosses the 1,200 ft<sup>2</sup>/ft<sup>3</sup> *g*-factor class boundary, there is a drop in rate of spread. Compare this to live and dead herbaceous fuel SAV of 1,201 ft<sup>2</sup>/ft<sup>3</sup> (fig. 12b). Rate of spread is higher if the fine fuels are in the same class (1-h SAV >1,200 ft<sup>2</sup>/ft<sup>3</sup>) and lower when they are in different classes (1-h SAV <1,200 ft<sup>2</sup>/ft<sup>3</sup>).

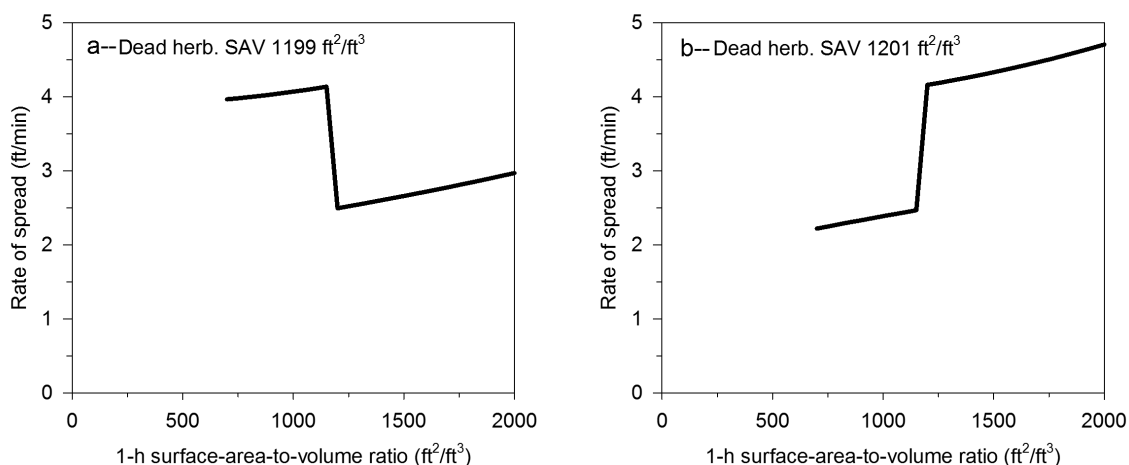


**Figure 12**—Rate of spread for a range of 1-h SAV and dead herbaceous (a) SAV = 1199 ft<sup>2</sup>/ft<sup>3</sup> and (b) SAV = 1201 ft<sup>2</sup>/ft<sup>3</sup>. The step change at SAV 1200 ft<sup>2</sup>/ft<sup>3</sup> results from 1-h SAV moving from one *g*-factor class to the other. If 1-h and dead herbaceous fuel are in the same class, rate of spread is higher.

### 5.2.3 Fuel Particle Properties

The intrinsic fuel particle properties are particle density, mineral content, and heat content. These are properties of the fuel particle itself, not fuel size, shape, quantity, or arrangement. While the fire model allows these parameters to vary, they are generally treated as constants.

#### 5.2.3.1 Particle Density

Packing ratio ( $\beta$ ) is the portion of the fuel array volume that is occupied by fuel. Packing ratio is bulk density ( $\rho_b$ ) divided by particle density ( $\rho_p$ ). As particle density increases, packing ratio decreases. Particle density plays a role via packing ratio in each of the components of the numerator. Propagating flux ratio ( $\zeta$ ) and reaction intensity ( $I_R$ ) decrease with increasing particle density. Wind factor and slope factor ( $\phi_w, \phi_s$ ) increase with increasing particle density. If there is no wind or slope, rate of spread decreases with increasing particle density. When there is wind or slope, rate of spread generally increases because of the strong influence of the wind and slope factors (fig. 13). The effect of particle density was not experimentally tested (Richard C. Rothermel, retired Missoula Fire Sciences Laboratory, personal communication, August 16, 2016).

The influence of particle density on calculated rate of spread is minor; note the scale of the plots in figure 13. A value of 32 lb/ft<sup>3</sup> is used for all standard and custom fire behavior fuel models. However, other values have been used. For example, in their special case palmetto-gallberry fuel model, Hough and Albini (1978) used 30 lb/ft<sup>3</sup> for dead fuel and 46 lb/ft<sup>3</sup> for live fuel.

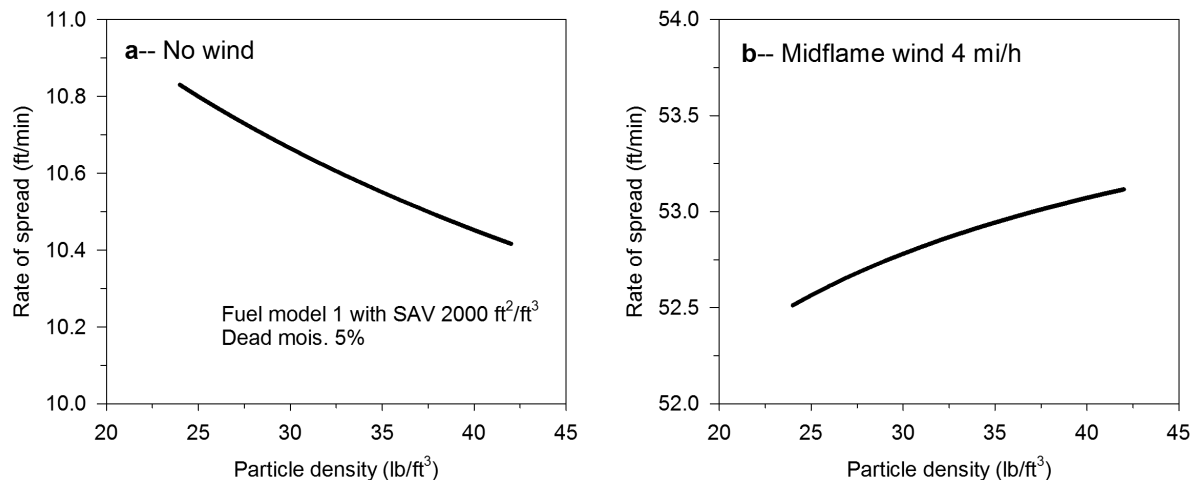


**Figure 13**—Effect of particle density on rate of spread for no wind and 4 mi/h midflame wind. Fuel model 1 with SAV changed to 2000 ft<sup>2</sup>/ft<sup>3</sup> (dead moisture 5 percent). The effect is minor. Note the scale of the x-axis, rate of spread.

### 5.2.3.2 Mineral Content

The quantity and type of inorganic material in the fuel affects the rate at which it burns. Total mineral content is quantified as pounds of minerals per pound of wood and is used to find net fuel load from oven-dry fuel load. For total mineral content of 0.0555, oven-dry fuel load is multiplied by  $1 - 0.0555 = 0.9445$ , a reduction of 5.55 percent.

Effective mineral content is defined as silica-free minerals per pound of wood. Increasing mineral content reduces reaction intensity and therefore rate of spread. Mineral damping coefficient is a function of effective mineral content (fig. 14). For effective mineral content of 0.010, the mineral damping coefficient is 0.4174.

All standard fire behavior fuel models use 0.0555 for total mineral content and 0.01 for effective mineral content. However, other values have been used. For example, in their special case palmetto-gallberry fuel model, Hough and Albin (1978) used 0.030 for total mineral content, and for effective mineral content they used 0.010 for dead fuel and 0.015 for live fuel.

### 5.2.3.3 Heat Content

Heat content enters into the spread rate calculations as a factor in the numerator (heat source). Higher heat content values increase the reaction intensity and therefore rate of spread. Net load ( $w_n$ ) multiplied by heat content ( $h$ ) is the total energy that could be obtained by burning all of the fuel.

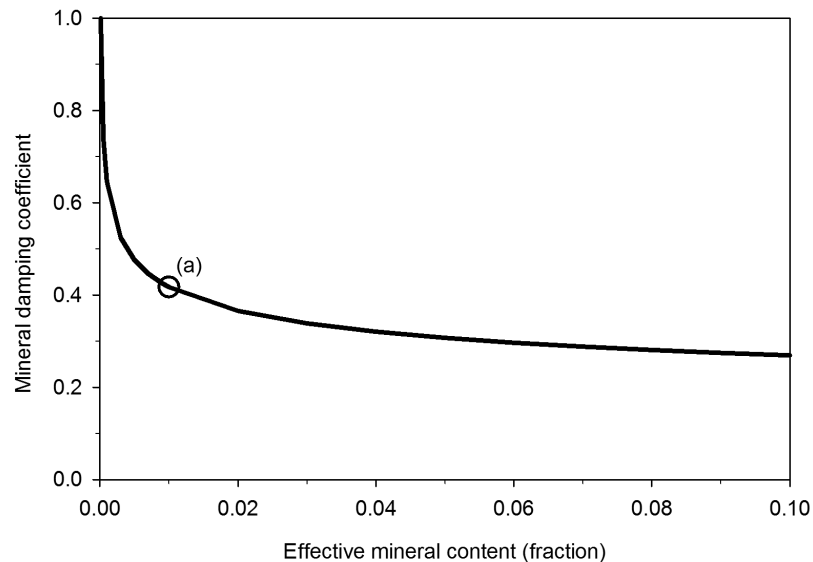


**Figure 14**—Mineral damping coefficient as a function of effective mineral content. Mineral damping coefficient is (a) 0.4174 for effective mineral content 0.010, the commonly used value.

While there is no verification of the role of volatiles, heat content is sometimes used to refine custom fuel models. According to Burgan and Rothermel (1984, page 32), “The heat content is lowest for those fuels with few volatiles—oils and waxes—and higher for those with more of them. Fuels having higher heat contents have more heat available per pound of fuel.”

The 53 standard fuel models all use heat content of 8,000 Btu/lb. Other values for live and dead fuel can be used for custom fuel models. Hough and Albini (1978) used 8,300 Btu/lb for their special case palmetto-gallberry fuel model.

Consider the effect of changing heat content for fuel model 5 (brush) from 8,000 Btu/lb to live and dead heat content ranging from 6,000 to 12,000 Btu/lb. The linear effect of a change in the heat content values on spread rate is shown in figure 15.

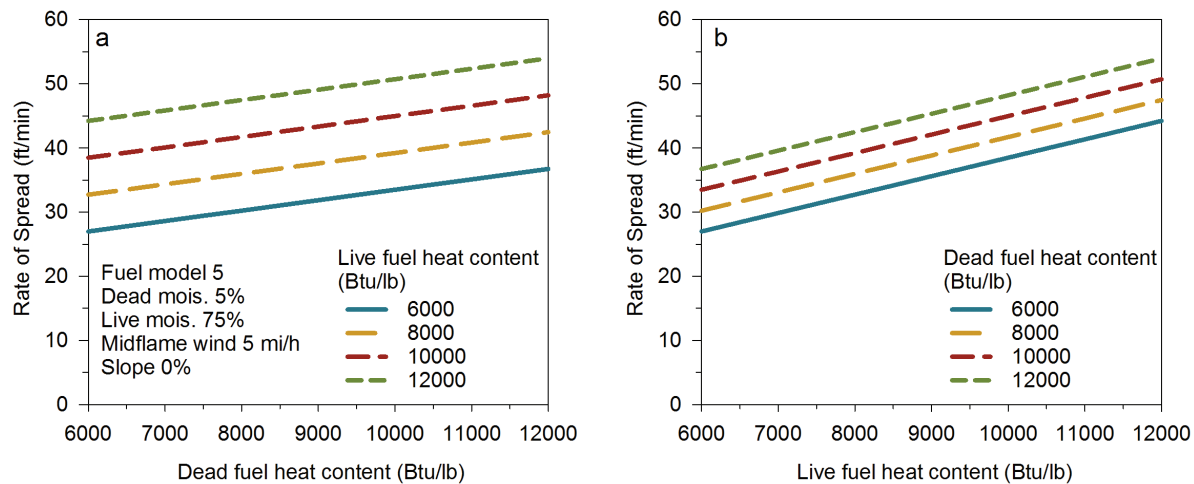


**Figure 15**—Heat content for dead and live fuel has a linear effect on rate of spread, shown for fuel model 5 (dead moisture 5 percent, live moisture 75 percent, midflame wind 5 mi/h, 0 percent slope).

### 5.2.4 Fuel Bed Properties

The fuel bed parameters are surface-area-to-volume ratio, fuel bed depth, and fuel load. Dead fuel moisture of extinction, the fourth parameter, is addressed in the fuel moisture section.

A single value for fuel bed depth is specified. Load and SAV are defined for each size class, live and dead. Values for each class and category are used to calculate characteristic values for the fuel bed: surface-area-to-volume ratio, bulk density, mean packing ratio, and relative packing ratio.

#### 5.2.4.1 Surface-Area-to-Volume Ratio

In the fire model, sizes are characterized by surface-area-to-volume ratio ( $\sigma$ ). Table 15 shows fuel particle diameter in inches associated with selected SAV values.

**Table 15**—Relationship between fuel particle diameter and surface-area-to-volume ratio.

<b>Diameter</b>	<b>SAV</b>
-----inches-----	-----feet <sup>2</sup> /feet <sup>3</sup> -----
0.014	3,500
0.024	2,000
0.04	1,200
0.06	750
0.25	192
0.44	109
0.50	96
1.00	48
1.60	30
3.00	16

Table 16 shows the defined diameter and associated SAV for 1-h, 10-h, and 100-h fuels; values for the standard fuel models are given. One-hour fuels are defined as 0 to ¼ inch diameter. SAV for 1-h fuel for the 53 fuel models ranges from 3,500 to 750 ft<sup>2</sup>/ft<sup>3</sup>. Ten-hour fuels are ¼-1 inch, which corresponds to an SAV of 192 to 48 ft<sup>2</sup>/ft<sup>3</sup>; a value of 109 ft<sup>2</sup>/ft<sup>3</sup> is used for 10-h fuel.

One-hour SAV for fuel model 1 (short grass) is 3,500 ft<sup>2</sup>/ft<sup>3</sup>, which is equivalent to a diameter of 0.014 in. Compare this to ¼ inch (0.25) diameter fuel with SAV of 192 ft<sup>2</sup>/ft<sup>3</sup>. Standard and custom fuel models have one class of 1-h fuel. Given the wide range of possible 1-h SAV, it might have been better to allow more than one class of 1-h fuel.

Characteristic SAV includes both dead and live fuel. The characteristic SAV for the 53 fuel models ranges from 3,500 to 1,144 ft<sup>2</sup>/ft<sup>3</sup>. Although 10-h SAV is 109 ft<sup>2</sup>/ft<sup>3</sup> and 100-h is 30 ft<sup>2</sup>/ft<sup>3</sup>, the lowest characteristic SAV is 1,144 ft<sup>2</sup>/ft<sup>3</sup>, illustrating that the weighting method puts most weight on fine fuel.

As SAV increases (finer fuels), reaction intensity, propagating flux ratio, wind and slope coefficients, and effective heating number all increase. Heat source therefore increases with increasing SAV. Heat sink also increases with increasing SAV. In general, the effects in the numerator will dominate, so the spread rate tends to increase.

**Table 16**—Diameter and surface-area-to-volume ratio associated with dead fuel size classes of standard fire behavior fuel models.

<b>Fuel size class</b>	<b>Size class definition</b>	<b>Associated SAV</b>	<b>Standard fuel model SAV</b>
	-----Inches-----	-----feet <sup>2</sup> /feet <sup>3</sup> -----	-----feet <sup>2</sup> /feet <sup>3</sup> -----
1-h	< ¼	>192	3,500 - 750
10-h	¼ - 1	192 - 48	109
100-h	1 - 3	48 - 16	30

Flame residence time decreases with increasing SAV. Heat per unit area ( $H_A$ ) is the product of reaction intensity and flame residence time, which have opposing influences. Response of heat per unit area to SAV depends on the relative values of the factors.

Consider fuel model 1 (short grass), which has single size class of dead fuel with SAV of  $3,500 \text{ ft}^2/\text{ft}^3$ . Figure 16 shows the effect of a range of SAV from 500 to  $3,500 \text{ ft}^2/\text{ft}^3$  (dead moisture 6 percent, midflame wind speed 4 mi/h, 0 slope) on rate of spread, reaction intensity, flame residence time and heat per unit area. Note that heat per unit area increases, then decreases with increasing SAV because of the effects of increasing reaction intensity and decreasing residence time.

#### 5.2.4.2 Fuel Bed Depth

The fire model requires a single value for fuel bed depth and it is sensitive to that input. Depth is a hard parameter to quantify, given the variation in real-world fuel. Defining a value for fuel bed depth is therefore part of the “fuel modeling” process. Strong reliance on a parameter that is hard to characterize is a weakness of the surface fire spread model.

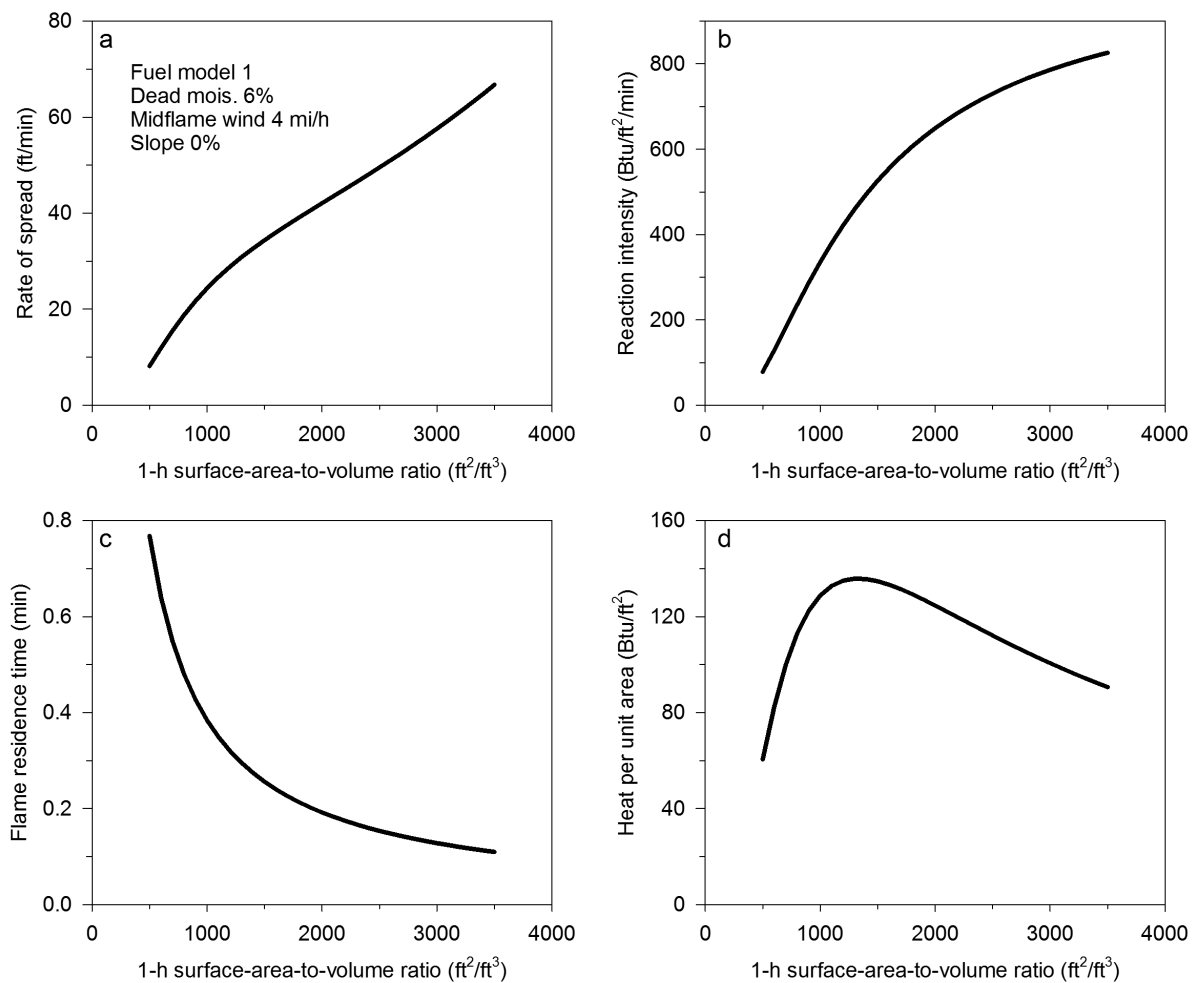


**Figure 16**—Effect of 1-hr SAV on (a) rate of spread, (b) reaction intensity, (c) flame residence time, and (d) heat per unit area for fuel model 1, dead moisture 6 percent, midflame wind 4 mi/h, no slope.

Fuel bed depth plays a role in the fire model through bulk density (fuel load divided by fuel bed depth) and packing ratio (bulk density divided by particle density). Increasing depth reduces packing ratio, thereby increasing wind and slope factors. Increasing depth also reduces heat sink. These influences both increase rate of spread.

Increasing depth increases propagating flux and therefore reaction intensity if the packing ratio is greater than optimum and decreases if the packing ratio is less than optimum. Thus a change in depth may either increase or decrease the heat source term.

Fuel model SB4 (high load blowdown) has packing ratio 0.00744, which is close to the optimum packing ratio of 0.006896. Relative packing ratio is 1.07996. Depth for this fuel model is 2.7 ft. Figure 17 shows the effect of depth values from 0.5 to 6 ft (dead fuel moisture 4 percent, no wind or slope). Reaction intensity increases to the point of optimum packing ratio, then decreases. In this case, the relative values of heat source and heat sink result in increasing rate of spread with increasing depth.

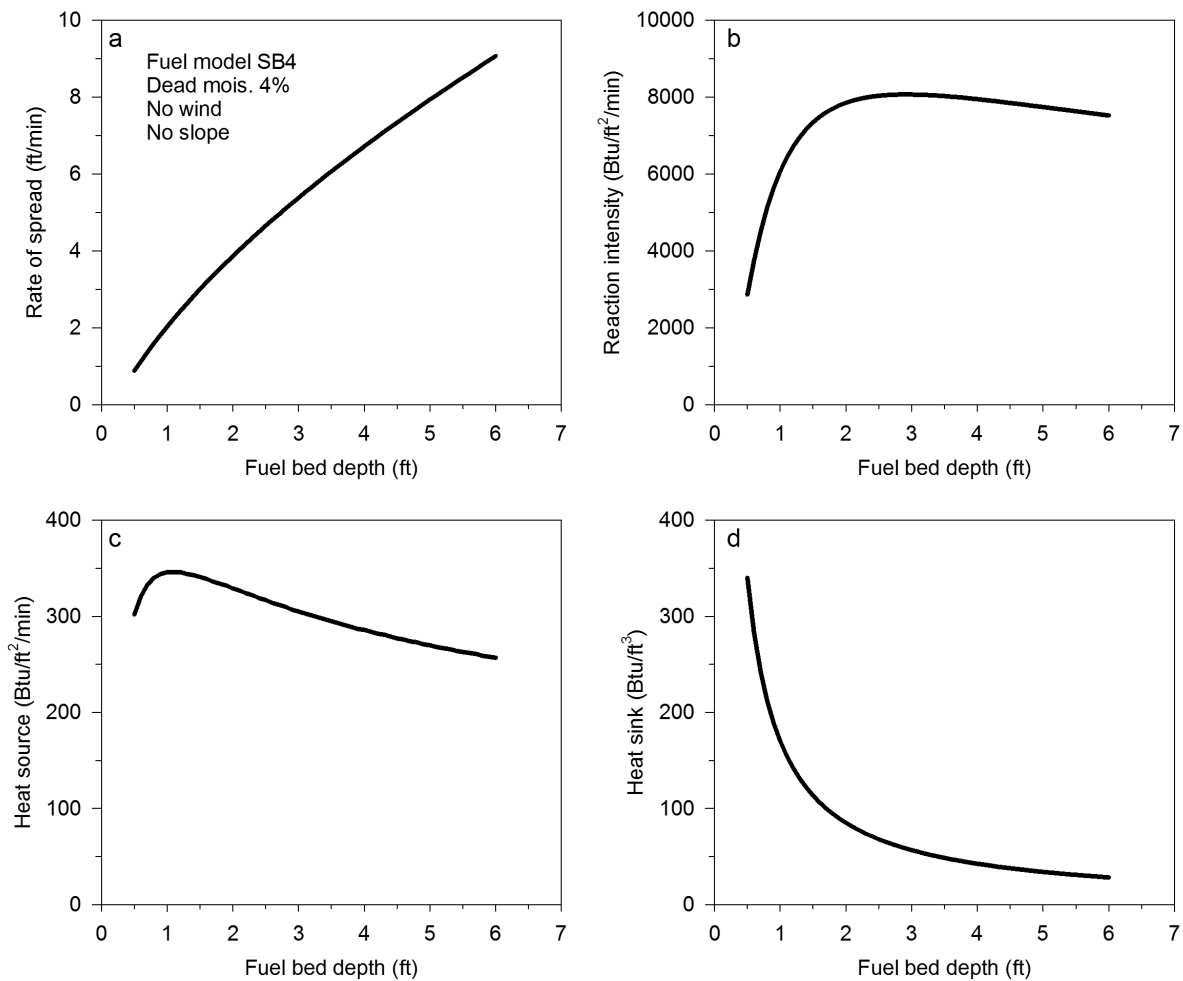


**Figure 17**—Effect of depth on (a) rate of spread, (b) reaction intensity, (c) heat source, and (d) heat sink for fuel model SB4, dead moisture 4 percent, no wind, no slope.

### 5.2.4.3 Fuel Load

Fuel load is the weight of fuel for an area on the ground ( $\text{lb}/\text{ft}^2$  or  $\text{tons}/\text{ac}$ ). A value for oven-dry fuel load is specified for each size class, live and dead. Adjustment of fuel load values for dynamic fuel models is done prior to fire spread model calculations. The total oven-dry load, including live and dead fuel, is used to determine bulk density and packing ratio. Net fuel load is total load reduced by the total ash content. Live and dead net load are used to find reaction intensity. Figure 18 shows the relationship between total oven-dry load and total net load for the 53 fuel models. Fuel model 13 has total oven-dry load of 58  $\text{tons}/\text{ac}$  and total net load of 10.6  $\text{tons}/\text{ac}$ .

Consider an example where the total oven-dry load is 2  $\text{tons}/\text{ac}$ , with that load separated four ways: all load in 1-h, half in 1-h and 10-h, most in 10-h, and all in 10-h (table 17). Bulk density and packing ratio are based on total oven-dry load and

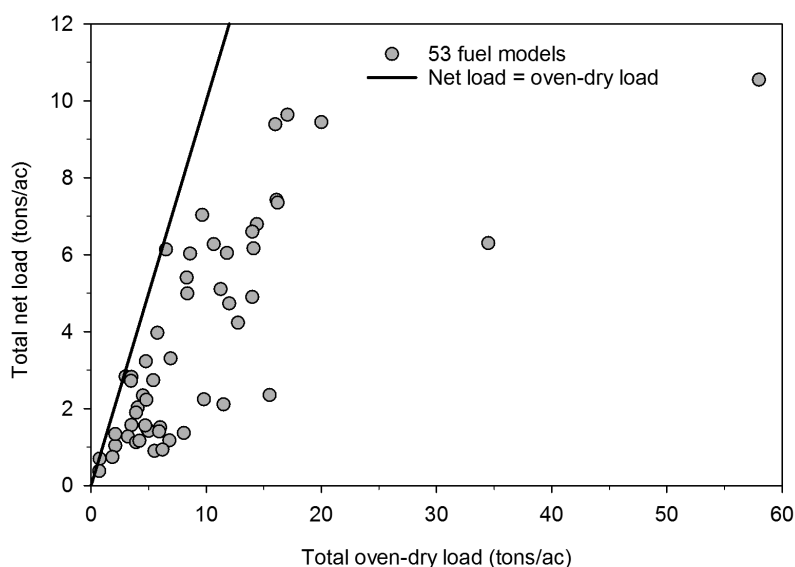


**Figure 18**—Total net load compared to total oven-dry load for the 53 standard fuel models. The line indicates total net load equal to total oven-dry load.

**Table 17**—The effect of dividing a total fuel load of 2  $\text{tons}/\text{ac}$  into 1-h and 10-h classes<sup>a</sup>.

Total oven-dry load <i>ton/ac</i>	1-h load <i>ton/ac</i>	10-h load <i>ton/ac</i>	Bulk density <i>lb/ft<sup>3</sup></i>	Packing ratio	Characteristic SAV <i>ft<sup>2</sup>/ft<sup>3</sup></i>	Optimum packing ratio	Relative packing ratio	Wind factor	Rate of spread <i>ft/min</i>
2	2	0	0.0918	0.0029	2,500	0.0055	0.5195	17.8	81.6
2	1	1	0.0918	0.0029	2,400	0.0057	0.5025	17.9	40.2
2	0.1	1.9	0.0918	0.0029	1,417	0.0088	0.3263	20.8	32.0
2	0	2	0.0918	0.0029	109	0.0718	0.0399	81.9	0

<sup>a</sup>1-h SAV 2,500  $\text{ft}^2/\text{ft}^3$ , 10-h SAV 109  $\text{ft}^2/\text{ft}^3$ , depth 1 ft, moisture of extinction 20 percent, dead fuel moisture 5 percent, midflame wind speed 5  $\text{mi}/\text{h}$ , no slope.

are therefore the same for the four cases. Optimum packing ratio is a function of characteristic SAV, which depends on the loads in each class. Even a small amount of 1-h fuel is very different from no fuel in the 1-h category because of the fuel weighting calculations. Relative packing ratio is almost 10 times higher (0.3263 vs. 0.0399) for 0.1 ton/ac of 1-h fuel than for no 1-h fuel. Rate of spread is more than double (81.6 vs. 40.2 ft/min) for 2 tons/ac in the 1-h class and none in the 10-h class than for 1 ton/ac in each class.

Fuel load affects every component of the fire spread model through net load, bulk density, and packing ratio. In the heat sink term as load increases, bulk density and heat sink increase because more fuel must be raised to ignition temperature. Increasing net load increases the heat source term. But optimum reaction velocity is also in the heat source term. It increases then decreases with increasing load, as the fuel bed becomes more tightly packed.

The result of the multiple effects of fuel load can be seen in an example with 1-h load ranging from 0.05 to 1 ton/acre and 10-h load of 0, 1, and 2 ton/ac (fig. 19).

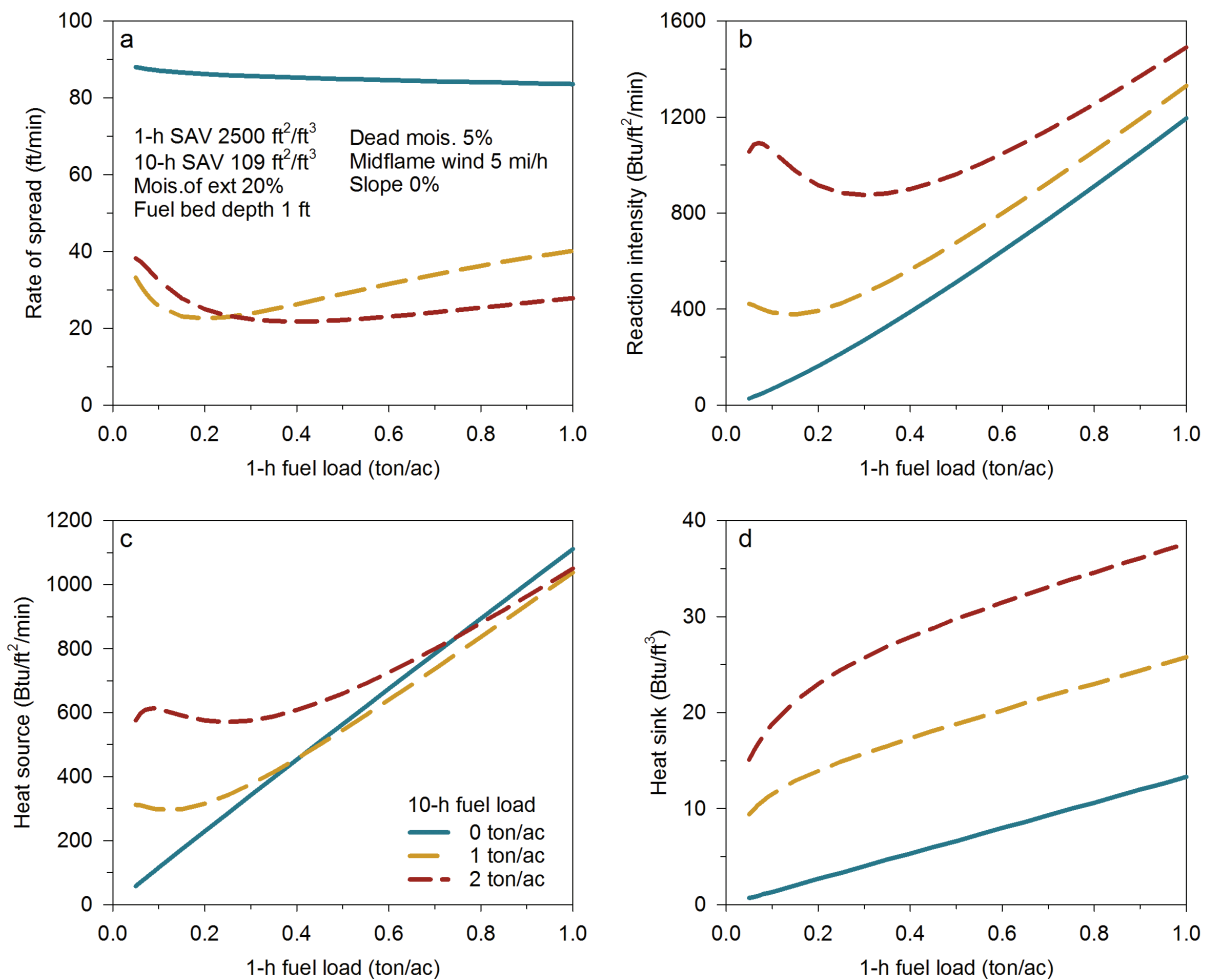


**Figure 19**—The result of multiple influences of changing fuel load is shown in plots for a range of 1-hr load and three values of 10-hr load (1-hr SAV 2,500 ft<sup>2</sup>/ft<sup>3</sup>, 10-hr SAV 109 ft<sup>2</sup>/ft<sup>3</sup>, moisture of extinction 20 percent, fuel bed depth 1 ft, dead moisture 5 percent, midflame wind 5 mi/h, 0 percent slope).

#### 5.2.4.4 Bulk Density

Bulk density ( $\rho_b$ ) is the amount of oven-dry fuel per cubic foot of fuel bed. It is the total oven-dry load divided by the depth. For a given depth, bulk density increases with increasing load. For a given load, bulk density decreases with increasing depth.

Bulk density for the 53 fuel models ranges from 0.034 lb/ft<sup>3</sup> for fuel model 1 (short grass) to 1.56 lb/ft<sup>3</sup> for fuel model TL1 (low load, compact conifer litter). Load vs. depth is plotted for the 53 standard fuel models, with lines indicating various bulk densities (fig. 20). The grass (GR) and timber litter (TL) fuel models are highlighted. Note the low bulk densities for vertically oriented grass fuels and higher bulk densities for the horizontally oriented compact litter fuels.

Figure 21 shows the relationship between heat sink and bulk density (via load and depth). As bulk density increases (for constant SAV and moisture), heat sink increases. This example uses one size class of dead fuel with SAV of 2,000 ft<sup>2</sup>/ft<sup>3</sup> and 5 percent fuel moisture.

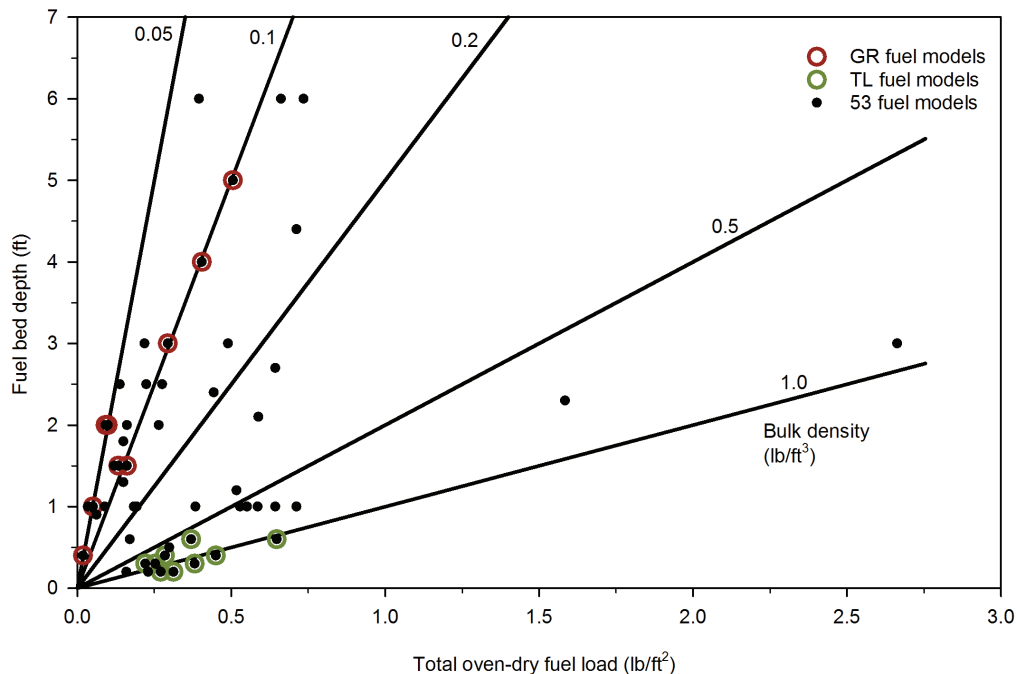


**Figure 20**—Fuel bed depth vs. total oven-dry load for the 53 standard fuel models. GR (grass) and TL (timber litter) fuel models are highlighted. Lines indicate various bulk densities. Vertically oriented fuels have a lower bulk density (load/depth) than do horizontally oriented fuels.

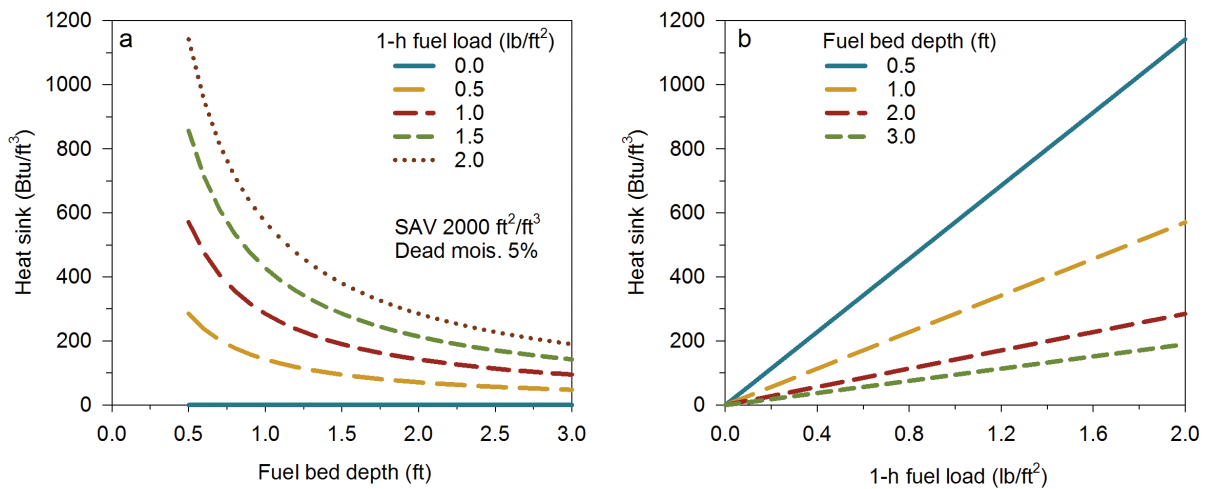


**Figure 21**—Relationship between heat sink and bulk density (load/depth) for one size class of dead fuel with SAV of 2,000 ft<sup>2</sup>/ft<sup>3</sup> and 5 percent dead fuel moisture: (a) range of fuel bed depth for several fuel load values, (b) range of loads for several depth values.

#### 5.2.4.5 Packing Ratio

Mean packing ratio ( $\beta$ ) is a fuel bed value. It is bulk density divided by particle density, ranging from 0.00106 to 0.04878 for the 53 fuel models. Mean packing ratio is the fraction of fuel bed volume that is occupied by fuel particles and is used in the calculation of wind factor and propagating flux ratio.

Optimum packing ratio ( $\beta_{op}$ ) is a function of SAV (fig. 22). It is lower for finer fuel.

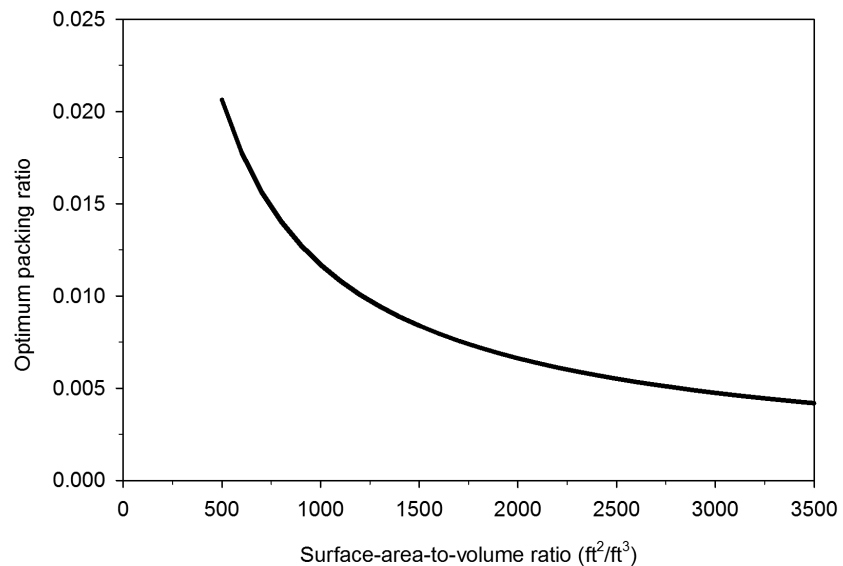


**Figure 22**—Optimum packing ratio is a function of SAV.

Relative packing ratio ( $\beta/\beta_{op}$ ) is mean packing ratio divided by the optimum packing ratio. It ranges from 0.15108 to 6.49054 for the 53 fuel models. Relative packing ratio is used in the calculation of wind factor and optimum reaction velocity.

Reaction velocity is at a maximum when the fuel bed density is optimized to provide the best fuel to air ratio. This occurs when the relative packing ratio is one.

Figure 23 shows optimum packing ratio and packing ratio for the 53 fuel models. The line indicates where they are equal. To the right of the line packing ratio is greater than optimum packing ratio; relative packing ratio is greater than one. The grass (GR) and timber litter (TL) fuel models are highlighted. Note that all of the GR fuel models have relative packing ratio less than one, and all TL fuel models have relative packing ratio greater than one.

### 5.3 Fuel Moisture

Fuel moisture content is expressed in the fire model as a fraction on a dry weight basis. The fraction of moisture content is the weight of the water (initial fuel weight minus oven-dry weight) divided by the weight of the oven-dry material.

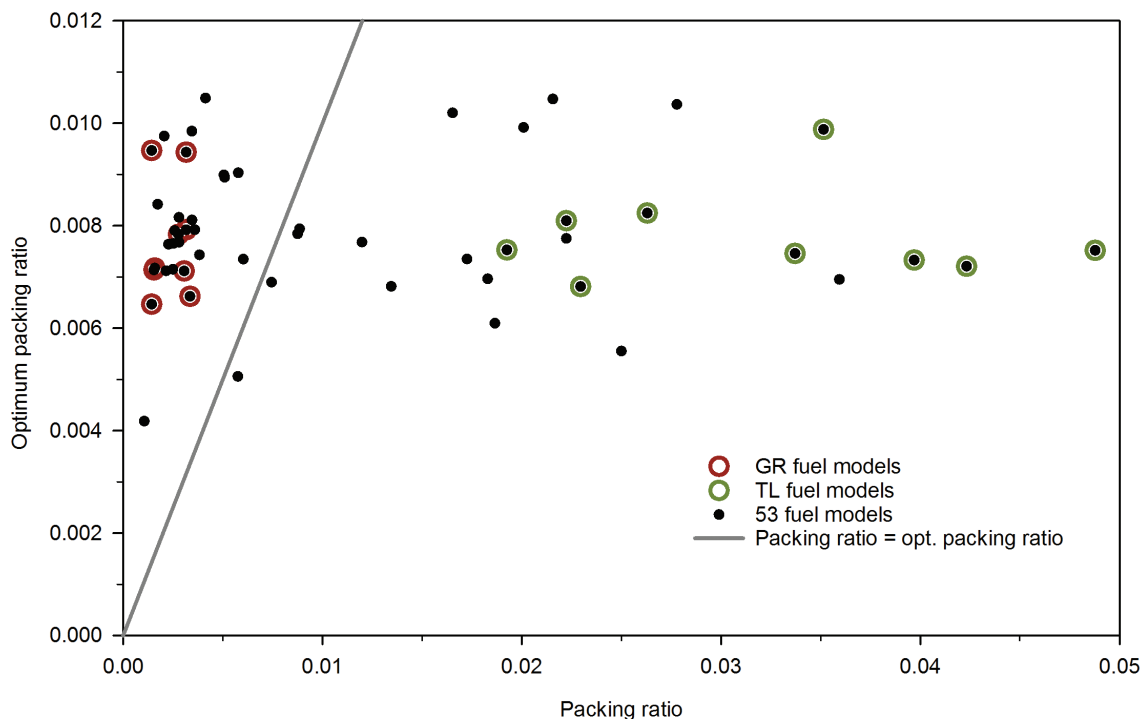


**Figure 23**—Optimum packing ratio vs. packing ratio for the 53 standard fuel models. The line shows where optimum packing ratio is equal to packing ratio, or where relative packing ratio is one. The highlighted grass fuel models have packing ratios that are less than optimum. Litter fuel models have packing ratios higher than optimum.

A moisture value is assigned to each fuel size class, for both live and dead fuel. Fuel moisture plays a role in the rate of spread calculation in both the heat source and heat sink terms. The reaction intensity is reduced by a moisture damping coefficient, which is calculated from the ratio of the fuel moisture to the moisture of extinction for live and dead fuel. The moisture content of each class of fuel is part of the calculation of heat of preignition ( $Q_{ig}$ ). Increasing moisture decreases the heat source term (numerator) and increases the heat sink term (denominator). Rate of spread then logically decreases with increasing fuel moisture.

In addition to the role that live fuel moisture plays in the fire spread model, live herbaceous moisture can be used to determine the amount of load that is transferred from the live-to-dead category to represent curing. The combined effects can sometimes be counterintuitive. Increasing live herbaceous fuel moisture can result in faster rates of spread for dynamic fuel models. A small change in moisture can have a large effect on resulting rate of spread. An option to separate the effects is to assign a curing level not dependent on herbaceous moisture.

Examination of the role of moisture in the fire model is followed by examples of the effect of the fuel load transfer function used for dynamic fuel models.

### **5.3.1 Characteristic Fuel Moisture**

A moisture content value is assigned to each size class of live and dead fuel. An intermediate step in the calculation of rate of spread is finding characteristic moisture content for live and for dead fuel, using the weighting factors.

Because fine fuels are weighted most heavily in the fire spread model, the moisture of that size class has the most influence. Rothermel (1983, page 14) suggested using  $10\text{-h} = 1\text{-h} + 1$  percent and  $100\text{-h} = 1\text{-h} + 2$  percent. The result is, however, essentially the same as using the same value for all dead fuel size classes. For 52 of the 53 standard fuel models, characteristic dead fuel moisture using this relationship is equal to 1-h moisture. Fuel model TL7 (large downed logs) has very little 1-h fuel relative to 10-h and 100-h fuel; characteristic dead fuel moisture is equal to 10-h moisture.

A larger difference between 1-h and 10-h moisture affects the characteristic moisture. Consider fuel model SH3 (moderate load, humid climate shrub), a static fuel model with no 100-h fuel and over 6 times as much load in the 10-h class as 1-h (3.0 tons/ac vs 0.45 tons/ac) (table 18). In this case, 10-h moisture has a large effect on characteristic dead fuel moisture. For 1-h moisture of 5 percent and 10-h moisture of 30 percent, the characteristic dead moisture is 13 percent. While this example illustrates calculation of characteristic fuel moisture, it is not likely that there would be such large differences between 1-h and 10-h moisture.

Characteristic live fuel moisture is calculated from live herbaceous and live woody fuel moisture using the weighting factors for the fuel model. Standard fuel models (except fuel model 2, timber grass and understory) with live herbaceous fuel are dynamic. If live herbaceous moisture is used to model curing, then live

**Table 18**—Characteristic dead fuel moisture (percent) for fuel model SH3, which has no 100-h fuel.

10-h fuel moisture -----percent-----	1-h fuel moisture -----percent-----					
	5	10	15	20	25	30
5	5	8	12	15	19	22
10	7	10	13	17	20	24
15	8	12	15	18	22	25
20	10	13	17	20	23	27
25	11	15	18	22	25	28
30	13	16	20	23	27	30

herbaceous moisture is used both in the fire spread model and to adjust fuel model parameters and thereby weighting factors. If the curing level is defined independently, then the role of moisture in the fire model can be examined without the compounding effects of fuel load changes.

Consider dynamic fuel model GS3 (moderate load, humid climate grass-shrub) with 50 percent curing (table 19). Live herbaceous fuel load is then 0.72 ton/ac; live woody is 1.25 ton/ac. Because there is more live woody fuel, its moisture has a larger influence on characteristic live fuel moisture. For live herbaceous moisture of 150 percent and live woody of 50 percent, characteristic moisture is 87 percent. For the reverse (live herbaceous moisture = 50 percent and live woody moisture = 150 percent), characteristic live moisture is 113 percent.

**Table 19**—Characteristic live fuel moisture for fuel model GS3, with 50 percent cured set for all live herbaceous moisture values.

Live herb. moisture -----percent-----	Live woody moisture -----percent-----			
	50	100	150	200
50	50	82	113	145
100	68	100	132	163
150	87	118	150	182
200	105	137	168	200

### 5.3.2 Moisture of Extinction

In the spread model there exists some value of dead fuel moisture content for which the dead fuel can no longer sustain a spreading surface fire. Dead fuel moisture of extinction is often referred to as simply “moisture of extinction” and is a fuel model parameter. Live fuel moisture of extinction is calculated from the ratio of dead-to-live fine fuel loads and the moisture content of the fine dead fuel.

If there is no dead fuel, or if the dead fuel is wetter than its moisture of extinction, the model predicts no spread and no reaction intensity. In reality, live fuel alone may propagate a fire. This restriction is an area of model incompleteness.

When sufficient fine dead fuel exists and the dead fuel moisture content is low enough relative to its moisture of extinction, both live and dead fuel will burn, according to the model. In this case, the reaction intensities from the dead and live fuels are added together.

If the fine dead fuel load is too light relative to that of the live fuel, or the dead fuel is too moist, the live fuel moisture of extinction may be less than the live fuel moisture content. In this case, only the dead fuel produces a reaction intensity, but because both dead and live fuel must be heated to the point of ignition, the fire spreads relatively slowly.

### 5.3.2.1 Dead Fuel Moisture of Extinction

The 11 fuel models published by Rothermel (1972) all had 30 percent moisture of extinction. Dead fuel moisture of extinction for the current 53 standard fire behavior fuel models varies from 12 to 40 percent (table 20). All the fuel models with “humid” in their name have dead fuel moisture of extinction of 30 or 40 percent, while those labeled “dry” have 15 percent moisture of extinction.

**Table 20**—Dead fuel moisture of extinction (a fuel model parameter) for the 53 standard fuel models.

Moisture of extinction --percent--	Fuel model
12	1, TU4
15	2, 11, GR1, GR2, GR4, GR7, GS1, GS2, SH1, SH2, SH5, SH7
20	4, 5, 12, TU1, TL3
25	3, 6, 9, 10, 13, TU5, TL2, TL4, TL5, TL6, TL7, SB1, SB3, SB4
30	8, GR3, GR8, SH4, SH6, TU2, TU3, TL1
35	TL8, TL9
40	7, GR5, GR6, GR9, GS3, GS4, SH3, SH8, SH9

### 5.3.2.2 Live Fuel Moisture of Extinction

While dead fuel moisture of extinction is an input (a fuel model parameter), live fuel moisture of extinction is an intermediate value calculated in the fire model. Live fuel moisture of extinction is calculated from dead fuel moisture, dead moisture of extinction, and dead-to-live load ratio. When characteristic live fuel moisture is less than live fuel moisture of extinction, live fuel contributes to the heat source term. When it is greater than that value, heat source is determined only by dead fuel.

Consider static fuel models SH2 (moderate load, dry climate shrub), SH6 (low load, humid climate shrub), and SH8 (high load, humid climate shrub), which have dead fuel moistures of extinction 15, 30, and 40 percent. If dead fuel moisture is more than the dead fuel moisture of extinction, the fire is predicted to not burn no matter what live fuel moisture is. Figure 24 and table 21 show calculated live fuel moisture of extinction. For dead fuel moisture of 10 percent and live fuel moisture of 100 percent, live fuel in SH6 and SH8 live fuel contributes to the heat source, but it does not in SH2.

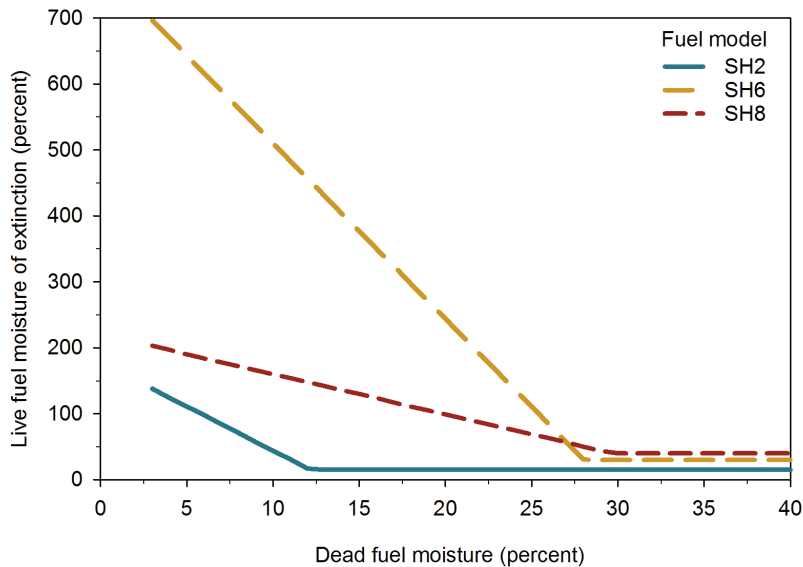


**Figure 24**—Live fuel moisture of extinction is a function of dead fuel moisture and fuel model parameters (dead fuel moisture of extinction and dead-to-live load ratio).

**Table 21**—Live fuel moisture of extinction (percent) calculated from fuel model parameters and dead fuel moisture.

Fuel model	Dead fuel moisture		
	-----percent-----		
	6	10	14
SH2	98	44	15
SH6	616	510	403
SH8	184	160	136

### 5.3.3 Moisture Damping Coefficient

Moisture damping coefficient is a multiplier in the calculation of reaction intensity, part of the heat source term. Reaction intensity is reduced as fuel moisture increases. Relative values of characteristic fuel moisture and moisture of extinction are used to define the moisture damping coefficient (fig. 25). The same relationship is used for both dead and live fuel. For very dry fuels the ratio of fuel moisture to moisture of extinction is low and the moisture damping coefficient is close to one so there is little reduction of reaction intensity. The reduction increases for wetter fuel, reducing reaction intensity. When the moisture content is equal to the moisture of extinction, the moisture damping coefficient is 0. The steep parts of the curve (fig. 25) indicate that fire behavior is most responsive to changes in fuel moisture when the fuels are either relatively wet or relatively dry.

Figure 26 shows dead fuel damping coefficient for various moisture of extinction values for a range of dead fuel moisture. The relationship is the same for all fuel models. For 20 percent dead fuel moisture, moisture damping coefficient is 0.4 for dead moisture of extinction of 25 percent and 0.55 for moisture of extinction of 45 percent. For the same fuel moisture, reaction intensity is reduced less for higher moisture of extinction.

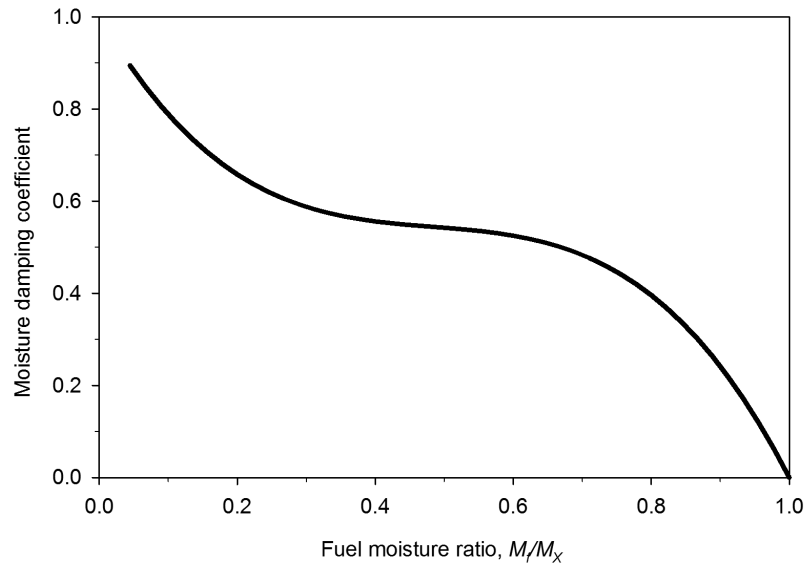


**Figure 25**—Moisture damping coefficient is found from the ratio of fuel moisture ( $M_f$ ) to moisture of extinction ( $M_x$ ). The same relationship is used for both dead and live fuel.

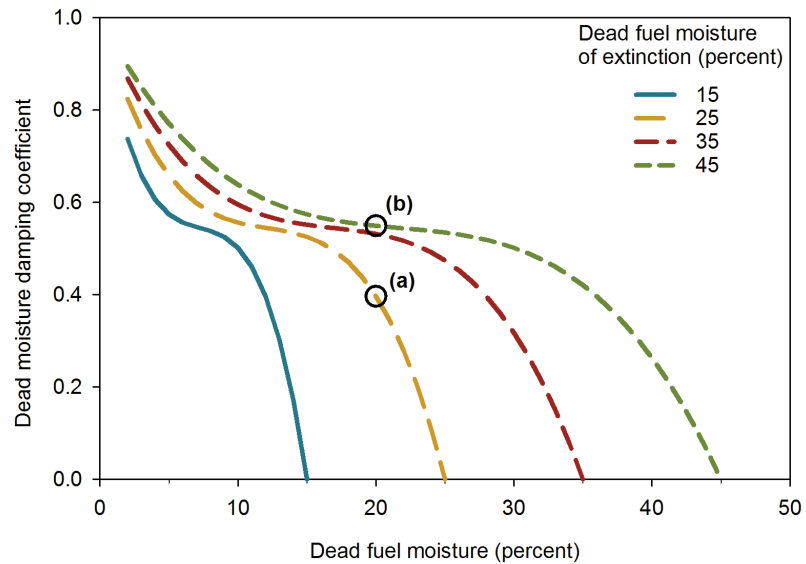


**Figure 26**—Dead moisture damping coefficient is a function of dead fuel moisture and dead fuel moisture of extinction. The relationship is the same for all fuel models. For 20 percent dead fuel moisture, moisture damping coefficient is (a) 0.4 for dead moisture of extinction of 25 percent and (b) 0.55 for moisture of extinction of 45 percent.

Moisture of extinction has an impact beyond defining the point at which rate of spread is 0 because it affects moisture damping coefficient. Consider static fuel model TL6 (moderate load broadleaf litter), which has a 25 percent moisture of extinction and no live fuel. Look at the result of changing only moisture of extinction with 6 mi/h midflame wind and 0 slope (fig. 27).

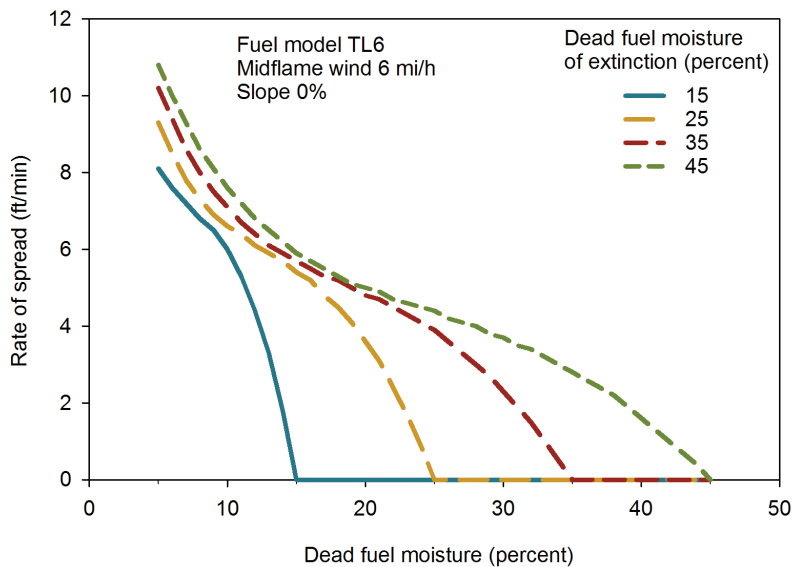


**Figure 27**—A change in dead fuel moisture of extinction changes not only the point at which rate of spread is 0, but also affects rate of spread for the range of dead fuel moisture values (fuel model TL6, midflame wind 6 mi/h, no slope).

While dead fuel moisture of extinction is a single input value, live fuel moisture of extinction is calculated from dead fuel moisture and fuel parameters. So live fuel moisture damping coefficient is a function of both live and dead moisture and varies by fuel model. Consider static fuel models SH2, SH6, and SH8 (see fig. 24 and table 21). Live fuel moisture of extinction is a function of dead fuel moisture and differs by fuel model. Figure 28 shows live moisture damping coefficient for SH8 for dead moisture values of 6, 10, and 14 percent. For live moisture of 30 percent and 6 percent dead moisture, live moisture damping is 0.7, meaning 70 percent of live reaction intensity contributes to the heat source.

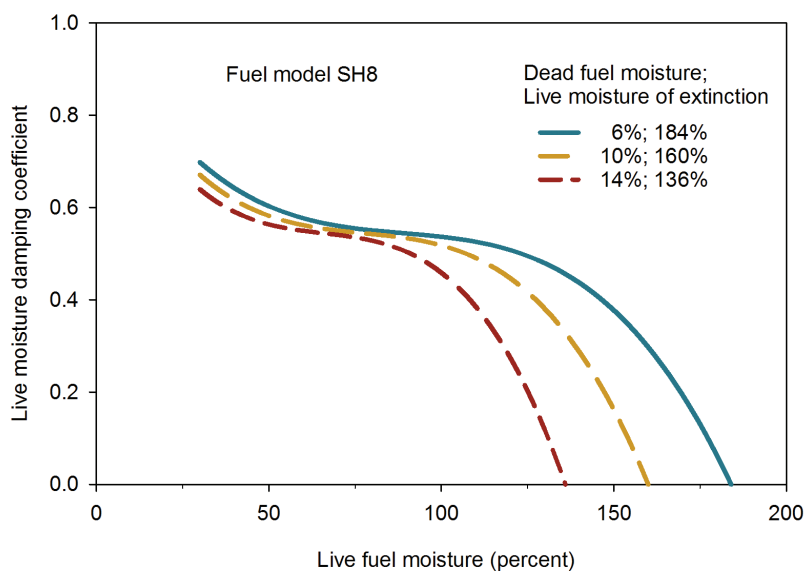


**Figure 28**—Live moisture damping coefficient for fuel model SH8 and dead fuel moistures of 6, 10, and 14 percent. The associated live moisture of extinction is calculated to be 184, 160, and 136 percent.

Figure 29 shows live moisture damping coefficient for the same three fuel models for 10 percent dead moisture. Live moisture of extinction for SH2 is 44 percent. Live moisture damping coefficient drops quickly from 0.49 at 30 percent live moisture to 0 at 44 percent moisture. At the other extreme, live fuel in fuel model SH6 will always contribute to the heat source since the moisture of extinction is 510 percent. At 200 percent moisture content, live moisture damping coefficient for SH6 is 0.56.

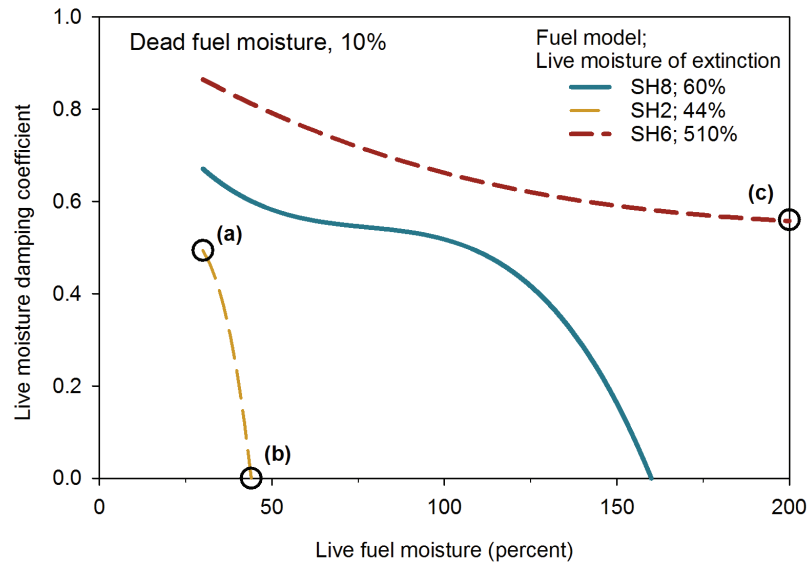


**Figure 29**—Live moisture damping coefficient for fuel models SH2, SH6, and SH8 and dead fuel moisture 10 percent. Live moisture of extinction is calculated. For SH2, with live moisture of extinction of 44 percent, live moisture damping coefficient drops quickly from (a) 0.49 at 30 percent live moisture to (b) 0 at 44 percent moisture. For fuel model SH6, live moisture of extinction is 510 percent, so live fuel always burns. Moisture damping coefficient is (c) 0.56 at 200 percent live moisture.

### 5.3.4 Fuel Moisture in the Heat Source and Heat Sink Terms

As fuel moisture increases, heat source decreases and heat sink increases. As a result, rate of spread decreases. The effect is monotonic. Heat source includes the transition from where live fuel contributes to where it does not. There can be a steep change in spread rate as live fuel moisture approaches that point.

Consider fuel model SH8 (high load, humid climate shrub) for ranges of live and dead moisture (midflame wind 6 mi/h, 0 slope) (fig. 30). Heat sink increases linearly with increasing live and dead fuel moisture, with live fuel having more influence. Heat source decreases with increasing moisture; live fuel contributes when moisture is less than live moisture of extinction. For 50 percent live fuel moisture, rate of spread is 14 ft/min for dead moisture 28 percent, and rate of spread is 26 ft/min for dead moisture 27 percent. The spread rate nearly doubles for a change of 1 percent dead fuel moisture.

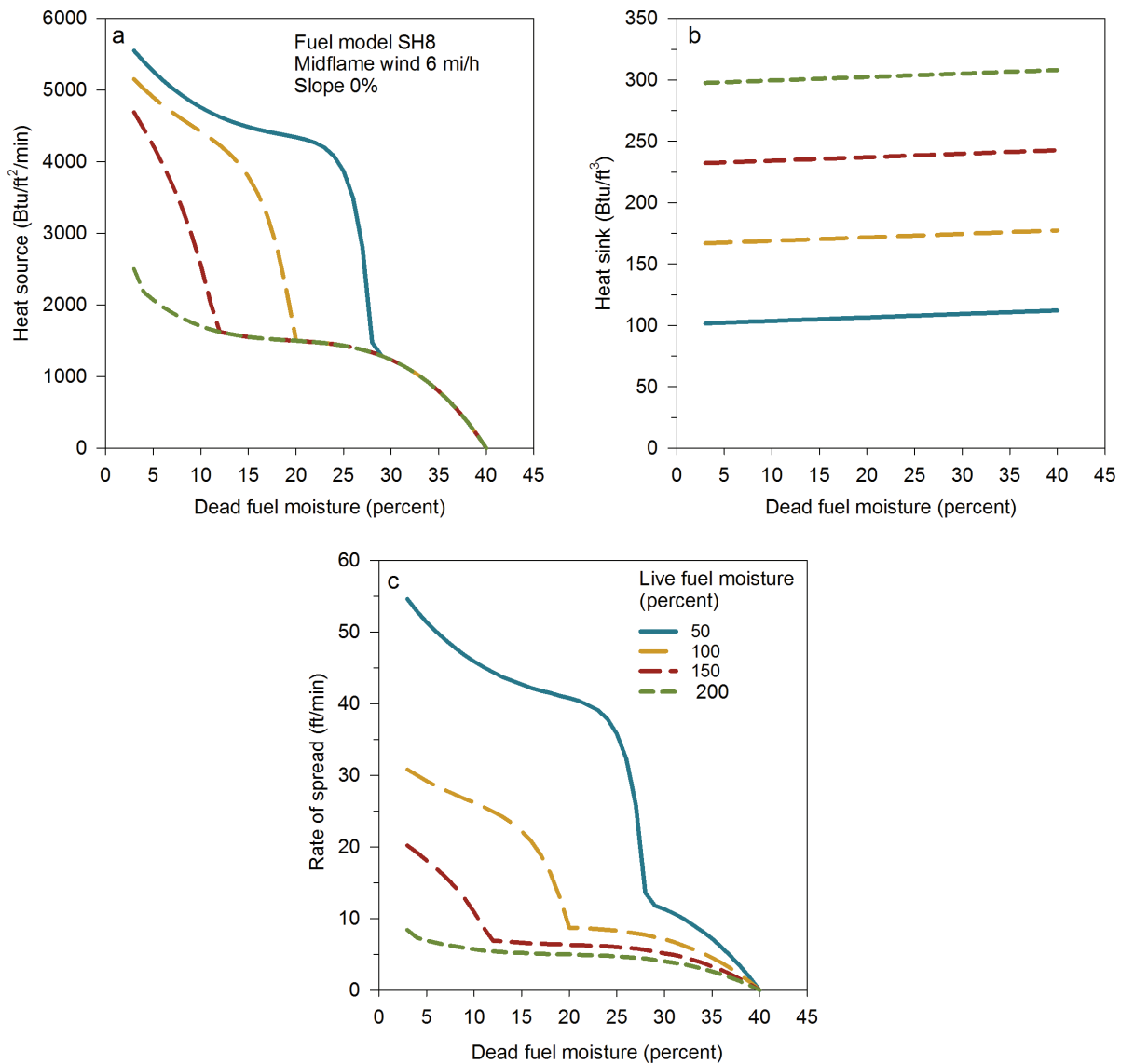


**Figure 30**—The effect of dead and live fuel moisture on (a) heat source, (b) heat sink, and (c) rate of spread for fuel model SH8, midflame wind speed 6 mi/h and 0 percent slope.

### 5.3.5 Live Herbaceous Moisture and Dynamic Fuel Models

The prior discussion addressed the role of fuel moisture in the fire spread model. Examples used fixed fuel model parameters: either static fuel models or dynamic fuel models where curing level was defined rather than calculated. The following is an examination of the additional effect of using the fuel load transfer function to change fuel model parameters as a function of live herbaceous moisture. The change to fuel loads affects rate of spread through changes to characteristic live and dead fuel moisture, fuel moisture of extinction, and moisture damping coefficient.

### 5.3.5.1 Characteristic Live Fuel Moisture for Dynamic Fuel Models

For fixed fuel loads, characteristic live moisture increases as both live herbaceous and live woody moisture increase. Consider dynamic fuel model GS3 (moderate load, humid climate grass-shrub) where curing is a function of live herbaceous moisture (dead moisture is 5 percent) (fig. 31). When live woody moisture is 200 percent, and live herbaceous moisture increases from 50 to 100 percent, characteristic moisture decreases from 169 to 153 percent because fuel loads and weighting factors change with the change in live herbaceous moisture.

### 5.3.5.2 Live Fuel Moisture of Extinction for Dynamic Fuel Models

For fixed fuel loads, live fuel moisture of extinction is constant for a given value of dead fuel moisture and does not depend on live fuel moisture. On the other hand, live herbaceous moisture has a significant effect on live fuel moisture of extinction when it determines how live and dead fuel loads change. Consider fuel model GR2 (low load, dry climate grass) with curing a function of live herbaceous moisture, and a range of dead and live moisture (fig. 32). When dead fuel moisture is defined as 10 percent, live fuel moisture of extinction is 250 percent for live moisture 60 percent and 55 percent for live moisture of 90 percent. The black line indicates where live fuel moisture is equal to live fuel moisture of extinction. Fuels contribute to the heat source for moistures above that line, where live fuel moisture is less than live fuel moisture of extinction.

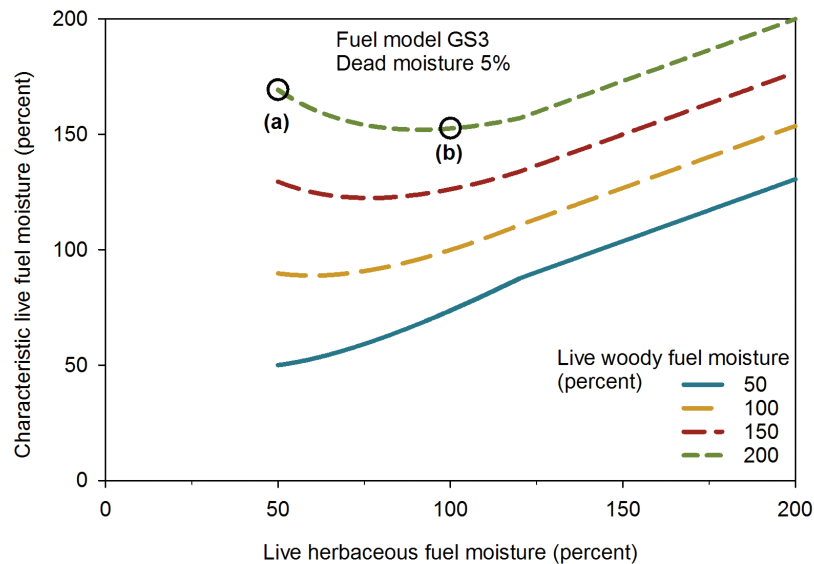


**Figure 31**—For dynamic fuel models, characteristic live moisture can decrease with increasing live herbaceous moisture because of the change in fuel load and the effect on weighting factors. The plot shows fuel model GS3, dead moisture 5 percent, and four live woody moisture values for a range of live herbaceous moisture. When live woody moisture is 200 percent and live herbaceous moisture is (a) 50 percent, characteristic live moisture is 169 percent. When live herbaceous moisture increases to (b) 100 percent, characteristic live moisture decreases to 153 percent.

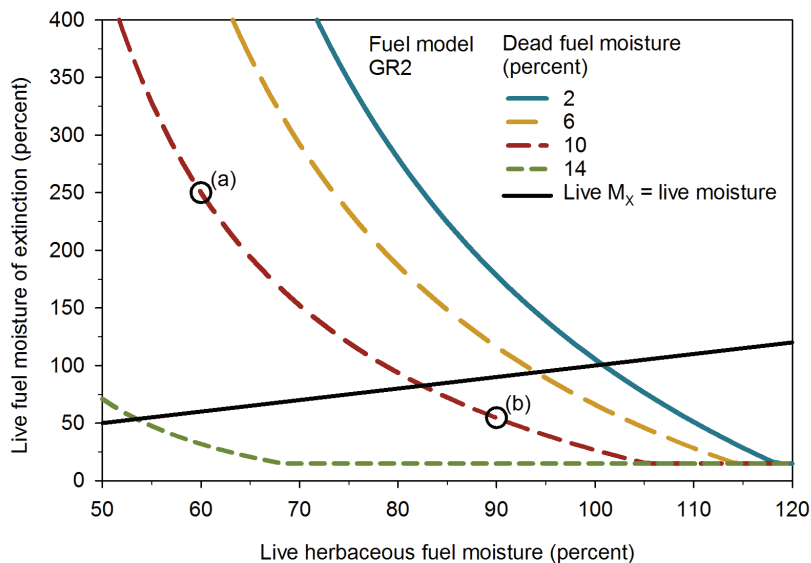


**Figure 32**—Live herbaceous fuel moisture affects live fuel moisture of extinction for dynamic fuel models because of the change in live to dead load ratio. The black line indicates where live fuel moisture is equal to live fuel moisture of extinction. Fuel model GR2 has no live woody fuel. For dead fuel moisture of 10 percent, live fuel moisture of extinction is (a) 250 percent for live herbaceous moisture 60 percent and (b) 55 percent for live herbaceous moisture of 90 percent.

### 5.3.5.3 Moisture Damping Coefficient for Dynamic Fuel Models

Moisture damping coefficient is determined by the ratio of fuel moisture to moisture of extinction. When live herbaceous moisture determines fuel load transfer, live moisture of extinction changes with live moisture. There is a different live fuel moisture of extinction value for each value of live herbaceous moisture. The resulting moisture damping coefficient is sensitive to live herbaceous moisture content, especially as live fuel moisture nears the moisture of extinction. Consider fuel model GR2 (low load, dry climate grass), curing as a function of live herbaceous moisture, dead moisture values of 2, 6, 10, 14 percent, and a range of live herbaceous moisture values (fig. 33). The live moisture damping coefficient drops quickly from 0.5 to 0. For dead fuel moisture of 10 percent, live moisture damping is 0.5 for 76 percent live herbaceous moisture and 0 for 82 percent.

### 5.3.5.4 Reaction Intensity for Dynamic Fuel Models

For fixed fuel loads, dead fuel reaction intensity decreases with increasing dead fuel moisture and does not depend on live fuel moisture. Similarly, live reaction intensity is a function of live fuel moisture and is not affected by dead fuel moisture. When live herbaceous moisture is used to transfer fuel loads in dynamic fuel models, both live and dead fuel moisture affect both live and dead reaction intensity.

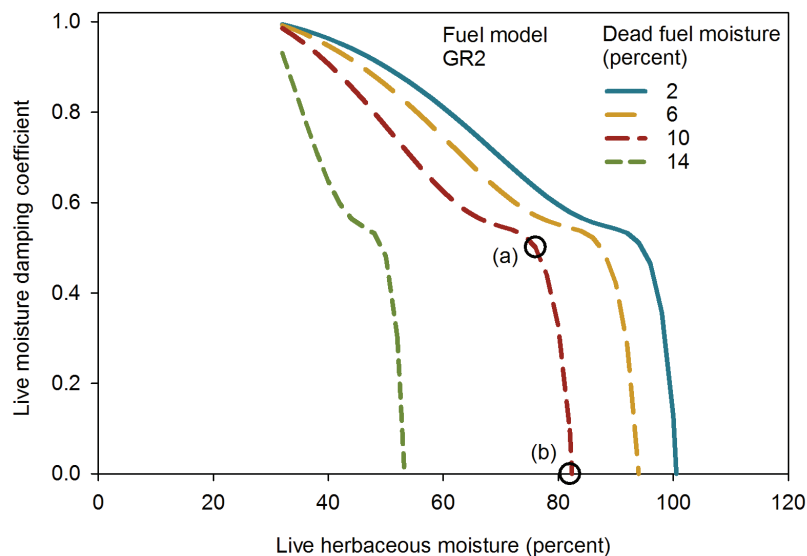


**Figure 33**—Live moisture damping coefficient for fuel model GR2 for a range of live herbaceous fuel moisture and four values of dead fuel moisture. For dead fuel moisture 10 percent, live moisture damping is (a) 0.5 for 76 percent live herbaceous moisture and (b) 0 for 82 percent.

Consider fuel model GR2 (low load, dry climate grass) with midflame wind speed of 6 mi/h, dead moisture values of 6, 10, 14 percent, and live herbaceous moisture ranging from 30 to 150 percent. Dead fuel reaction intensity (fig. 34) decreases with increasing live herbaceous moisture because there is less dead fuel at high live herbaceous moisture. The linear decrease is a reflection of the load transfer function. For 10 percent dead fuel moisture, there is an 11-fold difference in dead reaction intensity between 30 percent live herbaceous moisture, where all of the live herbaceous fuel is transferred to the dead fuel category (940 Btu/ft<sup>2</sup>/min), and 120 percent live herbaceous moisture, where no fuel load is transferred (86 Btu/ft<sup>2</sup>/min).

Live reaction intensity increases then decreases with increasing live herbaceous moisture (fig. 35). Live reaction intensity is 0 for live herbaceous moisture of 30 percent, where there is no live herbaceous fuel (GR2 has no live woody fuel). It is 0 for values above the live fuel moisture of extinction (a function of dead fuel moisture).

In calculating live reaction intensity, the two values that change with live herbaceous moisture are live net load and live moisture damping coefficient, shown in figure 36 for 10 percent dead fuel moisture. For increasing live herbaceous moisture, live net load increases (less load is transferred to dead) and moisture damping coefficient decreases. The product of the two factors (one increasing and one decreasing) increases then decreases (fig. 37).

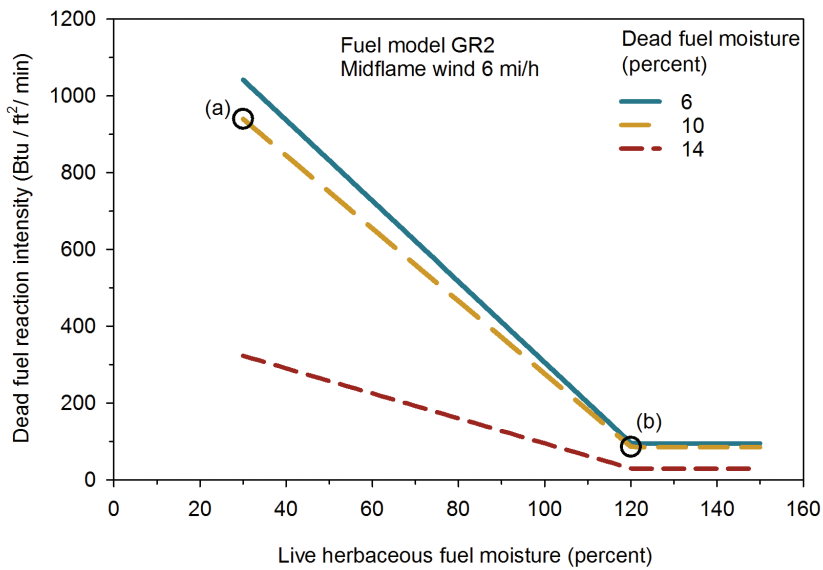


**Figure 34**—Dead reaction intensity changes according to live herbaceous moisture for dynamic fuel models because there is less dead fuel at high live herbaceous moisture. Fuel model GR2; midflame wind 6 mi/h. For 10 percent dead fuel moisture and (a) 30 percent live herbaceous moisture, reaction intensity is 940 Btu/ft<sup>2</sup>/min (all of the live herbaceous fuel is transferred to the dead fuel category). At (b) 120 percent live herbaceous moisture, reaction intensity is 86 Btu/ft<sup>2</sup>/min (no fuel load is transferred).

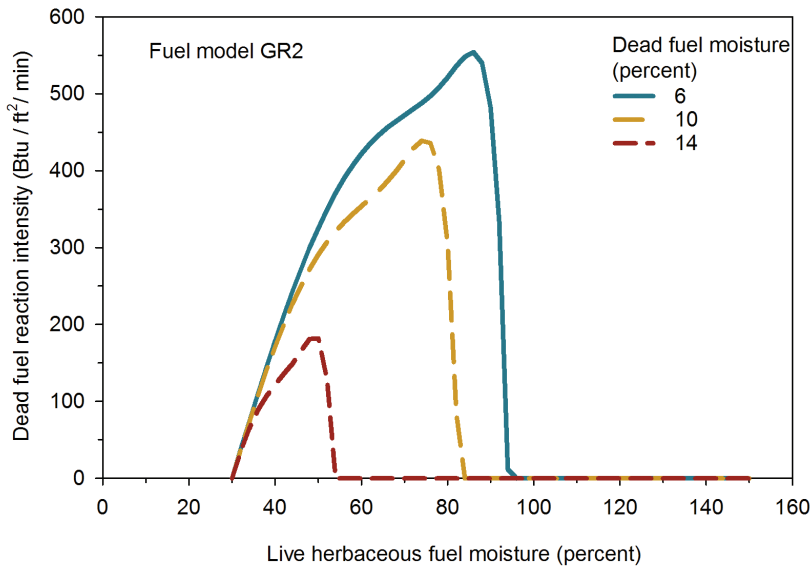


**Figure 35**—Live reaction intensity for fuel model GR2 increases then decreases rapidly as load is transferred as a function of live herbaceous fuel moisture.

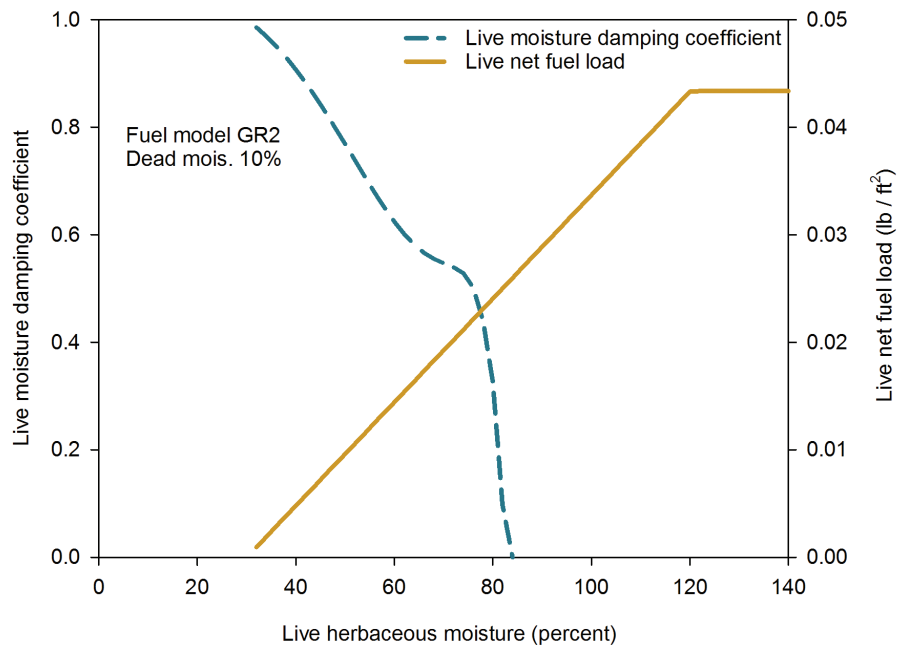


**Figure 36**—For dynamic fuel model GR2 (dead moisture 10 percent), as live herbaceous moisture increases, live net fuel load increases and live damping coefficient decreases.

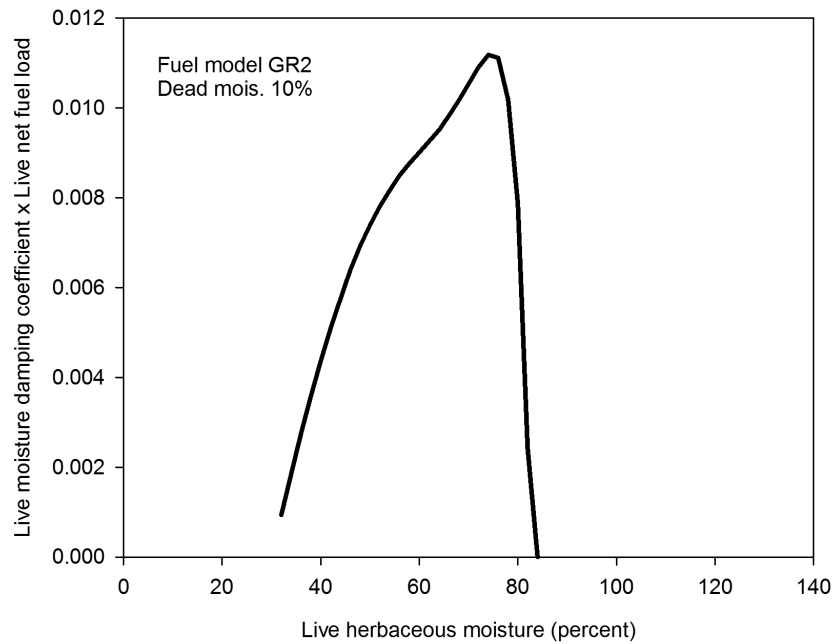


**Figure 37**—The product of live damping coefficient and net live load (from fig. 36) increases then decreases, having an effect on live reaction intensity (fig. 35).

### 5.3.5.5 Rate of Spread for Dynamic Fuel Models

There are numerous effects of live herbaceous fuel moisture on rate of spread for dynamic fuel models when load transfer from live-to-dead is a function of live herbaceous fuel moisture. Figure 38 shows rate of spread, heat source, and heat sink for dynamic fuel model GR2 (low load, dry climate grass), which has no live woody fuel and dead fuel moisture of extinction of 15 percent. Midflame wind speed is 6 mi/h; there is no slope. Heat sink increases with increasing live and dead fuel moisture values. Heat source is based in part on dead reaction intensity and live reaction intensity, thus the interesting shape of the resulting curve.

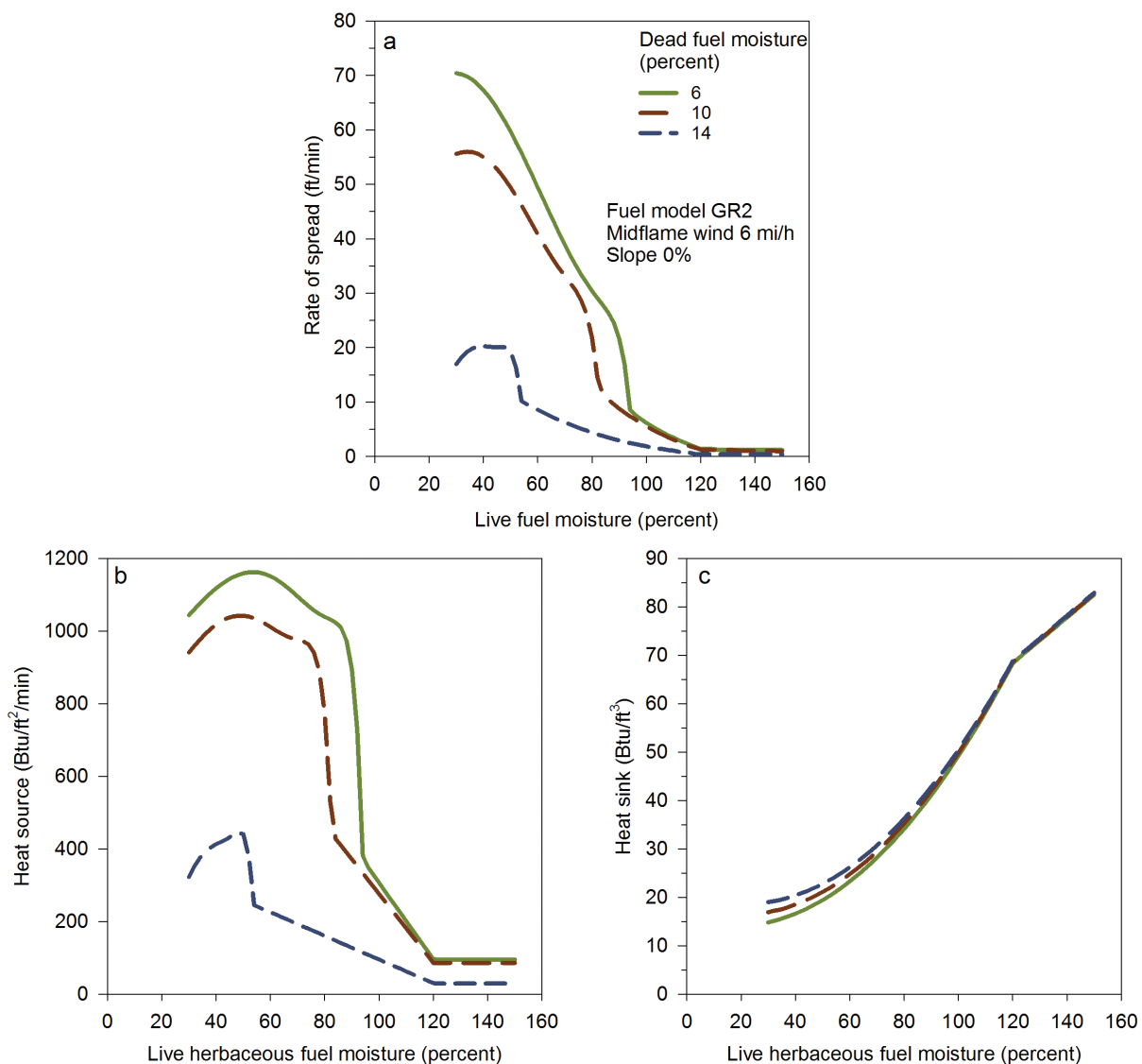


**Figure 38**—(a) Rate of spread, (b) heat source, and (c) heat sink for fuel model GR2 are influenced by live herbaceous fuel moisture through both the fire spread model and adjustment of fuel loads. Midflame wind speed is 6 mi/h; there is no slope.

## 5.4 Wind and Slope

The fire model was developed first for the no wind, no slope case ( $R_0$ ). Wind and slope factors ( $\phi_w$ ,  $\phi_s$ ) were then included to increase rate of spread. Wind and slope factors are in the numerator, in the heat source term.

$$R = R_0(1 + \phi_w + \phi_s)$$

The fire model itself applies only to upslope spread with the wind; adaptations for other directions are described in section 6.

Midflame wind speed is the average wind velocity that affects surface fire spread. While the term “midflame” wind indicates the wind at the midpoint of the flame, that is not a precise definition. The fire model was designed to use the fuel and environmental conditions in which the fire is expected to burn. Flame dimensions are not needed to determine the wind speed for calculating spread rate. The term “midflame” was coined to make the distinction between the “free wind” at 20 ft above the vegetation and the reduced wind that is used in calculating surface fire spread rate. The spread model is based, in part, on experimental burns in a wind tunnel. The wind velocity was not related to the height of the flames but was the average value for the uniform flow in the wind tunnel.

Rothermel (1983, preface) stated that it took 10 years to develop the spread model and another 10 years to learn how to obtain the inputs and interpret the outputs for field application. Development of concepts and models for wind adjustment factor to convert 20-ft wind speed to midflame wind speed is one of the steps taken to make the spread model useful for field applications (Andrews 2012).

### 5.4.1 Wind Factor

Wind factor is related to the geometrical properties of the fuel particles and fuel bed. The form of the wind factor equation is  $AU^B$ , where  $B$  is a function of SAV and  $A$  is found from SAV and relative packing ratio. In general,  $A$  is small for fine fuels and for tightly packed fuels and large for big and/or loosely packed fuels, while  $B$  is large for fine fuels and small for finer fuels.

Figure 39 shows the wind factor for five fuel models for midflame wind from 0 to 12 mi/h. Table 22 gives wind factor for 6 and 12 mi/h midflame wind and values that are used in the calculation.

Characteristic SAV and relative packing ratio are plotted in figure 40 for the 53 standard fuel models. Five selected fuel models are highlighted.

Figure 41 shows the relationship of wind factor for 6 mi/h midflame wind to relative packing ratio and surface-area-to-volume ratio. Values for the 53 standard fuel models are also shown. Wind factor decreases as relative packing ratio (fuel bed density) increases. Wind factor increases as the surface-area-to-volume ratio increases; the effect becomes greater as relative packing ratio decreases.

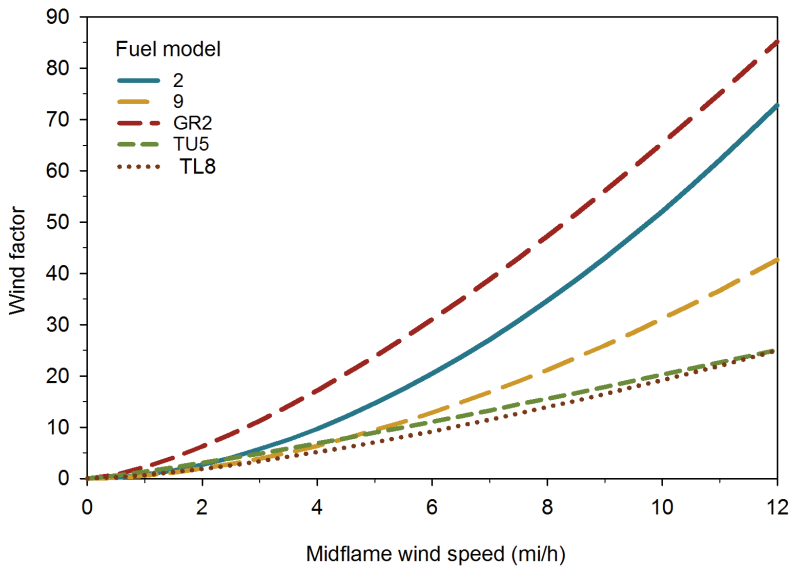


**Figure 39**—Wind factor for five standard fuel models for a range of mid-flame wind speed.

**Table 22**—Wind factor ( $AU^B$ ) is calculated from midflame wind speed and fuel model parameters.

Fuel model		Char. SAV $-\frac{ft^2}{ft^3}-$	Relative packing ratio	A	B	Wind factor, 6 mi/h	Wind factor, 12 mi/h
2	Timber grass and understory	2,784	1.14	0.000213	1.83	20.5	72.8
9	Long needle or hardwood litter	2,484	4.50	0.000267	1.72	12.9	42.7
GR2	Low load, dry climate grass	1,820	0.22	0.003398	1.46	31.1	85.2
TU5	Very high load, dry climate timber-shrub	1,224	2.03	0.007056	1.17	11.1	25.1
TL8	Long needle litter	1,770	5.42	0.001157	1.43	9.2	25.0

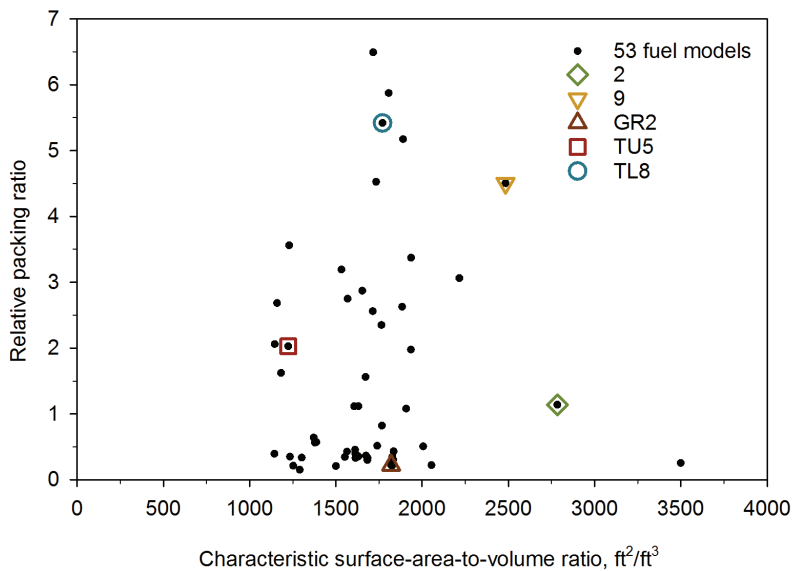


**Figure 40**—Relative packing ratio and characteristic surface-area-to-volume ratio are used to calculate wind factor. Values for the 53 standard fuel models are shown. Five selected fuel models are highlighted.

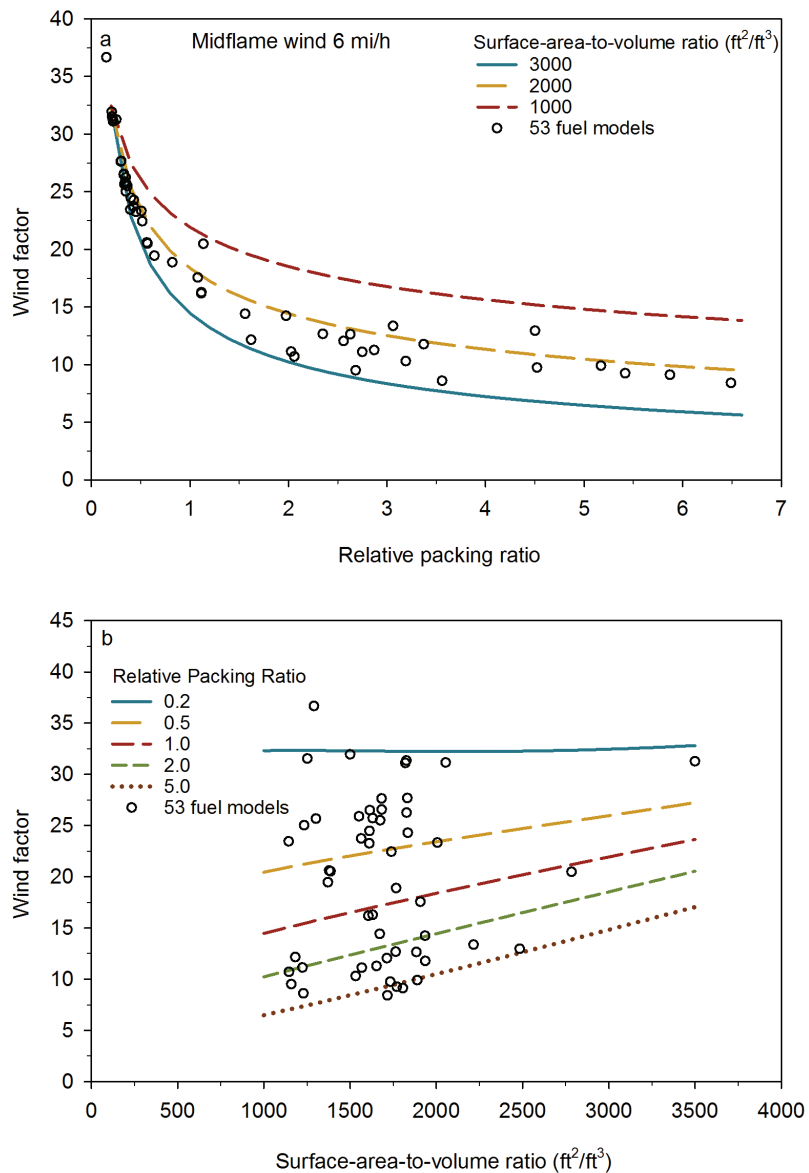


**Figure 41**—Wind factor is a function of relative packing ratio and SAV. For midflame wind 6 mi/h (a) range of relative packing ratio for several SAV values, (b) range of SAV for several packing ratio values. Values for the 53 standard fuel models are plotted to illustrate the range of values.

Wind factor is a significant part of the fire spread model. In table 22 note that for fuel model 2 (timber grass and understory) with midflame wind of 6 mi/h and 0 slope, rate of spread is over 20 times rate of spread for 0 wind and slope.

$$R = R_0(1 + \phi_w + \phi_s) = R_0(1 + 20.5)$$

#### 5.4.2 Slope Factor

Slope factor is a function of packing ratio (fig. 42 and table 23). As packing ratio increases, slope factor decreases. More tightly packed fuels have lower slope factors.

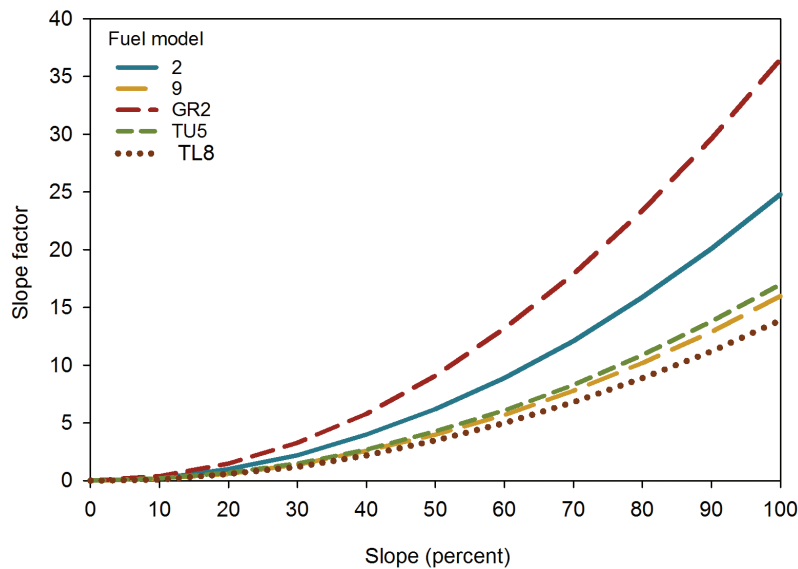


**Figure 42**—Slope factor for five standard fuel models for a range of slope values.

**Table 23**—Slope factor is calculated from slope steepness and packing ratio.

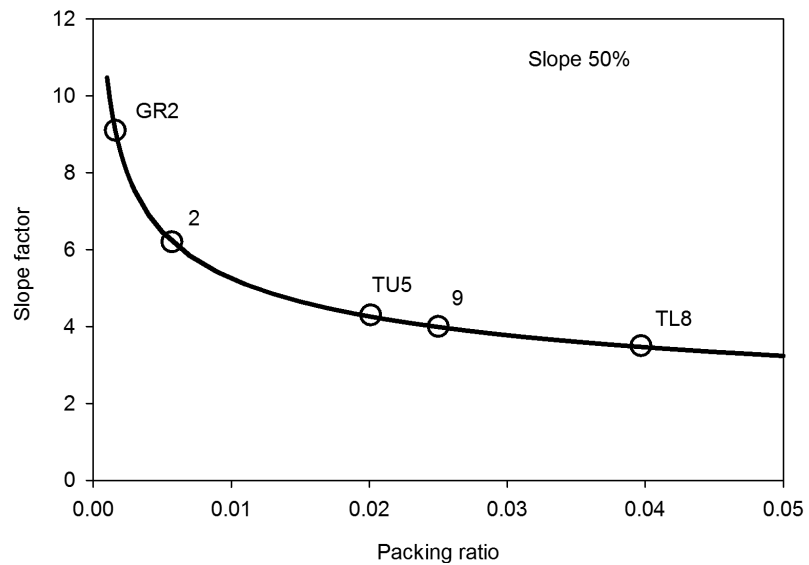
Fuel model		Packing ratio	Slope factor, 20% (11 deg)	Slope factor, 50% (27 deg)	Slope factor, 100% (45 deg)
2	Timber grass and understory	0.0057	1.0	6.2	24.8
9	Long needle or hardwood litter	0.0250	0.6	4.0	16.0
GR2	Low load, dry climate grass	0.0016	1.5	9.1	36.5
TU5	Very high load, dry climate timber-shrub	0.0201	0.7	4.3	17.0
TL8	Long needle litter	0.0397	0.6	3.5	13.9

Figure 42 shows slope factor for five fuel models with slope steepness ranging from 0 to 100 percent. Table 23 gives slope factor for 20, 50, and 100 percent slope for the same five fuel models.

Figure 43 shows slope factor for 50 percent slope for a range of packing ratio values. Values for the five fuel models in table 23 are indicated. Figure 44 shows slope factor for slope ranging from 0 to 100 percent for several packing ratio values.

### 5.4.3 Effective Wind Speed

Effective wind speed represents the combined effect of wind and slope. Effective wind factor is the sum of the wind factor and the slope factor. The wind factor equation is then used to find effective wind speed.



**Figure 43**—Slope factor for 50 percent slope as a function of packing ratio. Values for five fuel models are indicated.

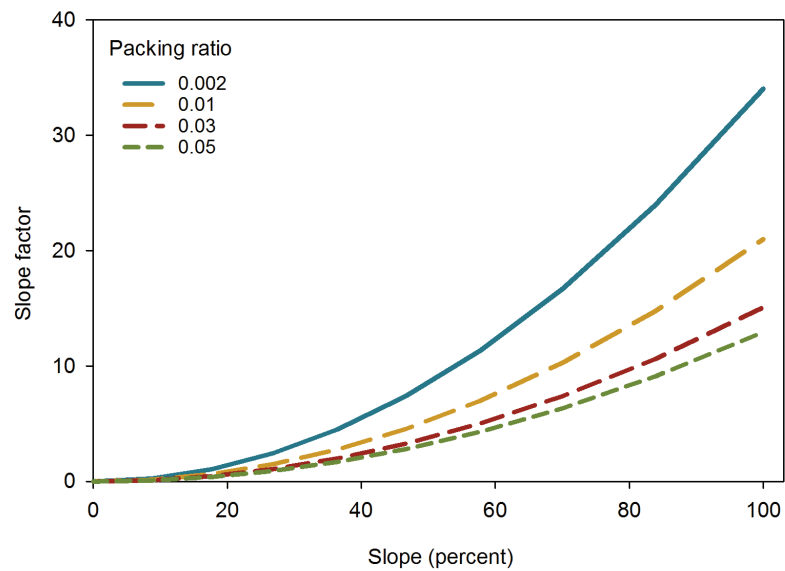


**Figure 44**—Slope factor for a range of slope values and selected packing ratios.

Calculation of effective wind speed depends on wind and slope factors, which are based on fuel model parameters. Table 24 gives effective wind for 0 wind speed and for three slope values for five fuel models. For fuel model TL8 (long-needle litter), a 50 percent slope has the same effect in the fire model as a 3 mi/h midflame wind. Note that both fuel model 9 (long-needle or hardwood litter) and TL8 have effective wind of 3.0 mi/h for 50 percent slope. But effective wind is different for 100 percent slope: 6.8 mi/h for fuel model 9 and 8.0 mi/h for fuel model TL8. A plot of effective wind speed for fuel models 9 and TL8 is in figure 45.

**Table 24**—Effective wind speed (mi/h) for no wind for five fuel models and three values for slope.

Fuel model	Slope steepness		
	percent		
	20	50	100
2	1.1	3.1	6.7
9	1.0	3.0	6.8
GR2	0.7	2.6	6.7
TU5	0.6	2.6	8.6
TL8	0.8	3.0	8.0

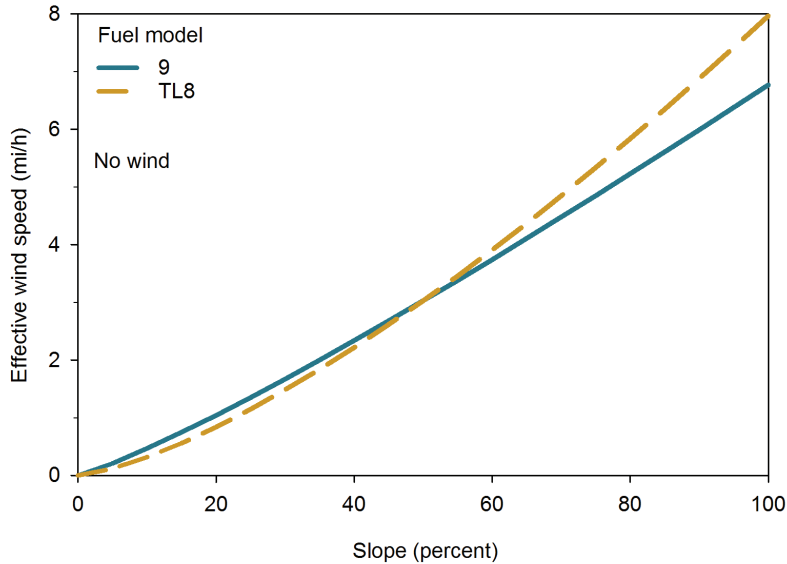


**Figure 45**—Effective wind speed for no wind and slope 0 to 100 percent for fuel models 9 and TL8.

#### 5.4.4 Wind Limit

Rothermel (1972, page 33) defined a wind speed limit as part of the model, above which predicted rate of spread is constant. Wind limit is a function of reaction intensity. It is now recommended that a wind limit not be imposed (Andrews et al. 2013).

Although the wind limit function was included in the Rothermel model to avoid over-prediction of fires burning in sparse fuels under high winds, it also plays a role in low intensity fires resulting from high moisture content. The influence is especially evident for dynamic grass fuel models with high live fuel moisture content (Jolly 2007; Scott and Burgan 2005). Figure 46 compares calculated rate of spread with and without the wind limit for dynamic fuel model GR1 (short, sparse, dry climate grass), dead moisture 8 percent, live moisture 100 percent, 0 slope, for a range of wind speed. For these conditions, the calculated wind limit is 1.6 mi/h. Rate of spread is then 0.7 ft/min for any wind over that value. For 9 mi/h midflame wind, rate of spread without the wind limit is 8.2 ft/min, which is over 10 times the spread rate (0.7 ft/min) when the wind limit is imposed.

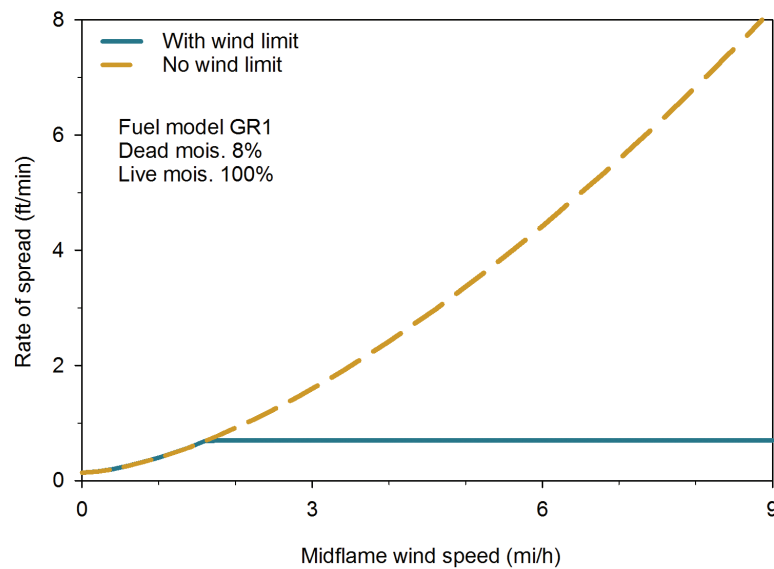


**Figure 46**—Comparison of rate of spread with and without imposition of the wind limit (fuel model GR1, dead moisture 8 percent and live moisture 100 percent). When the wind limit is imposed, rate of spread is constant for winds greater than 1.6 mi/h.

The Rothermel model is the foundation of many wildland fire modeling systems. Imposition of the wind limit can significantly affect results. When models are used to support fire management decisions, under-prediction of fire behavior is less acceptable than over-prediction. In addition to wildfire behavior prediction, contingency plans in a fire prescription include the potential spread of an escaped fire. Under-prediction would also be undesirable for low intensity fires burning under moist conditions, which are often modeled for prescribed fire planning.

## 6. Fire Spread Directions

The Rothermel surface fire spread model was developed for upslope spread with the wind. Adaptations have been made to find maximum rate of spread, fireline intensity, and flame length when the wind is not blowing upslope and spread in directions other than maximum. Various methods and models have been developed. Those described here are used in BehavePlus6 (tables 25, 26). Calculation of spread from the fire front and for fireline intensity associated with spread from an ignition point is from Catchpole et al. (1982).

**Table 25**—Input variables for spread direction equations.

Variable	Description	Notes
$R_0$	Zero-wind, zero-slope rate of spread	Calculated <sup>a</sup>
$\phi_w$	Wind factor	Calculated <sup>a</sup>
$\phi_s$	Slope factor	Calculated <sup>a</sup>
$\beta, \beta_{op}, E, C, B$	Intermediate values used to calculate effective wind speed	Calculated <sup>a</sup>
$H_A$	Heat per unit area <sup>b</sup>	Calculated <sup>a</sup>
$t$	Elapsed time	
$\omega$	Wind direction	Direction relative to upslope
$\gamma$	Direction from the ignition point (If $\psi$ in input, $\gamma$ is calculated.)	Direction relative to the direction of maximum spread
$\psi$	Direction normal to fire perimeter (If $\gamma$ is input, $\psi$ is calculated.)	Direction relative to the direction of maximum spread

<sup>a</sup>See table 6.<sup>b</sup>Used to calculate fireline intensity. Not affected by wind or slope.

## 6.1 Fire Behavior in the Direction of Maximum Spread

The basic surface spread equation assumes that the effects of wind and slope are in the same direction.

$$R = R_0(1 + \phi_w + \phi_s) = R_0 + R_0\phi_w + R_0\phi_s$$

where

$R_0$  = no-wind, no-slope rate of spread

$\phi_w$  = wind factor

$\phi_s$  = slope factor

In order to model fire spread with other than upslope wind, vector addition is used (fig. 47).

For elapsed time  $t$ , the slope vector has magnitude  $D_S$  and direction 0. The wind vector has magnitude  $D_W$  in direction  $\omega$  from upslope.

$$D_S = R_0\phi_s t$$

$$D_W = R_0\phi_w t$$

The slope vector is  $(D_S, 0)$  and the wind vector is  $(D_W \cos \omega, D_W \sin \omega)$ . The resultant vector is then  $(D_S + D_W \cos \omega, D_W \sin \omega)$ . The magnitude of the head fire vector is  $D_H$  in direction  $\alpha$ .

**Table 26**—Spread direction equations, as implemented in BehavePlus.

Description and equations	Source <sup>a</sup>
Rate of spread in direction of maximum spread, heading fire (see fig. 47)	
$R_H = R_0 + D_H/t$	
where	
$D_H = (X^2 + Y^2)^{1/2}$	
$X = D_S + D_W \cos \omega$	
$Y = D_W \sin \omega$	
$D_S = R_0 \phi_s t$	
$D_W = R_0 \phi_w t$	
Direction of maximum spread, relative to upslope	
$\alpha = \sin^{-1}( Y /D_H)$	
Effective wind factor in direction of maximum spread	
$\phi_E = R_H/R_0 - 1$	
Effective wind speed in direction of maximum spread (ft/min)	
$U_E = [\phi_E (\beta/\beta_{op})^E / C]^{-B}$	
Length-to-width ratio, ( $U_E$ in mi/h)	
$Z = L/W = 1 + .25 U_E$	
Rate of spread from ignition point, direction $\gamma$ relative to direction of maximum spread (see fig. 48)	
$R_\gamma = R_H (1 - e)/(1 - e \cos \gamma)$	
where	
$e = (Z^2 - 1)^{0.5}/Z$	
Rate of spread of backing fire (see fig. 48)	
$R_B = R_H (1 - e)/(1 + e)$	
Heading spread distance	
$D_H = R_H t$	
Backing spread distance	
$D_B = R_B t$	
Fire length	
$L = D_H + D_B$	
Maximum fire width	
$W = Z/L$	
Flanking spread distance	
$D_F = W/2$	
Ellipse dimensions (see fig. 49)	
$f = L/2$	
$g = D_H - f$	
$h = D_F = W/2$	
Rate of spread normal to fire perimeter ( $\psi$ ) at the point associated with the direction from ignition point ( $\gamma$ ), directions relative to direction of maximum spread.	
$R_\psi = R_H h(g \cos \theta + f)/(h^2 \cos^2 \theta + f^2 \sin^2 \theta)^{0.5}$	[4]
where	
$\cos \theta = (h \cos \gamma (h^2 \cos^2 \gamma + (f^2 - g^2) \sin^2 \gamma)^{0.5} - fg \sin^2 \gamma)/(h^2 \cos^2 \gamma + f^2 \sin^2 \gamma)$	[5]
Rate of spread, normal to the perimeter in direction $\psi$ , directions relative to direction of maximum spread	
$R_\psi = R_H (g \cos \psi + (f^2 \cos^2 \psi + h^2 \sin^2 \psi)^{0.5})$	[6]
Direction from ignition point ( $\gamma$ ) associated with associated with the input direction normal to fire perimeter ( $\psi$ ), directions relative to the direction of maximum spread	
$\tan \gamma = (h \sin \theta)/(g + f \cos \theta)$	[7]
where	
$\cos \theta = (h \cos \gamma (h^2 \cos^2 \gamma + (f^2 - g^2) \sin^2 \gamma)^{0.5} - fg \sin^2 \gamma)/(h^2 \cos^2 \gamma + f^2 \sin^2 \gamma)$	[5]
Fireline intensity ( $\psi$ is either input or calculated from $\gamma$ )	
$I_B = H_A R_\psi$	

<sup>a</sup>Equation number in Catchpole et al. (1982).

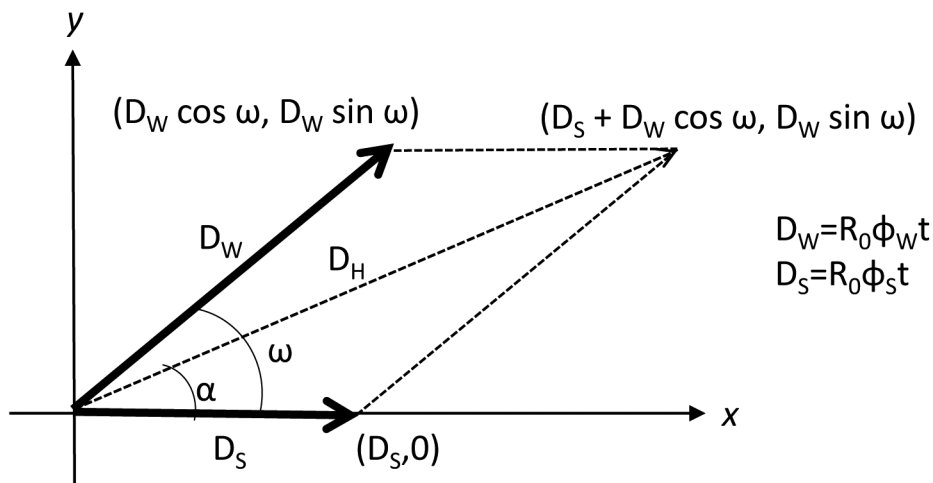


Figure 47—Vector addition to find head fire rate of spread when wind is not blowing upslope.

$$D_H = (X^2 + Y^2)^{1/2}$$

$$X = D_S + D_W \cos \omega$$

$$Y = D_W \sin \omega$$

$$\alpha = \sin^{-1}(|Y|/D_H)$$

The rate of spread in direction  $\alpha$  is then

$$R_H = R_0 + D_H/t$$

The effective wind factor ( $\phi_E$ ) in the direction of maximum spread (head fire) is found from the form of the spread equation

$$R_H = R_0(1 + \phi_E)$$

$$\phi_E = (R_H/R_0) - 1$$

The effective wind speed associated with that effective wind factor is a function of fuel variables

$$U_E = [\phi_E(\beta/\beta_{op})^E/C]^{-B}$$

The vector addition described above differs from the manual methods described by Rothermel (1983). A computer allows calculations that manual vectoring cannot; the difference is not great. The wind vector is based on calculated rate of spread for wind and no slope and the slope vector is from slope and no wind.

$$R_w = R_0(1 + \phi_w)$$

$$R_s = R_0(1 + \phi_s)$$

Consider upslope wind

$$\begin{aligned}
 R_H &= R_w + R_s \\
 &= R_0(1 + \phi_w) + R_0(1 + \phi_s) \\
 &= R_0(2 + \phi_w + \phi_s)
 \end{aligned}$$

This is not equal to

$$R_H = R_0(1 + \phi_w + \phi_s)$$

## 6.2 Fire Spread from a Single Ignition Point

When a fire starts from a single ignition point, it is assumed to be elliptically shaped (fig. 48) with the fire spreading at a steady rate throughout the projection time. The direction of maximum spread and the spread rate in that direction are as described above. Directions in the following equations are relative to the direction of maximum spread.

The ellipse length-to-width ratio is determined from the effective wind speed ( $U_E$ , mi/h) in the direction of maximum spread.

$$Z = L/W = 1 + .25 U_E$$

The eccentricity of the ellipse is

$$e = (Z^2 - 1)^{0.5}/Z$$

Rate of spread in direction  $\gamma$  from the ignition point is

$$R_\gamma = R_H(1 - e)/(1 - e \cos \gamma)$$

Backing fire spreads in the direction opposite of the heading fire. Rate of spread of the backing fire is

$$R_B = R_H(1 - e)/(1 + e)$$

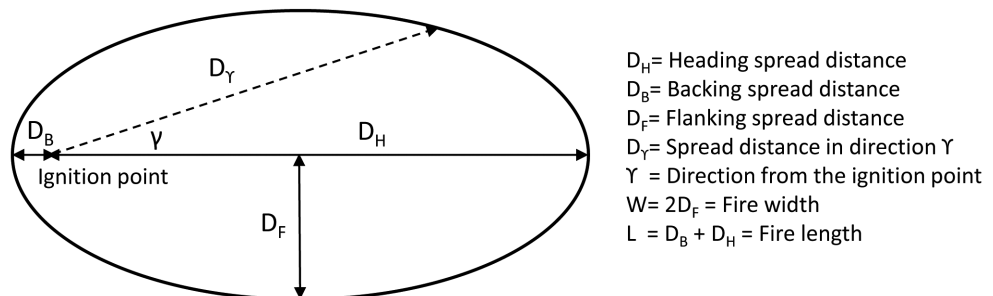


Figure 48—Fires that start from a single ignition point are assumed to be elliptically shaped.

Heading and backing spread distances are

$$D_H = R_H t$$

$$D_B = R_B t$$

Fire length and width are

$$L = D_H + D_B$$

$$W = Z/L$$

Flanking spread distance is

$$D_F = W/2$$

Ellipse dimensions (fig. 49) used in the following equations are

$$f = L/2$$

$$g = D_H - f$$

$$h = D_F$$

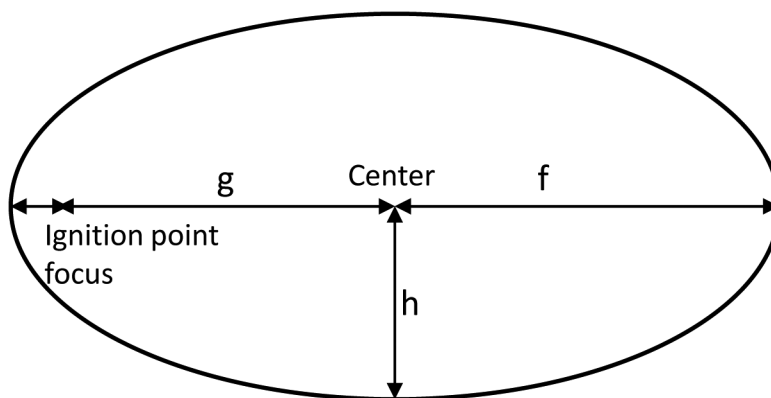


**Figure 49**—Ellipse dimensions; the ignition point is at a focus;  $f$ ,  $g$ , and  $h$  are used in equations for spread rate from the perimeter.

### 6.3 Fire Spread from Fire Perimeter

Fire spread rate and intensity on the perimeter of a fire are described by Catchpole et al. (1982). Details and derivation can be found in that paper. Their equation numbers are given in table 26. Given the direction from the ignition point ( $\gamma$ ), it is possible to find the associated direction normal to the perimeter ( $\psi$ ) and the rate of spread in that direction ( $R_\psi$ ) (fig. 50a).

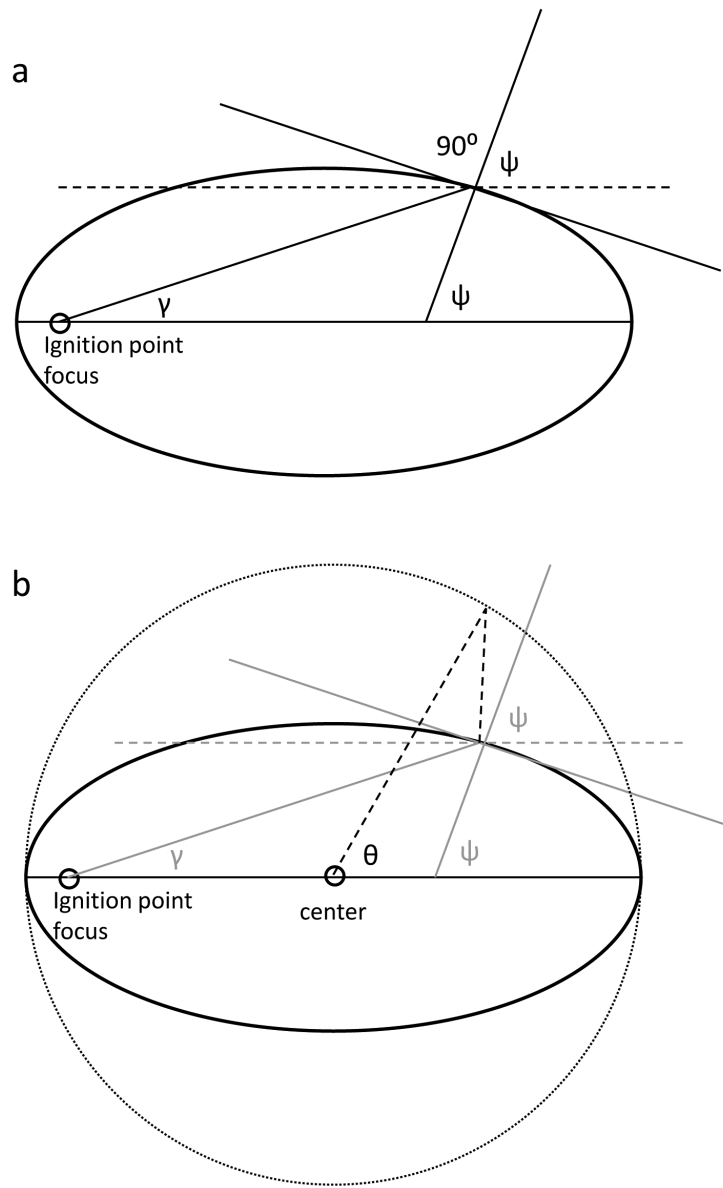


**Figure 50**—(a) Direction from ignition point ( $\gamma$ ) and from fire perimeter ( $\psi$ ) with respect to the direction of maximum spread. (b)  $\theta$  is an intermediate value needed to find  $\psi$  given  $\gamma$ .

An intermediate step is to find  $\theta$ , measured from the center of the ellipse (fig. 50b).

$$\cos \theta = (h \cos \gamma (h^2 \cos^2 \gamma + (f^2 - g^2) \sin^2 \gamma)^{0.5} - fg \sin^2 \gamma) / (h^2 \cos^2 \gamma + f^2 \sin^2 \gamma)$$

Rate of spread in the direction  $\psi$  is

$$R_\psi = (R_H h (g \cos \theta + f)) / (h^2 \cos^2 \theta + f^2 \sin^2 \theta)^{0.5}$$

The direction  $\psi$  is

$$\tan \psi = f / h \tan \theta$$

$$\psi = \tan^{-1} (f / h \tan \theta)$$

For a specified direction  $\psi$ , it is possible to find the spread rate in that direction ( $R_\psi$ ) and the associated direction from the ignition point ( $\gamma$ ).

$$R_\psi = g \cos \psi + (f^2 \cos^2 \psi + h^2 \sin^2 \psi)^{0.5}$$

$$\tan \gamma = (h \sin \theta) / (g + f \cos \theta)$$

## 6.4 Fireline Intensity

Byram's fireline intensity ( $I_B$ ) is

$$I_B = H_A R$$

Heat per unit area ( $H_A$ ) is not affected by wind or slope.  $R$  is rate of spread of the head fire (fig. 51a).

For directions other than head fire, the calculation uses rate of spread in the direction  $\psi$  (Catchpole et al. 1982) (fig. 51b).

$$I_B = H_A R_\psi$$

This relationship applies whether the direction  $\psi$  is specified or if it is the calculated direction associated with a specified  $\gamma$ .

Prior to version 6 of BehavePlus, when spread rate was calculated for spread from the ignition point in direction  $\gamma$ ,  $R_\gamma$  was used to find  $I_B$  (fig. 51c). This is the relationship used to develop the fire characteristics chart (Andrews et al. 2011; Andrews and Rothermel 1982). The relationship based on  $R_\psi$  does not lend itself to fire characteristics chart plots, except for heading and backing fire.

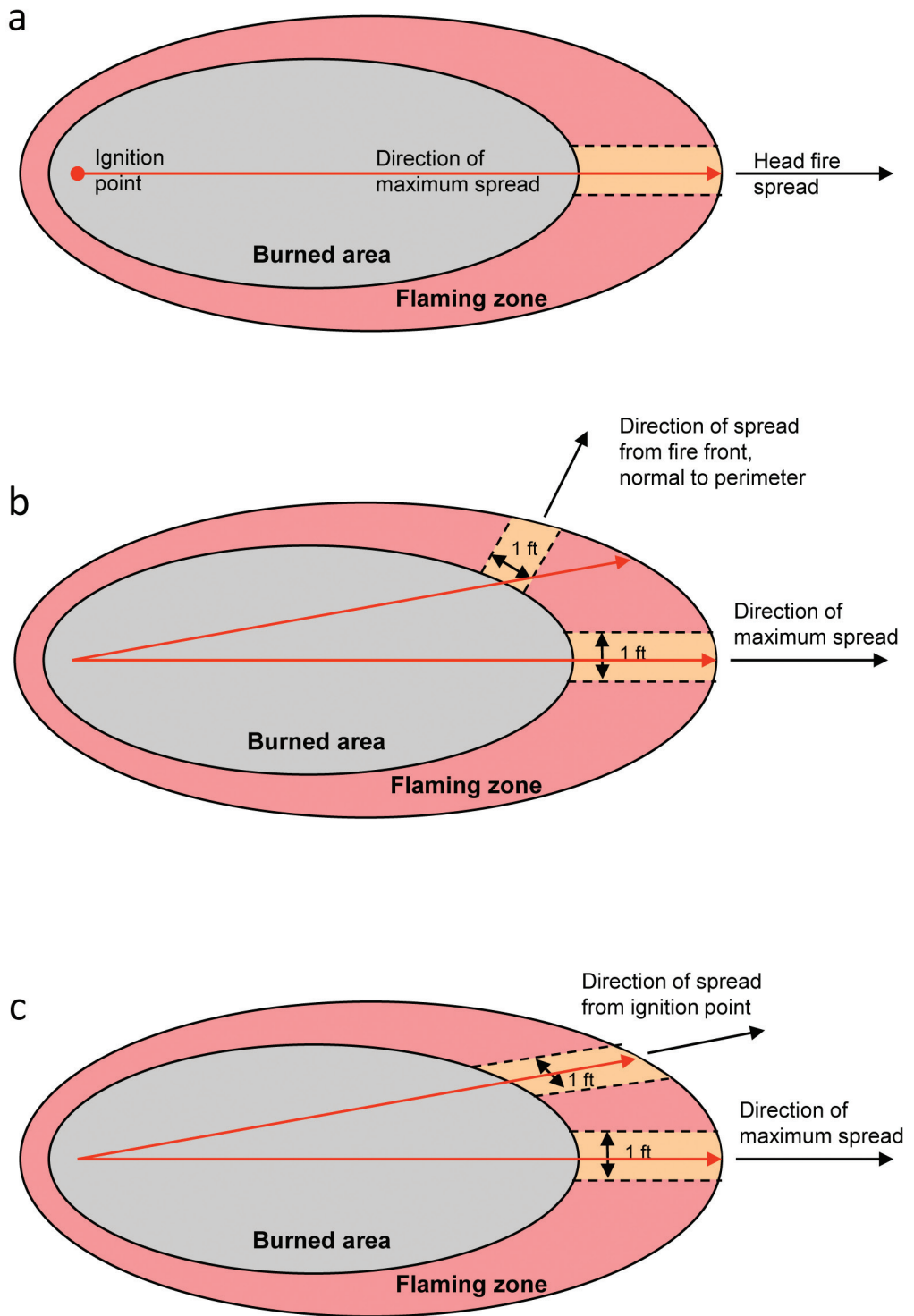


**Figure 51**—Portion of the burning front used to calculate fireline intensity: (a) head fire, the basic equation, (b) segment normal to the perimeter, used in BehavePlus6, (c) segment in the direction of spread from the ignition point, used in BehavePlus prior to version 6.

## 7. Rothermel Fire Spread Model in NFDRS

The first application of the Rothermel fire spread model was in the 1972 National Fire Danger Rating System (NFDRS) (Deeming et al. 1972). Subsequent updates to NFDRS are also based on that model. NFDRS produces integer indices designed to reflect seasonal changes in conditions in fire potential. While fire-danger indices and components are based on the same mathematical models used for fire behavior modeling, there are some significant computation differences.

At the time of this writing, the operational NFDRS is the 1978 version with optional 1988 revisions (Burgan 1988; Deeming et al. 1977). An update is in progress (W.M. Jolly, Missoula Fire Sciences Laboratory, personal communication, June 2016) but the basic equations remain the same.

Technical documentation of the 1978 NFDRS is found in Bradshaw et al. (1984). The basic equations, using FORTRAN variable names, are found in Cohen and Deeming (1985). Cohen (1985) compares fire danger and fire behavior equations.

Calculation of Spread Component (SC), Energy Release Component (ERC), and Burning Index (BI) is based on fuel model, fuel moisture, wind speed, and slope, which correspond to fire behavior rate of spread, heat per unit area, and flame length. The mathematical nomenclature of the body of this report is used to facilitate comparison of fire behavior and fire danger calculations.

### 7.1 Input Variables

Input variables for fire danger (FD) index calculations are essentially the same as for fire behavior (FB) (table 27; see table 5). Much of NFDRS is devoted to calculation of live and dead fuel moisture values as they change through the season. Fuel particle and fuel array variables are assigned values through fuel models. Some fuel model parameters also change through the season to reflect changes in fire danger. Wind speed is measured at 20-ft height and converted to midflame height based on a wind adjustment factor (WAF) assigned to each fuel model. Slope steepness is assigned through a slope class specified for a site.

### 7.2 Fuel Models

Parameters for the 20 1978 NFDRS fuel models are given in table 28; the 1988 fuel models are in table 29; and the five 2016 fuel models are in table 30 (c.f. FB fuel models table 8). The 1988 fuel model parameters that differ from those for the 1978 fuel models are highlighted. Moisture of extinction was changed for some to better predict fire danger in humid climates; some fuel loads were changed and a reservoir of dead fuel was added to improve drought response (Burgan 1988). The

**Table 27**—Input parameters for the fire spread model in NFDRS.

Type	Symbol <sup>a</sup>	Parameter	Notes
Fuel particle	$h_{ij}$	Heat content (Btu/lb)	Fuel model parameter. The same heat content is used for all live and dead components of a fuel model.
	$(S_T)_{ij}$	Total mineral content (fraction)	Constant = 0.0555
	$(S_e)_{ij}$	Effective mineral content (fraction)	Constant = 0.010
	$(\rho_p)_{ij}$	Particle density (lb/ft <sup>3</sup> )	Constant = 32 lb/ft <sup>3</sup>
Fuel array	$\sigma_{ij}$	Surface-area-to-volume ratio (ft <sup>2</sup> /ft <sup>3</sup> )	Fuel model parameter.
	$(w_0)_{ij}$	Oven-dry fuel load (tons/ac) [lb/ft <sup>2</sup> for fire behavior, (FB)]	Fuel model parameter. All loads are converted to lb/ft <sup>2</sup> by multiplying by 0.0459137. Initial value can change due to herbaceous curing, drought, and/or deciduous woody.
	$\delta$	Fuel bed depth (ft)	Fuel model parameter. Initial value can change due to addition of drought fuel.
	$(M_x)_1$	Dead fuel moisture of extinction (percent) [fraction for FB]	Fuel model parameter.
Environmental	$(M_f)_{ij}$	Fuel moisture (percent) [fraction for FB]	A large part of NFDRS is aimed at calculation of live and dead fuel moisture values as they change through the season.
	$U_{20}$	20-ft wind speed (mi/h) [U = midflame wind speed, ft/min for FB]	Wind adjustment factor (WAF) is assigned to each fuel model.
	$\tan \phi$	Slope steepness (fraction)	22.5% for slope class 1 31.8% for slope class 2 44.5% for slope class 3 63.6% for slope class 4 90.0% for slope class 5

<sup>a</sup>For dead fuel  $i = 1$ ;  $j = 1$  for 1-h,  $j = 2$  for 10-h,  $j = 3$  for 100-h,  $j = 4$  for 1,000-h. For live fuel  $i = 2$ ;  $j = 1$  for herbaceous,  $j = 2$  for woody. [c.f. fire behavior (FB) table 5].

2016 fuel models are derived from fire behavior fuel models; 1,000-h fuel has been added to two of them and other fuel model parameters (such as fuel bed depth) are changed. The tables give initial fuel model values, representing fully green conditions before curing and without any addition of drought fuel load.

Development of 1978 fuel models was based in part on NFDRS index calculations. According to Bradshaw et al. (1984, page 12), “The fuel modeling procedure incorporated a great deal of repetitive building and evaluating.” Fire danger fuel models are designed specifically to work with NFDRS. Because of differences in the calculations for fire danger versus fire behavior, it is not valid to use an NFDRS fuel model for fire behavior or vice versa.

Table 28—Fuel model parameters for the 1978 NFDERS.

Fuel model	Fuel load						Surface-area-to-volume ratio <sup>a</sup>				Fuel bed depth ft	Heat content Btu/lb	Dead fuel mois. ext. %
	1-h	10-h	100-h	1,000-h	Live herb	Live woody	1-h	Live herb	Live woody				
	-----	-----	-----	-----	-----	-----	-----	-----	-----	-----	-----	-----	-----
	tons/acre	ft <sup>2</sup> /ft <sup>3</sup>	ft <sup>2</sup> /ft <sup>3</sup>	ft <sup>2</sup> /ft <sup>3</sup>	ft <sup>2</sup> /ft <sup>3</sup>	ft <sup>2</sup> /ft <sup>3</sup>	ft <sup>2</sup> /ft <sup>3</sup>	ft <sup>2</sup> /ft <sup>3</sup>					
A	0.20	0	0	0	0.30	0	3,000	3,000	--	--	8,000	0.80	15
B	3.50	4.00	0.50	0	0	11.50	700	--	1,250	--	9,500	4.50	15
C	0.40	1.00	0	0	0.80	0.50	2,000	2,500	1,500	1,500	8,000	0.75	20
D	2.00	1.00	0	0	0.75	3.00	1,250	1,500	1,500	1,500	9,000	2.00	30
E	1.50	0.50	0.25	0	0.50	0.50	2,000	2,000	1,500	1,500	8,000	0.40	25
F	2.50	2.00	1.50	0	0	9.00	700	--	1,250	--	9,500	4.50	15
G	2.50	2.00	5.00	12.00	0.50	0.50	2,000	2,000	1,500	1,500	8,000	1.00	25
H	1.50	1.00	2.00	2.00	0.50	0.50	2,000	2,000	1,500	1,500	8,000	0.30	20
I	12.00	12.00	10.00	12.00	0	0	1,500	--	--	--	8,000	2.00	25
J	7.00	7.00	6.00	5.50	0	0	1,500	--	--	--	8,000	1.30	25
K	2.50	2.50	2.00	2.50	0	0	1,500	--	--	--	8,000	0.60	25
L	0.25	0	0	0	0.50	0	2,000	2,000	--	--	8,000	1.00	15
N	1.50	1.50	0	0	0	2.00	1,600	--	1,500	--	8,700	3.00	25
O	2.00	3.00	3.00	2.00	0	7.00	1,500	--	1,500	--	9,000	4.00	30
P	1.00	1.00	0.50	0	0.50	0.50	1,750	2,000	1,500	1,500	8,000	0.40	30
Q	2.00	2.50	2.00	1.00	0.50	4.00	1,500	1,500	1,200	1,200	8,000	3.00	25
R	0.50	0.50	0.50	0	0.50	0.50	1,500	2,000	1,500	1,500	8,000	0.25	25
S	0.50	0.50	0.50	0.50	0.50	0.50	1,500	1,500	1,200	1,200	8,000	0.40	25
T	1.00	0.50	0	0	0.50	2.50	2,500	2,000	1,500	1,500	8,000	1.25	15
U	1.50	1.50	1.00	0	0.50	0.50	1,750	2,000	1,500	1,500	8,000	0.50	20

<sup>a</sup>10-h = 109, 100-h = 30, 1,000-h = 8 ft<sup>2</sup>/ft<sup>3</sup>.

**Table 29**—Fuel model parameters for the 1988 NFDRS. Bold indicates a change from 1978 fuel models.

Fuel model	Fuel load				Surface-area-to-volume ratio <sup>a</sup>				Heat content Btu/lb	Fuel bed depth ft	Dead fuel mois. ext. %		
	1-h	10-h	100-h	1,000-h	Live herb	Live woody	Drought	1-h				Live herb	Live woody
	tons/acre	ft <sup>2</sup> /ft <sup>3</sup>	ft <sup>2</sup> /ft <sup>3</sup>	ft <sup>2</sup> /ft <sup>3</sup>	ft <sup>2</sup> /ft <sup>3</sup>				ft <sup>2</sup> /ft <sup>3</sup>	ft <sup>2</sup> /ft <sup>3</sup>			
A Western grasses (annual)	0.20	0	0	0	0.30	0	<b>0.2</b>	3,000	3,000	--	8,000	0.80	15
B California chaparral	3.50	4.00	0.50	0	0	11.50	<b>3.5</b>	700	--	1,250	9,500	4.50	15
C Pine-grass savanna	0.40	1.00	0	0	0.80	<b>0.80</b>	<b>1.8</b>	2,000	2,500	1,500	8,000	0.75	20
D Southern rough	2.00	1.00	0	0	<b>1.00</b>	3.00	<b>1.5</b>	1,250	1,500	1,500	9,000	2.00	<b>40</b>
E Hardwood litter (winter)	<b>1.00</b>	0.50	0.25	0	0.50	1.00	<b>1.5</b>	2,000	2,000	1,500	8,000	0.40	25
F Intermediate brush	2.50	2.00	1.50	0	<b>1.00</b>	7.00	<b>2.5</b>	700	<b>1,500</b>	1,250	9,500	4.50	15
G Short needle (heavy dead)	2.50	2.00	5.00	12.00	0.50	0.50	<b>5.0</b>	2,000	2,000	1,500	8,000	1.00	25
H Short needle (normal dead)	1.50	1.00	2.00	2.00	0.50	0.50	<b>2.0</b>	2,000	2,000	1,500	8,000	0.30	20
I Heavy slash	12.0	12.0	10.00	12.00	0	0	<b>12.0</b>	1,500	--	--	8,000	2.00	25
J Intermediate slash	7.00	7.00	6.00	5.50	0	0	<b>7.0</b>	1,500	--	--	8,000	1.30	25
K Light slash	2.50	2.50	2.00	2.50	0	0	<b>2.5</b>	1,500	--	--	8,000	0.60	25
L Western grasses (perennial)	0.25	0	0	0	0.50	0	<b>0.25</b>	2,000	2,000	--	8,000	1.00	15
N Sawgrass	1.50	1.50	0	0	0	2.00	<b>2.0</b>	1,600	--	1,500	8,700	3.00	<b>40</b>
O High pocosin	2.00	3.00	3.00	2.00	0	7.00	<b>3.5</b>	1,500	--	1,500	9,000	4.00	30
P Southern pine plantation	1.00	1.00	0.50	0	0.50	0.50	<b>1.0</b>	1,750	2,000	1,500	8,000	0.40	30
Q Alaskan black spruce	<b>2.50</b>	<b>5.40</b>	<b>2.90</b>	1.00	<b>1.00</b>	<b>3.00</b>	<b>3.5</b>	<b>3,500</b>	1,500	<b>1,500</b>	8,000	3.00	<b>18</b>
R Hardwood litter (summer)	0.50	0.50	0.50	0	0.50	0.50	<b>0.5</b>	1,500	2,000	1,500	8,000	0.25	25
S Tundra	0.50	0.50	0.50	0.50	0.50	0.50	<b>1.5</b>	1,500	1,500	1,200	8,000	0.40	25
T Sagebrush-grass	1.00	0.50	0	0	0.50	2.50	<b>1.0</b>	2,500	2,000	1,500	8,000	1.25	15
U Western pines	1.50	1.50	1.00	0	0.50	0.50	<b>2.0</b>	1,750	2,000	1,500	8,000	0.50	20

<sup>a</sup>10-h = 109, 100-h = 30, 1,000-h = 8 ft<sup>2</sup>/ft<sup>3</sup>.

Table 30—Fuel model parameters for the 2016 NFDRS.

NFDRS	Fuel model	Related fire behavior	Fuel load					Surface-area-to-volume ratio					Dead fuel moisture of extinction								
			1-h	10-h	100-h	1,000-h	Live herb Live woody	Drought	1-h	10-h	100-h	1,000-h	Live herb Live woody	Heat content	Fuel bed depth	Arid	Humid				
			tons/acre	ft <sup>2</sup> /ft <sup>3</sup>																	
V	Grass	GR2	0.1	0	0	0	1.0	0	0	0	0	2,000	109	30	8	2,000	1,500	8,000	1.0	15	40
W	Grass/shrub	GS2	0.5	0.5	0	0	0.6	1.0	1.0	1.0	1.0	2,000	109	30	8	2,000	1,500	8,000	1.5	15	40
X	Brush	SH9	4.5	2.45	0	0	1.55	7.0	2.5	2.5	2.5	2,000	109	30	8	2,000	1,500	8,000	4.4	25	40
Y	Timber litter	TL1	2.5	2.2	3.6	10.16	0	0	5.0	5.0	5.0	2,000	109	30	8	2,000	1,500	8,000	0.6	25	40
Z	Slash	SB2	4.5	4.25	4.0	4.0	0	0	7.0	7.0	7.0	2,000	109	30	8	2,000	1,500	8,000	1.0	25	40

## **7.3 Fuel Model Adjustments**

Fuel model parameters are adjusted before the fire model calculations are done. These relationships were developed to reflect changes in fuel throughout the season, which result in changes in fire danger. Equations for the three fuel model adjustments are given in table 31.

### ***7.3.1 Dynamic Herbaceous Fuel Load Transfer***

A dynamic fuel curing model was added to the 1978 NFDRS (Burgan 1979). All NFDRS fuel models with live herbaceous fuel are dynamic. Fuel load is transferred from the live herbaceous category to 1-h dead fuel as a function of live herbaceous moisture in the 1978 and 1988 NFDRS. Curing fraction for the 2016 NFDRS is calculated from the Growing Season Index (GSI).

When live herbaceous fuel is transferred to the 1-h category, its SAV changes for most 1978 and 1988 fuel models. A minor difference between FD and FB is that fire behavior modeling systems transfer fuel to a dead herbaceous category with the same SAV.

### ***7.3.2 Dynamic Deciduous Woody Fuel Load Transfer***

The 1988 NFDRS update gives the option of specifying live woody fuel as either coniferous (static) or deciduous (dynamic). Deciduous live woody fuel load is transferred to the 1-h dead fuel class as a function of the live woody greenness factor. This option is not used in the 2016 NFDRS.

### ***7.3.3 Drought Fuel Addition***

The 1988 NFDRS update includes a reservoir of additional fuel that can be used to simulate increased fuel availability as drought progresses. A portion of the drought load value is added to each dead fuel size class as a function of Keetch Byram Drought Index (KBDI). The initial fuel model depth is changed to preserve the bulk density of the initial fuel model. The drought fuel addition is done after dynamic fuel load transfers. This option is included in NFDRS 2016.

## **7.4 SC, ERC, BI Equations**

The equations for implementation of the Rothermel fire spread model for NFDRS indices SC, ERC, and BI are given in table 32. The fire behavior (FB) modeling equations (see tables 6 and 7) are compared to those used for SC and for ERC. BI is calculated from SC and ERC. These equations are the same for 1978, 1988, and 2016 NFDRS.

**Table 31**—Equations for NFDRS fuel model adjustments.

Element	Equation	Notes
<b>Dynamic herbaceous load transfer (curing)</b>		
Portion of fuel transferred from live herbaceous to dead (fraction)	$T = -0.0111(M_f)_{21} + 1.33$ $0 \leq T \leq 1.0$	For the 1978 and 1988 NFDRS. $(M_f)_{21}$ is herbaceous fuel moisture (percent).
	$T = -\left(\left(\frac{1.0}{1.0 - GU_H}\right) * GSI'\right)$ $+ \left(\frac{1.0}{1.0 - GU_H}\right)$ $0 \leq T \leq 1$	For the 2016 NFDRS. GSI is daily Growing Season Index (calculated from weather). GSI' is running average of daily GSI. $GU_H$ is GSI threshold for herbaceous greenup (input).
Live herbaceous fuel load, adjusted (lb/ft <sup>2</sup> )	$(w_0)_{21,new} = (w_0)_{21} - T (w_0)_{21}$	Reduced live herbaceous fuel load for dynamic fuel models
1-h fuel load, adjusted (lb/ft <sup>2</sup> )	$(w_0)_{11,new} = (w_0)_{11} + T (w_0)_{21}$	Increased dead 1-h load for dynamic fuel models. For NFDRS, the transferred live herbaceous fuel load uses the SAV of the 1-h fuel. [FB uses the SAV of the live herbaceous class]
<b>Dynamic live woody load transfer (deciduous). Not in 2016 NFDRS.</b>		
Live woody greenness factor	$G_w$	Input value
Dynamic live woody deciduous fuel load transfer (fraction)	$T = (1 - G_w)/20, \quad 0 \leq T \leq 1.0$	The fraction of fuel transferred from live woody to dead for fuel models designated as deciduous (dynamic). A 1988 NFDRS option.
Live woody fuel load, adjusted (lb/ft <sup>2</sup> )	$(w_0)_{22,new} = (w_0)_{22} - T (w_0)_{22}$	
1-h fuel load, adjusted (lb/ft <sup>2</sup> )	$(w_0)_{11,new} = (w_0)_{11} + T (w_0)_{21}$	
<b>Drought fuel addition</b>		
Keetch Byram Drought Index	$KBDI$	Calculated in NFDRS
Drought Load (lb/ft <sup>2</sup> )	$W_D$	Fuel model parameter for 1988 and 2016 fuel models. Potential total dead load that could be added due to drought. Converted from tons/ac to lb/ft <sup>2</sup> before calculations.
Fraction of dead load in each size class	$k_{1j} = (w_0)_{1j}/L_1$ where $L_1 = \sum_j (w_0)_{1j}$	The initial fuel model parameters may have been changes due to dynamic load transfer.
Total dead fuel load to add per unit increase in KBDI above 100 (lb/ft <sup>2</sup> )	$U_i = W_D / 700$	
Total dead fuel load to be added at the current level of drought (lb/ft <sup>2</sup> )	$W_a = (KBDI - 100) U_i$	
Dead fuel load, adjusted (lb/ft <sup>2</sup> )	$(w_0)_{1j,new} = (w_0)_{1j} + k_{1j} W_a$	
Bulk density (lb/ft <sup>3</sup> )	$\rho_b = \frac{1}{\delta} \sum_i \sum_j (w_0)_{ij}$	Initial pre-drought fuel model parameters. Total live and dead load divided by depth.
Fuel bed depth, adjusted (ft)	$\delta_{new} = (L_T - (w_0)_{14}) / \rho_b$  where $L_i = \sum_j (w_0)_{ij,new}$ $L_T = \sum_i L_i$	Adjustment to preserve the pre-drought bulk density

**Table 32a**—Equations for Spread Component (SC) and Energy Release Component (ERC) compared to those used for fire behavior (FB) modeling (see table 6a,b,c).

Element	FB equation	SC equation	ERC equation <sup>a</sup>	Notes
<b>Weighting factors</b>				
Weighting factors based on surface area	$A_{ij} = (\sigma)_{ij}(w_0)_{ij}/(\rho_p)_{ij}$ $A_i = \sum_j A_{ij}$ $A_T = \sum_i A_i$ $f_{ij} = A_{ij}/A_i$ $f_i = A_i/A_T$	$A_{ij} = (\sigma)_{ij}(w_0)_{ij}/(\rho_p)_{ij}$ $A_i = \sum_j A_{ij}$ $A_T = \sum_i A_i$ $f_{ij} = A_{ij}/A_i$ $f_i = A_i/A_T$	$A_{ij} = (\sigma)_{ij}(w_0)_{ij}/(\rho_p)_{ij}$ $A_i = \sum_j A_{ij}$ $A_T = \sum_i A_i$ $f_{ij} = A_{ij}/A_i$ $f_i = A_i/A_T$	Same
Weighting factors based on fuel load	<p>Fuel is partitioned by size into six subclasses:</p> <ul style="list-style-type: none"> <li><math>\sigma \geq 1,200</math></li> <li><math>1,200 &gt; \sigma \geq 192</math></li> <li><math>192 &gt; \sigma \geq 96</math></li> <li><math>96 &gt; \sigma \geq 48</math></li> <li><math>48 &gt; \sigma \geq 16</math></li> <li><math>16 &gt; \sigma</math></li> </ul> <p>Members of each subclass are given the same weighting factor:</p> $g_{ij} = \sum_{\substack{\text{subclass} \\ \text{to which} \\ j \text{ belongs}}} f_{ij}$ <p>for <math>\sigma &lt; 16, g_{ij} = 0</math></p>	<p>Fuel is partitioned by size into six subclasses:</p> <ul style="list-style-type: none"> <li>N/A</li> </ul>	<p>N/A</p>	<p>Used for net fuel load for FB.</p> <p>Not used in NFDRS due to an oversight. There is an effect for fuel models with both live herbaceous and live woody fuel, with SAV <math>\geq 1,200 \text{ ft}^2/\text{ft}^3</math>.</p>
Weighting factors based on fuel load	N/A	N/A	$L_i = \sum_j (w_0)_{ij}$ $L_T = \sum_i L_i$ $k_{ij} = (w_0)_{ij}/L_i$ $k_i = L_i/L_T$	Developed for NFDRS ERC calculation. Includes 1,000-h fuel.

N/A, not applicable, indicates that the equation is not needed.

<sup>a</sup>The umlaut (pair of dots) above the variable indicates a difference from FB, either because the equation is different or because the result is different due to a change in a prior equation.

**Table 32b**—Equations for Spread Component (SC) and Energy Release Component (ERC) compared to those used for fire behavior (FB) modeling (see table 6a, b, c).

Element	FB equation	SC equation	ERC equation <sup>a</sup>	Notes
<b>Moisture of extinction</b>				
Live fuel moisture of extinction (fraction for FB) (percent for FD)	$(M_x)_2 = 2.9W \frac{(1 - M_{f,dead})}{(\min = (M_x)_1)} - 0.226$ <p>where, Dead-to-live load ratio  <math display="block">W = \frac{\sum_j (w_0)_{1j} \exp(-138/\sigma_{1j})}{\sum_j (w_0)_{2j} \exp(-500/\sigma_{2j})}</math> </p>	$(M_x)_2 = 2.9W \frac{(1 - M_{f,dead})}{(\min = (M_x)_1)} - 0.226$ <p>where, Dead-to-live load ratio  <math display="block">W = \frac{\sum_j (w_0)_{1j} \exp(-138/\sigma_{1j})}{\sum_j (w_0)_{2j} \exp(-500/\sigma_{2j})}</math> </p>	$(M_x)_2 = 2.9W \frac{(1 - M_{f,dead})}{(\min = (M_x)_1)} - 0.226$ <p>where, Dead-to-live load ratio  <math display="block">W = \frac{\sum_j (w_0)_{1j} \exp(-138/\sigma_{1j})}{\sum_j (w_0)_{2j} \exp(-500/\sigma_{2j})}</math> </p>	Same 1,000-h fuel not in ERC calculation.
	<p>“Fine” dead fuel moisture  <math display="block">\frac{M_{f,dead}}{\sum_j (M_f)_{1j} (w_0)_{1j} \exp(-138/\sigma_{1j})} = \frac{M_{f,dead}}{\sum_j (w_0)_{1j} \exp(-138/\sigma_{1j})}</math> </p>	<p>“Fine” dead fuel moisture  <math display="block">\frac{M_{f,dead}}{\sum_j (M_f)_{1j} (w_0)_{1j} \exp(-138/\sigma_{1j})} = \frac{M_{f,dead}}{\sum_j (w_0)_{1j} \exp(-138/\sigma_{1j})}</math> </p>	<p>“Fine” dead fuel moisture  <math display="block">\frac{M_{f,dead}}{\sum_j (M_f)_{1j} (w_0)_{1j} \exp(-138/\sigma_{1j})} = \frac{M_{f,dead}}{\sum_j (w_0)_{1j} \exp(-138/\sigma_{1j})}</math> </p>	
<b>Characteristic values for live and dead categories</b>				
Net fuel load (lb/ft <sup>2</sup> )	$(w_n)_{ij} = (w_0)_{ij} (1 - (S_T)_{ij})$ $(w_n)_i = \sum_j g_{ij} (w_n)_{ij}$	$(w_n)_{ij} = (w_0)_{ij} (1 - (S_T)_{ij})$ $(w_n)_i = \sum_j f_{ij} (w_n)_{ij}$	$(w_n)_{ij} = (w_0)_{ij} (1 - (S_T)_{ij})$ $(w_n)_i = \sum_j (w_n)_{ij}$	Same g weighting factor inadvertently not used in NFDRS SC. No weighting for ERC.
Heat content (Btu/lb)	$h_i = \sum_j f_{ij} h_{ij}$	$h_1 = h_2$	$h_1 = h_2$	Weighting not needed for NFDRS because the same value is used for all classes, live and dead in a fuel model.
Effective mineral content (fraction)	$(S_e)_i = \sum_j f_{ij} (S_e)_{ij}$	$(S_e)_1 = (S_e)_2 = 0.0100$	$(S_e)_1 = (S_e)_2 = 0.0100$	Weighting not needed for NFDRS because the same value is used for all classes, live and dead.
Mineral damping coefficient	$(\eta_s)_i = 0.174 (S_e)_i^{-0.19}$ $(\max = 1)$	$(\eta_s)_i = 0.174 (S_e)_i^{-0.19}$ $(\max = 1)$	$(\eta_s)_i = 0.174 (S_e)_i^{-0.19}$ $(\max = 1)$	Same

N/A, not applicable, indicates that the equation is not needed.

<sup>a</sup>The umlaut (pair of dots) above the variable indicates a difference from FB, either because the equation is different or because the result is different due to a change in a prior equation.

**Table 32c**—Equations for Spread Component (SC) and Energy Release Component (ERC) compared to those used for fire behavior (FB) modeling (see table 6a,b,c).

Element	FB equation	SC equation	ERC equation <sup>a</sup>	Notes
<b>Characteristic values for live and dead categories (continued)</b>				
Moisture content (fraction for FB) (percent for FD)	$(M_f)_i = \sum_j f_{ij} (M_f)_{ij}$	$(M_f)_i = \sum_j f_{ij} (M_f)_{ij}$	$(\dot{M}_f)_i = \sum_j k_{ij} (M_f)_{ij}$	Surface area weighted for SC and load weighted for ERC
Moisture damping coefficient	$(\eta_M)_i = 1 - 2.59(r_M)_i + 5.11(r_M)_i^2 - 3.52(r_M)_i^3$ $(r_M)_i = (M_f)_i / (M_x)_i$ , max = 1	$(\eta_M)_i = 1 - 2.59(r_M)_i + 5.11(r_M)_i^2 - 3.52(r_M)_i^3$ $(r_M)_i = (M_f)_i / (M_x)_i$ , max = 1	$(\dot{\eta}_M)_i = 1 - 2.0(\dot{r}_M)_i + 1.5(\dot{r}_M)_i^2 - 0.5(\dot{r}_M)_i^3$ $(\dot{r}_M)_i = (\dot{M}_f)_i / (M_x)_i$ , max = 1	ERC uses fuel load weighted moisture. ERC equation developed for NFDRS.
Surface-area-to-volume ratio (ft <sup>2</sup> /ft <sup>3</sup> )	$\sigma_i = \sum_j f_{ij} \sigma_{ij}$	$\sigma_i = \sum_j f_{ij} \sigma_{ij}$	$\ddot{\sigma}_i = \sum_j k_{ij} \sigma_{ij}$	ERC uses load weighted SAV
<b>Fuel bed characteristic values</b>				
Surface-area-to-volume ratio (ft <sup>2</sup> /ft <sup>3</sup> )	$\sigma = \sum_i f_i \sigma_i$	$\sigma = \sum_i f_i \sigma_i$	$\ddot{\sigma} = \sum_{ij} k_{ij} \ddot{\sigma}_i$	ERC uses load weighted SAV
Mean bulk density (lb/ft <sup>3</sup> )	$\rho_b = \frac{1}{\delta} \sum_i \sum_j (w_o)_{ij}$	$\rho_b = \frac{1}{\delta} \sum_i \sum_j (w_o)_{ij}$	$\rho_b = \frac{1}{\delta} \sum_i \sum_j (w_o)_{ij}$	1,000-h fuel not in ERC calculation.
Mean packing ratio	$\beta = \sum_i \sum_j (\rho_b)_{ij} / (\rho_p)_{ij}$	$\beta = \sum_i \sum_j (\rho_b)_{ij} / (\rho_p)_{ij}$	$\beta = \sum_i \sum_j (\rho_b)_{ij} / (\rho_p)_{ij}$	Same. For NFDRS $\rho_p = 32$ lb/ft <sup>3</sup>
Optimum packing ratio	$\beta_{op} = 3.348(\sigma)^{-0.8189}$	$\beta_{op} = 3.348(\sigma)^{-0.8189}$	$\beta_{op} = 3.348(\ddot{\sigma})^{-0.8189}$	ERC uses load weighted SAV

N/A, not applicable, indicates that the equation is not needed.

<sup>a</sup>The umlaut (pair of dots) above the variable indicates a difference from FB, either because the equation is different or because the result is different due to a change in a prior equation.

**Table 32d**—Equations for Spread Component (SC) and Energy Release Component (ERC) compared to those used for fire behavior (FB) modeling (see table 6a,b,c).

Element	FB equation	SC equation	ERC equation <sup>a</sup>	Notes
<b>Wind and slope</b>				
Slope factor	$\phi_s = 5.275\beta^{-0.3}(\tan\phi)^2$	$\phi_s = 5.275\beta^{-0.3}(\tan\phi)^2$	N/A	Same
Wind factor	$\phi_w = CU^B(\beta/\beta_{op})^{-E}$ where $C = 7.47\exp(-0.133\sigma^{0.55})$ $B = 0.02526\sigma^{0.54}$ $E = 0.715\exp(-3.59\times 10^{-4}\sigma)$	$\phi_w = C(U_{20} * 88 * WAF)^B(\beta/\beta_{op})^{-E}$ where $C = 7.47\exp(-0.133\sigma^{0.55})$ $B = 0.02526\sigma^{0.54}$ $E = 0.715\exp(-3.59\times 10^{-4}\sigma)$	N/A	FB wind input (U) is midflame (ft/min). NFDRS wind input (U <sub>20</sub> ) is 20-ft (mi/h). Conversion to midflame in ft/min is in the equation. A wind adjustment factor (WAF) is assigned to each NFDRS fuel model.
Wind limit (ft/min)	$U = 0.9I_R$	$U = 0.9I_R$	N/A	The wind limit applied to midflame wind in NFDRS and to effective wind speed in BehavePlus. BehavePlus also offers the option of not applying the wind limit.
<b>Heat source</b>				
Maximum reaction velocity (min <sup>-1</sup> )	$\Gamma'_{max} = \sigma^{1.5}(495 + 0.0594\sigma^{1.5})^{-1}$	$\Gamma'_{max} = \sigma^{1.5}(495 + 0.0594\sigma^{1.5})^{-1}$	$\ddot{\Gamma}'_{max} = \sigma^{1.5}(495 + 0.0594\sigma^{1.5})^{-1}$	
Optimum reaction velocity (min <sup>-1</sup> )	$\Gamma' = \Gamma'_{max}(\beta/\beta_{op})^A \exp[A(1 - \beta/\beta_{op})]$ $A = 133\sigma^{-0.7913}$	$\Gamma' = \Gamma'_{max}(\beta/\beta_{op})^A \exp[A(1 - \beta/\beta_{op})]$ $A = 133\sigma^{-0.7913}$	$\ddot{\Gamma}' = \ddot{\Gamma}'_{max}(\beta/\beta_{op})^A \exp[\dot{A}(1 - \beta/\beta_{op})]$ $\ddot{A} = 133\sigma^{-0.7913}$	
Reaction intensity (Btu/ft <sup>2</sup> -min)	$I_R = \Gamma' \sum_i (w_{n_i})_i h_i (\eta_M)_i (\eta_S)_i$	$I_R = \Gamma' \sum_i (w_{n_i})_i h_i (\eta_M)_i (\eta_S)_i$	$\ddot{I}_R = \ddot{\Gamma}' \sum_i k_i (\ddot{w}_{n_i})_i h_i (\ddot{\eta}_M)_i (\eta_S)_i$	ERC includes an additional weighting factor

N/A, not applicable, indicates that the equation is not needed.

<sup>a</sup>The umlaut (pair of dots) above the variable indicates a difference from FB, either because the equation is different or because the result is different due to a change in a prior equation.

**Table 32e**—Equations for Spread Component (SC) and Energy Release Component (ERC) compared to those used for fire behavior (FB) modeling (see table 6a,b,c).

Element	FB equation	SC equation	ERC equation <sup>a</sup>	Notes
<b>Heat source (continued)</b>				
Propagating flux ratio	$\xi = (192 + 0.2595\sigma)^{-1} \exp[(0.792 + 0.681\sigma^{0.5})(\beta + 0.1)]$	$\xi = (192 + 0.2595\sigma)^{-1} \exp[(0.792 + 0.681\sigma^{0.5})(\beta + 0.1)]$	N/A	Same
Heat source	$I_R \xi (1 + \phi_w + \phi_s)$	$I_R \xi (1 + \phi_w + \phi_s)$	N/A	
<b>Heat sink</b>				
Heat of preignition for each size class, live and dead	$(Q_{ig})_{ij} = 250 + 1116(M_r)_{ij}$	$(Q_{ig})_{ij} = 250 + 11.16(M_r)_{ij}$	N/A	FB moisture is fraction. FD is percent
Heat sink (Btu/ft <sup>3</sup> )	$\rho_b \epsilon Q_{ig} = \rho_b \sum_i \sum_j f_{ij} [ \exp(-138/\sigma_{ij}) ] (Q_{ig})_{ij}$	$\rho_b \epsilon Q_{ig} = \rho_b \sum_i \sum_j f_{ij} [ \exp(-138/\sigma_{ij}) ] (Q_{ig})_{ij}$	N/A	Same
<b>Rate of Spread</b>				
Zero-wind, zero-slope rate of spread (ft/min)	$R_0 = \frac{I_R \xi}{\rho_b \epsilon Q_{ig}}$	$R_0 = \frac{I_R \xi}{\rho_b \epsilon Q_{ig}}$	N/A	
Rate of spread (ft/min)	$R = R_0(1 + \phi_w + \phi_s)$	$R = R_0(1 + \phi_w + \phi_s)$	N/A	SC is essentially the same as R for FB. The difference is in wind limit and g factor.
<b>Flame Length</b>				
Residence time (min)	$t_r = 384/\sigma$	N/A	$t_r = 384/\sigma$	Same
Heat per unit area (Btu/ft <sup>2</sup> )	$H_A = I_R t_r$	N/A	$\dot{H}_A = \dot{I}_R t_r$	Surface area weighted SAV.
Flame length (ft)	$F_B = 0.45 I_B^{0.46}$	N/A	$\dot{F}_B = 0.45 \dot{I}_B^{0.46}$	
Fireline Intensity (Btu/ft/sec)	$I_B = I_R t_r R/60$		$\dot{I}_B = \dot{I}_R t_r R/60$	

N/A, not applicable, indicates that the equation is not needed.

<sup>a</sup>The umlaut (pair of dots) above the variable indicates a difference from FB, either because the equation is different or because the result is different due to a change in a prior equation.

**Table 32f**—Equations for Spread Component (SC) and Energy Release Component (ERC) compared to those used for fire behavior (FB) modeling (see table 6a,b,c).

Element	FB equation	SC equation	ERC equation <sup>a</sup>	Notes
<b>NFDRS indices and components</b>				
Spread Component (SC)	N/A	$SCx = R$ $SC = RND(SCx)$	N/A	Rounded to give an integer SC; unrounded value is used for BI calculation.
Energy Release Component (ERC)	N/A	N/A	$ERCx = (0.04\ddot{I}_{R,t_r}) = 0.04H_A$ $ERC = RND(ERCx)$	Rounded to give an integer ERC; unrounded value is used for BI calculation.
Burning Index (BI)	N/A	N/A	$BI = RND[3.01(SCx \cdot ERCx)^{0.46}]$	Uses unrounded SC and ERC then rounded to give an integer BI.

N/A, not applicable, indicates that the equation is not needed.

<sup>a</sup>The umlaut (pair of dots) above the variable indicates a difference from FB, either because the equation is different or because the result is different due to a change in a prior equation.

### **7.4.1 Spread Component, SC**

Calculation of Spread Component (SC) is very similar to that of rate of spread (R). The SC calculation uses the Rothermel spread model with surface area weighting factors. The 1,000-h fuel in NFDRS fuel models plays no role in calculation of SC. SC is equal to the rounded value of rate of spread in ft/min. The unrounded SC is used to calculate Burning Index (BI).

Three differences between calculation of SC in NFDRS and rate of spread (R) in fire behavior modeling systems affect results.

1. Fuel load is transferred from live herbaceous to 1-h dead fuel for fire danger and to dead herbaceous fuel for fire behavior. The surface-area-to-volume ratio of the 1-h and dead herbaceous classes might be different.
2. The wind limit is applied to midflame wind speed for fire danger and generally to effective wind speed (which includes the effect of slope) for fire behavior. BehavePlus includes the recommended option of not imposing a wind limit.
3. The g factors of Albin (1976) are used in fire behavior systems, but not in fire danger. This can affect results for NFDRS fuel models that include both live herbaceous and woody fuel.

The SC calculation uses the original f weighting factors in Rothermel (1972) rather than the revised g factors by Albin (1976). This affects results when there is more than one fuel component in a fuel subclass. For the 20 NFDRS fuel models, there is no effect on dead fuel because the surface-area-to-volume ratios of 1-h, 10-h, and 100-h fuel put them each in a separate subclass, and the load transfer method moves the live herbaceous fuel to the 1-h class. There is, however, an effect for fuel models with both live herbaceous and live woody fuel, with surface-area-to-volume ratio greater than or equal to  $1,200 \text{ ft}^2/\text{ft}^3$ . This is the case for 11 of the 20 1978/1988 NFDRS fuel models.

This difference and the reason were noted by Cohen (1985).

A technical oversight is responsible for the NFDRS [reaction intensity] not being calculated exactly the same as the [fire behavior reaction intensity]. ... When Albin's (1976) technical changes were incorporated, the loading computation change was missed. ... the NFDRS live fuel classes, herbaceous and woody, have surface-area-to-volume ratios that usually fall into a single surface-area-to-volume ratio subclass. Without Albin's modification, when herbaceous and woody loadings are present in a fuel model, the live loadings are mathematically reduced.

### **7.4.2 Energy Release Component, ERC**

Energy Release Component (ERC) is based on the calculation of heat per unit area, which is the product of reaction intensity and residence time. Residence time uses surface area weighting, the same as for fire behavior modeling. The reaction intensity calculation was changed for NFDRS to use a weighting scheme based on fuel load rather than on surface area to give more influence to the heavy fuels.

As noted by Bradshaw et al. (1984, page 24), “This solution had no experimental basis.” When 1,000-h fuel is part of the fuel model, it plays an important part in the calculation of ERC.

There are three differences between the calculation of ERC in NFDRS and heat per unit area for fire behavior.

1. Reaction intensity includes fuel load weighting factors for fire danger, while surface area weighting is used for fire behavior.
2. The reaction intensity equation for fire danger includes an additional weighting factor not used in fire behavior.
3. The moisture damping coefficient equation is different for fire danger and fire behavior.

In the following equations, the umlaut (pair of dots) above the variable indicates a difference between fire behavior and fire danger, either because the equation is different or because the result is different due to a change in a prior equation.

Calculation of reaction intensity for ERC includes weighting factors based on fuel load to reflect the role of larger fuels on fire intensity. The weighting factors for each size class of fuel ( $k_{ij}$ ) are based on the fraction of the total fuel load contributed by that size class in its category (live or dead). The weighting factors for live and dead fuel ( $k_i$ ) are based on the fraction of the total fuel load contributed by the dead and the live categories.

$$L_i = \sum_j (w_0)_{ij}$$

$$L_T = \sum_i L_i$$

$$k_{ij} = (w_0)_{ij} / L_i$$

$$k_i = L_i / L_T$$

Net fuel load for the live and dead categories is the sum of the fuel load values. For fire behavior the net fuel load includes the surface area weighting factor.

$$(\ddot{w}_n)_i = \sum_j (w_n)_{ij}$$

Characteristic live and dead fuel moisture is based on the load weighting factor.

$$(\ddot{M}_f)_i = \sum_j k_{ij} (M_f)_{ij}$$

The moisture damping coefficient used to calculate fire behavior rate of spread and heat per unit area and SC is different from that used to calculate ERC (fig. 52). The alternate moisture damping coefficient was developed to provide a continuing increase in the ERC as fuel moistures in the midrange decrease (Schroeder et al. 1972).

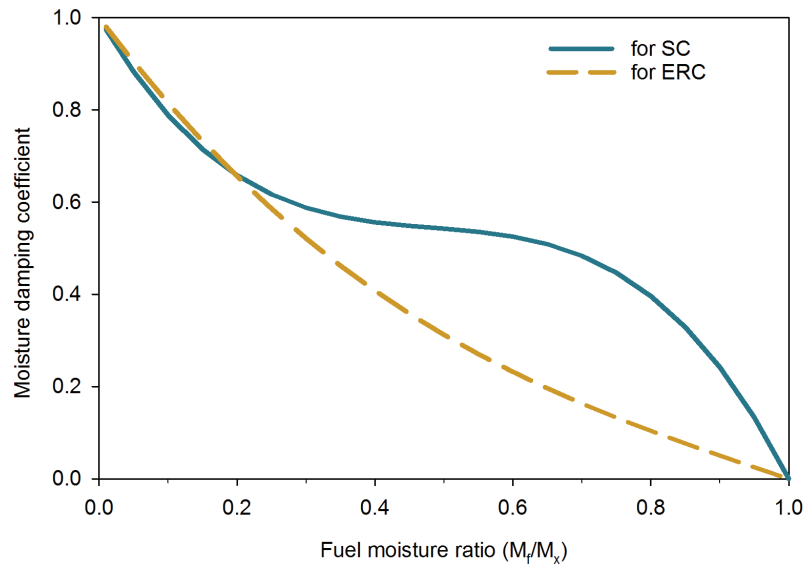


**Figure 52**—The moisture damping coefficient in the Rothermel (1972) fire spread model is used for Spread Component (SC). An alternate version was developed to calculate Energy Release Component (ERC).

SC calculation uses the moisture damping coefficient from Rothermel (1972).

$$(\eta_M)_i = 1 - 2.59(r_M)_i + 5.11 (r_M)_i^2 - 3.52(r_M)_i^3$$

$$(r_M)_i = (M_f)_i / (M_x)_i \text{ (max = 1.0)}$$

ERC calculation uses different coefficients in the equation.

$$(\check{\eta}_M)_i = 1 - 2.0(\check{r}_M)_i + 1.5(\check{r}_M)_i^2 - 0.5(\check{r}_M)_i^3$$

$$(\check{r}_M)_i = (\check{M}_f)_i / (M_x)_i \text{ (max = 1.0)}$$

The characteristic surface-area-to-volume ratio ( $\sigma$ ) used for residence time in NFDRS is the same as for fire behavior, using the surface area weighting factors. For ERC, the load weighted surface-area-to-volume ratio ( $\check{\sigma}$ ) is used to find optimum packing ratio ( $\check{\beta}_{op}$ ), maximum reaction velocity ( $\check{\Gamma}'$ ), and optimum reaction velocity ( $\check{\Gamma}'_{max}$ ), which are used to calculate reaction intensity ( $\check{I}_R$ ).

$$\check{\sigma}_i = \sum_j k_{ij} \sigma_{ij}$$

$$\check{\sigma} = \sum_{ij} k_i \check{\sigma}_i$$

For NFDRS fuel models, the same heat content value is used for the live and dead categories ( $h_i$ ). Heat content ranges from 8,000 to 9,500 Btu/lb for the 20 fuel models.

For ERC there is a difference in reaction intensity ( $\ddot{I}_R$ ) due to a difference in net load ( $(\ddot{w}_n)_i$ ), moisture damping coefficient ( $(\ddot{\eta}_M)_i$ ), and optimum reaction velocity ( $\ddot{\Gamma}'$ ).

$$\ddot{I}_R = \ddot{\Gamma}' \sum_i k_i (\ddot{w}_n)_i h_i (\ddot{\eta}_M)_i (\eta_s)_i$$

The equation for reaction intensity in the 1978 NFDRS also includes a weighting factor ( $k_i$ ) not in the 1972 NFDRS (Schroeder et al. 1972, page 43) or in fire behavior calculations. The reason is not stated in technical documentation of NFDRS (Bradshaw et al. 1984). Based on the memory of one of the developers, that factor was added because it produced better results with 1,000-h fuels, which were added to fuel models in the 1978 NFDRS (Jack D. Cohen, Missoula Fire Sciences Laboratory, personal communication, July 2011).

The final calculation of ERC includes a scaling factor (0.04 ft<sup>2</sup>/Btu) such that a unit value of ERC is equal to 25 Btu of available energy per square foot. The unrounded ERC value ( $ERCx$ ) is used to calculate BI.

$$ERCx = 0.04 \ddot{H}_A = 0.04 \ddot{I}_R t_r$$

$$ERC = RND(ERCx)$$

### 7.4.3 Burning Index, BI

BI is based on the flame length model and is calculated from the fuel load weighted reaction intensity ( $\ddot{I}_R$ ), the surface area weighted rate of spread ( $R$ ), and the surface area weighted residence time ( $t_r$ ). BI is a function of SC and ERC, with a scaling factor such that BI is 10 times the calculated flame length. This is, however, not equal to flame length used in fire behavior modeling.

$$BIx = 10 \ddot{F}_B = 10 \cdot 0.45 (\ddot{I}_R t_r R / 60)^{0.46}$$

$$BIx = 10 \cdot 0.45 [(25ERCx)(SCx/60)]^{0.46}$$

$$BIx = 3.01 (SCx \cdot ERCx)^{0.46}$$

$$BI = RND[BIx]$$

Technical documentation (Bradshaw et al. 1984; Cohen and Deeming 1985) gives the relationship to calculate BI from SC and ERC, not stating that the unrounded values are used rather than the final rounded index values. The computer code, however, uses unrounded SC and ERC values (Larry S. Bradshaw, Missoula Fire Sciences Laboratory, personal communication, July 2011).

#### 7.4.4 Burning Index Compared to Flame Length

While SC, ERC, and BI are related to rate of spread, heat per unit area, and flame length, they are not the same due to differences in the calculations. Burning Index is not technically equal to 10 times flame length. NFDRS components and indices are relative values, which are interpreted in terms of climatology.

Consider fuel model G with for selected moisture, wind, and slope conditions. BI is calculated using the calculator option in FireFamilyPlus 4.1 (Bradshaw and McCormick 2000). Flame length is calculated using BehavePlus with the fuel parameters for fuel model G. For the same inputs, flame length is significantly less than BI/10 (table 33). For dead moisture of 5 percent and live moisture of 50 percent, BI/10 is 7.7 ft compared to flame length of 5.4 ft.

**Table 33**—Burning Index (BI) divided by 10 is not equal to flame length due to differences in fire danger and fire behavior calculations. Comparison for fuel model G, slope class 1 (22.5 percent), wind adjustment factor 0.4.

<b>Dead fuel moisture</b>	<b>Live fuel moisture</b>	<b>20-ft wind</b>	<b>BI</b>	<b>BI/10</b>	<b>Flame length</b>
<i>-----percent-----</i>	<i>----percent----</i>	<i>---miles per hour---</i>			<i>-----feet-----</i>
5	50	10	77	7.7	5.4
5	50	20	117	11.7	8.1
10	100	10	46	4.6	3.8
10	100	20	72	7.2	5.7

## 8. References

- Albini, Frank A. 1976a. Computer-based models of wildland fire behavior: A user's manual. Ogden, UT: U.S. Department of Agriculture, Forest Service, Intermountain Forest and Range Experiment Station. 68 p.
- Albini, Frank A. 1976b. Estimating wildfire behavior and effects. Gen. Tech. Rep. INT-30. Ogden, UT: U.S. Department of Agriculture, Forest Service, Intermountain Forest and Range Experiment Station. 92 p.
- Albini, Frank A. 1984. Wildland fires. *American Scientist*. 72: 590–597.
- Anderson, Hal E. 1969. Heat transfer and fire spread. Res. Pap. INT-69. Ogden, UT: U.S. Department of Agriculture, Forest Service, Intermountain Forest and Range Experiment Station. 20 p.
- Anderson, Hal E. 1982. Aids to determining fuel models for estimating fire behavior. Gen. Tech. Rep. INT-122. Ogden, UT: U.S. Department of Agriculture, Forest Service, Intermountain Forest and Range Experiment Station. 22 p.
- Anderson, Hal E. 1983. Predicting wind-driven wild land fire size and shape. Gen. Tech. Rep. INT-305. Ogden, UT: U.S. Department of Agriculture, Forest Service, Intermountain Forest and Range Experiment Station. 26 p.
- Andrews, Patricia L. 1986. BEHAVE: Fire behavior prediction and fuel modeling system—BURN subsystem, part 1. Gen. Tech. Rep. INT-194. Ogden, UT: U.S. Department of Agriculture, Forest Service, Intermountain Forest and Range Experiment Station. 130 p.
- Andrews, Patricia L. 2012. Modeling wind adjustment factor and midflame wind speed for Rothermel's surface fire spread model. Gen. Tech. Rep. RMRS-GTR-266. Fort Collins, CO: U.S. Department of Agriculture, Forest Service. 39 p.
- Andrews, Patricia L. 2014. Current status and future needs of the BehavePlus fire modeling system. *International Journal of Wildland Fire*. 23(1): 21–33.
- Andrews, Patricia L.; Queen, Lloyd P. 2001. Fire modeling and information system technology. *International Journal of Wildland Fire*. 10(3/4): 343–352.
- Andrews, Patricia L.; Rothermel, Richard C. 1982. Charts for interpreting wildland fire behavior characteristics. Gen. Tech. Rep. INT-131. Ogden, UT: U.S. Department of Agriculture, Forest Service, Intermountain Forest and Range Experiment Station. 21 p.
- Andrews, Patricia L.; Anderson, Stuart A. J.; Anderson, Wendy R. 2006. Evaluation of a dynamic load transfer function using grassland curing data. In: Andrews, Patricia L.; Butler, Bret W., comps. 2006. Fuels management—How to measure success: Conference Proceedings. 2006 March 28–30; Portland, OR. Proceedings RMRS-P-41. Fort Collins, CO: U.S. Department of Agriculture, Forest Service, Rocky Mountain Research Station: 381–394.
- Andrews, Patricia L.; Cruz, Miguel G.; Rothermel, Richard C. 2013. Examination of the wind speed limit function in the Rothermel surface fire spread model. *International Journal of Wildland Fire*. 22(7): 959–969.
- Andrews, Patricia L.; Finney, Mark; Fishetti, Mark. 2007. Predicting wildfires. *Scientific American*. (August): 47–55.

- Andrews, Patricia L.; Heinsch, Faith Ann; Schelvan, Luke. 2011. How to generate and interpret fire characteristics charts for surface and crown fire behavior. Gen. Tech. Rep. RMRS-GTR-253. Fort Collins, CO: U.S. Department of Agriculture, Forest Service, Rocky Mountain Research Station. 40 p.
- Bradshaw, Larry; McCormick, Erin. 2000. FireFamily Plus user's guide, version 2.0. Gen. Tech. Rep. RMRS-GTR-67WWW. Ogden, UT: U.S. Department of Agriculture, Forest Service, Rocky Mountain Research Station. 122 p.
- Bradshaw, Larry S.; Deeming, John E.; Burgan, Robert E.; [et al.], comps. 1984. The 1978 National Fire Danger Rating System: Technical documentation. Gen. Tech. Rep. INT-169. Ogden, UT: U.S. Department of Agriculture, Forest Service, Intermountain Forest and Range Experiment Station. 44 p.
- Brown, Arthur A.; Davis, Kenneth P. 1973. Forest fire control and use. 2nd ed. New York: McGraw-Hill Book Co. 163 p.
- Brown, James K.; Simmerman, Dennis G. 1986. Appraising fuels and flammability in western aspen: A prescribed fire guide. Gen. Tech. Rep. INT-205. Ogden, UT: U.S. Department of Agriculture, Forest Service, Intermountain Research Station. 48 p.
- Burgan, Robert E. 1979a. Estimating live fuel moisture for the 1978 National Fire Danger Rating System. Res. Pap. INT-226. Ogden, UT: U.S. Department of Agriculture, Forest Service, Intermountain Forest and Range Experiment Station. 16 p.
- Burgan, Robert E. 1979b. Fire danger/fire behavior computations with the Texas Instruments TI-59 calculator: User's manual. Gen. Tech. Rep. INT-61. Ogden, UT: U.S. Department of Agriculture, Forest Service, Intermountain Forest and Range Experiment Station. 25 p.
- Burgan, Robert E. 1987. Concepts and interpreted examples in advanced fuel modeling. Gen. Tech. Rep. INT-238. Ogden, UT: U.S. Department of Agriculture, Forest Service, Intermountain Research Station. 40 p.
- Burgan, Robert E. 1988. 1988 Revisions to the 1978 National Fire Danger Rating System. Res. Pap. SE-273. Asheville, NC: U.S. Department of Agriculture, Forest Service, Southeastern Forest Experiment Station. 144 p.
- Burgan, Robert E.; Rothermel, Richard C. 1984. BEHAVE: Fire behavior prediction and fuel modeling system—FUEL subsystem. Gen. Tech. Rep. INT-167. Ogden, UT: U.S. Department of Agriculture, Forest Service, Intermountain Forest and Range Experiment Station. 110 p.
- Byram, George M. 1959. Combustion of forest fuels. In: Davis, Kenneth P. Forest fire control and use. New York, NY: McGraw-Hill Book Co.: 61–89.
- Catchpole, E. A.; deMestre, N. J.; Gill, A. M. 1982. Intensity of fire at its perimeter. *Australian Forest Research*. 12: 47–54.
- Cohen, Jack D. 1985. Should the 1978 national fire danger rating system be updated: A technical comparison to fire behavior prediction. In: Donoghue, Linda R.; Martin, Robert E., eds. *Weather—The drive train connecting the solar engine to forest ecosystems*. Proceedings of the Eighth Conference on Fire and Forest Meteorology; 1985 April 29–May 2. Detroit, MI: Society of American Foresters: 163–168.

- Cohen, Jack D.; Deeming, John E. 1985. The National Fire Danger Rating System: Basic equations. Gen. Tech. Rep. PSW-82. Berkeley, CA: U.S. Department of Agriculture, Forest Service, Pacific Southwest Forest and Range Experiment Station. 16 p.
- Deeming, John E. 1973. Fuel modeling: The key to applying Rothermel's mathematical fire spread model to fire-danger rating. In: Papers presented at the 1973 spring meeting, Western States Section, the Combustion Institute; 1973 April 16–17. Tempe, AZ: Arizona State University. 10 p.
- Deeming, John E.; Brown, James K. 1975. Fuel models in the National Fire Danger Rating System. *Journal of Forestry*. 73(6): 347–350.
- Deeming, John E.; Burgan, Robert E.; Cohen, Jack D. 1977. The National Fire Danger Rating System—1978. Gen. Tech. Rep. INT-39. Ogden, UT: U.S. Department of Agriculture, Forest Service, Intermountain Forest and Range Experiment Station. 63 p.
- Deeming, John E.; Lancaster, James W.; Fosberg, Michael A.; [et al.]. 1972. National Fire Danger Rating System. Res. Pap. RM-84. Fort Collins, CO: U.S. Department of Agriculture, Forest Service, Rocky Mountain Forest and Range Experiment Station. 165 p.
- Finney, Mark A. 1998. FARSITE: Fire Area Simulator—Model development and evaluation. Res. Pap. RMRS-RP-4. Ogden, UT: U.S. Department of Agriculture, Forest Service, Rocky Mountain Research Station. 47 p.
- Finney, Mark A. 2006. An overview of FlamMap fire modeling capabilities. In: Andrews, Patricia L.; Butler, Bret W., comps. 2006. Fuels management—How to measure success: Conference Proceedings. 2006 March 28–30; Portland, OR. Proceedings RMRS-P-41. Fort Collins, CO: U.S. Department of Agriculture, Forest Service, Rocky Mountain Research Station: 213–220.
- Fons, Wallace L. 1946. Analysis of fire spread in light forest fuels. *Journal of Agricultural Engineering Research*. 72(3): 93–121.
- Fosberg, Michael A.; Schroeder, Mark J. 1971. Fine herbaceous fuels in fire-danger rating. Res. Note. RM-185. Fort Collins, CO: U.S. Department of Agriculture, Forest Service, Rocky Mountain Forest and Range Experimental Station. 7 p.
- Frandsen, William H. 1971. Fire spread through porous fuels from the conservation of energy. *Combustion and Flame*. 16(1): 9–16.
- Frandsen, William H. 1973. Using the effective heating number as a weighting factor in Rothermel's fire spread model. Gen. Tech. Rep. INT-10. Ogden, UT: U.S. Department of Agriculture, Forest Service, Intermountain Forest and Range Experiment Station. 7 p.
- Frandsen, William H.; Andrews, Patricia L. 1979. Fire behavior in non-uniform fuels. Res. Pap. INT-232. Ogden, UT: U.S. Department of Agriculture, Forest Service, Intermountain Research Station. 34 p.
- Heinsch, Faith Ann; Andrews, Patricia L. 2010. BehavePlus fire modeling system, version 5.0: Design and features. Gen. Tech. Rep. RMRS-GTR-249. Fort Collins, CO: U.S. Department of Agriculture, Forest Service, Rocky Mountain Research Station. 111 p.
- Hough, Walter A.; Albini, Frank A. 1978. Predicting fire behavior in palmetto-gallberry fuel complexes. Res. Pap. SE-174. Asheville, NC: U.S. Department of Agriculture, Forest Service, Southeastern Forest Experiment Station. 44 p.

- Jolly, W. Matt. 2007. Sensitivity of a surface fire spread model and associated fire behaviour fuel models to changes in live fuel moisture. *International Journal of Wildland Fire*. 16(4): 503–509.
- McArthur Alan G. 1969. The Tasmanian bushfires of 7th February 1967 and associated fire behaviour characteristics. In: *Mass Fire Symposium: The Technical Cooperation Programme, 1969 February 10–12; Canberra, Australia*. Volume 1, Paper A7. Melbourne, Australia, Defence Standards Laboratories. 23 p.
- Rothermel, Richard C. 1968. Mechanisms of fire spread. In: *Northern Forest Fire Laboratory, Problem Analysis*. U.S. Department of Agriculture, Forest Service, Intermountain Forest and Range Experiment Station, Missoula MT. Unpublished paper on file with: U.S. Department of Agriculture, Forest Service, Rocky Mountain Research Station, Fire Sciences Laboratory, Missoula, MT. 24 p.
- Rothermel, Richard C. 1969. A fire behavior model for field applications. In: *Northern Forest Fire Laboratory, Study Plan*. Unpublished paper on file with: U.S. Department of Agriculture, Forest Service, Rocky Mountain Research Station, Fire Sciences Laboratory, Missoula, MT. 25 p.
- Rothermel, Richard C. 1972. A mathematical model for predicting fire spread in wildland fuels. Res. Pap. INT-115. Ogden, UT: U.S. Department of Agriculture, Forest Service, Intermountain Forest and Range Experiment Station. 40 p.
- Rothermel, Richard C. 1983. How to predict the spread and intensity of forest and range fires. Gen. Tech. Rep. INT-143. Ogden, UT: U.S. Department of Agriculture, Forest Service, Intermountain Forest and Range Experiment Station. 161 p.
- Rothermel, Richard C.; Anderson, Hal E. 1966. Fire spread characteristics determined in the laboratory. Res. Pap. INT-30. Ogden, UT: U.S. Department of Agriculture, Forest Service, Intermountain Forest and Range Experiment Station. 34 p.
- Rothermel, Richard C.; Philpot, Charles W. 1973. Predicting changes in chaparral flammability. *Journal of Forestry*. 71(10): 640–643.
- Schroeder, Mark J.; Fosberg, Michael A.; Lancaster, James W.; [et al.]. 1972. Technical development of the National Fire Danger Rating System. Review Draft. Unpublished paper on file with: U.S. Department of Agriculture, Forest Service, Rocky Mountain Research Station, Fire Sciences Laboratory, Missoula, MT. 151 p.
- Scott, Joe H. 1999. NEXUS: A system for assessing crown fire hazard. *Fire Management Notes*. 59: 20–24.
- Scott, Joe H. 2007. Nomographs for estimating surface fire behavior characteristics. Gen. Tech. Rep. RMRS-GTR-192. Fort Collins, CO: U.S. Department of Agriculture, Forest Service, Rocky Mountain Research Station. 119 p.
- Scott, Joe H.; Burgan, Robert E. 2005. Standard fire behavior fuel models: A comprehensive set for use with Rothermel's surface fire spread model. Gen. Tech. Rep. RMRS-GTR-153. Fort Collins, CO: U.S. Department of Agriculture, Forest Service, Rocky Mountain Research Station. 72 p.

- Smith, Diane M. 2012. The Missoula Fire Sciences Laboratory: A 50-year dedication to understanding wildlands and fire. Gen. Tech. Rep. RMRS-GTR-270. Fort Collins, CO: U.S. Department of Agriculture, Forest Service, Rocky Mountain Research Station. 62 p.
- Sullivan, Andrew L. 2009a. Wildland surface fire spread modelling, 1990–2007. 1: Physical and quasi-physical models. *International Journal of Wildland Fire*. 18(4): 349–368.
- Sullivan, Andrew L. 2009b. Wildland surface fire spread modelling, 1990–2007. 2: Empirical and quasi-empirical models. *International Journal of Wildland Fire*. 18(4): 369–386.
- Sullivan, Andrew L. 2009c. Wildland surface fire spread modelling, 1990–2007. 3: Simulation and mathematical analogue models. *International Journal of Wildland Fire*. 18(4): 387–403.
- Van Wagner, Charles E. 1978. Metric units and conversion factors for forest fire quantities. Information Report PS-X-71. Chalk River, ON: Canadian Forestry Service, Petawawa Forest Experiment Station. 15 p.
- Wells, G. 2008. The Rothermel fire-spread model: Still running like a champ. *Fire Science Digest*. 2: 1–12. <http://www.firescience.gov/Digest/FSdigest2.pdf>. (Accessed May 18, 2017).
- Wilson, Ralph. 1980. Reformulation of forest fire spread equations in SI units. Res. Note. INT-292. Ogden, UT: U.S. Department of Agriculture, Forest Service, Intermountain Forest and Range Experiment Station. 5 p.
- Ziel, Robert; Jolly, W. Matt 2009. Performance of fire behavior fuel models developed for the Rothermel surface fire spread model. In: Hutchinson, Todd F., ed. *Proceedings of the 3rd fire in eastern oak forests conference; 2008 May 20–22; Carbondale, IL*. Gen. Tech. Rep. NRS-P-46. Newtown Square, PA: U.S. Department of Agriculture, Forest Service, Northern Research Station: 78–87.

## Appendix A—Basic Fire Spread Equations in Metric Units

Wilson (1980) reformulated fire model equations (Rothermel 1972; Albini 1976) using metric units suggested by Van Wagner (1978). These equations are included for completeness and to correct errors in the original publication. Fire modeling systems, however, generally do the calculations in the “native” units of the model as published, with unit conversions applied to input and output.

The input parameters with metric units are given in table A.1. The basic spread equations in metric are given in table A.2. Equations that are not affected by the units change are noted as “Same.” “Change” indicates that the equation is reformulated for metric units. Equations found to be in error in the original publication (Wilson 1980) have been corrected and are noted as “Errata.” Metric equations for fireline intensity and flame length are in table A.3

Wilson (1980) also gave an alternate equation for reaction intensity ( $I_R$ ) in  $\text{kW/m}^2$ , which leads to rate of spread ( $R$ ) in  $\text{m/s}$ .

**Table A.1**—Input parameters for the basic spread model equations with metric units (Wilson 1980).

Type	Symbol	Parameter and units
Fuel particle	$h$	Low heat content (kJ/kg)
	$S_T$	Total mineral content (fraction)
	$S_E$	Effective mineral content (fraction)
	$\rho_p$	Oven-dry particle density ( $\text{kg/m}^3$ )
Fuel array	$\sigma$	Surface-area-to-volume ratio ( $\text{cm}^2/\text{cm}^3$ )
	$w_o$	Oven-dry fuel load ( $\text{kg/m}^2$ )
	$\delta$	Fuel bed depth (m)
	$M_x$	Dead fuel moisture of extinction (fraction)
Environmental	$M_f$	Moisture content (fraction)
	$U$	Wind velocity at midflame height (m/min)
	$\tan \varphi$	Slope steepness, maximum (fraction)

**Table A.2**—Basic spread model equations using metric units based on (Wilson 1980).

Element and units	Equation	Note <sup>a</sup>
Rate of spread (m/min)	$R = \frac{I_R \xi (1 + \phi_w + \phi_s)}{\rho_b \epsilon Q_{ig}}$	Same
Reaction intensity (kJ/min/m <sup>2</sup> )	$I_R = \Gamma' w_n h \eta_M \eta_S$	Same
Optimum reaction velocity (min <sup>-1</sup> )	$\Gamma' = \Gamma'_{max} (\beta / \beta_{op})^A \exp[A(1 - \beta / \beta_{op})]$ $\Gamma' = \Gamma'_{max} [(\beta / \beta_{op}) \exp(1 - (\beta / \beta_{op}))]^A$	Same (Alternate form)
	$A = 8.9033\sigma^{-0.7913}$	Change
Maximum reaction velocity (min <sup>-1</sup> )	$\Gamma'_{max} = (0.0591 + 2.926\sigma^{-1.5})^{-1}$	Change
Optimum packing ratio	$\beta_{op} = 0.20395\sigma^{-0.8189}$	Change
Packing ratio	$\beta = \rho_b / \rho_p$	Same
Oven-dry bulk density (kg/m <sup>3</sup> )	$\rho_b = w_0 / \delta$	Same
Net fuel load (kg/m <sup>2</sup> )	$w_n = w_0(1 - S_T)$	Same
Moisture damping coefficient	$\eta_M = 1 - 2.59r_M + 5.11(r_M)^2 - 3.52(r_M)^3$ $r_M = M_f / M_x$ (max=1.0)	Same
Mineral damping coefficient	$\eta_S = 0.174S_e^{-0.19}$ (max = 1.0)	Same
Propagating flux ratio	$\xi = (192 + 7.9095\sigma)^{-1} \exp[(0.792 + 3.7597\sigma^{0.5})(\beta + 0.1)]$	Change
Wind factor	$\phi_w = C(3.281U)^B (\beta / \beta_{op})^{-E}$ where $C = 7.47 \exp(-0.8711\sigma^{0.55})$ $B = 0.15988\sigma^{0.54}$ $E = 0.715 \exp(-0.01094\sigma)$	Change Errata
Slope factor	$\phi_s = 5.275\beta^{-0.3} (\tan \varphi)^2$	Same
Effective heating number	$\epsilon = \exp(-4.528/\sigma)$	Change
Heat of preignition (kJ/kg)	$Q_{ig} = 581 + 2,594M_f$	Change

<sup>a</sup>Equations that are not affected by the units change are noted as "Same." "Change" indicates that the equation is reformulated for metric units. Equations found to be in error in the original publication (Wilson 1980) are noted as "Errata."

**Table A.3**—Models related to the Rothermel fire spread model in metric units from Wilson (1980).

Element and Units	Equation	Note <sup>a</sup>
Fireline intensity (kW/m)	$I_B = (1/60)I_R R(12.6/\sigma)$	Change Errata
Flame length (m)	$F_B = 0.0775I_B^{0.46}$	Change Errata

<sup>a</sup>"Change" indicates that the equation is reformulated for metric units. Equations found to be in error in the original publication (Wilson 1980) are noted as "Errata."

## References

- Albini, Frank A. 1976. Computer-based models of wildland fire behavior: A user's manual. Ogden, UT: U.S. Department of Agriculture, Forest Service, Intermountain Forest and Range Experiment Station. 68 p.
- Rothermel, Richard C. 1972. A mathematical model for predicting fire spread in wildland fuels. Res. Pap. INT-115. Ogden, UT: U.S. Department of Agriculture, Forest Service, Intermountain Forest and Range Experiment Station. 40 p.
- Van Wagner, Charles E. 1978. Metric units and conversion factors for forest fire quantities. Information Report PS-X-71. Chalk River, ON: Canadian Forestry Service, Petawawa Forest Experiment Station. 15 p.
- Wilson, Ralph. 1980. Reformulation of forest fire spread equations in SI units. Res. Note. INT-292. Ogden, UT: U.S. Department of Agriculture, Forest Service, Intermountain Forest and Range Experiment Station. 5 p.

## Appendix B—People Behind the Equations

To add a personal touch to this equation-laden document, we include photographs of some of those involved in the development and application of the surface fire spread model. Dick Rothermel is the primary developer of the surface fire spread model. He presented a seminar on development of the model at the Missoula Fire Sciences Laboratory in 2011 (fig. B.1). He also devoted much of his career to application of the model (Rothermel 1983).



**Figure B.1**—Dick Rothermel gave a seminar on development of the fire model at the Missoula Fire Sciences Lab in 2011 (photo by Emily Schembra).

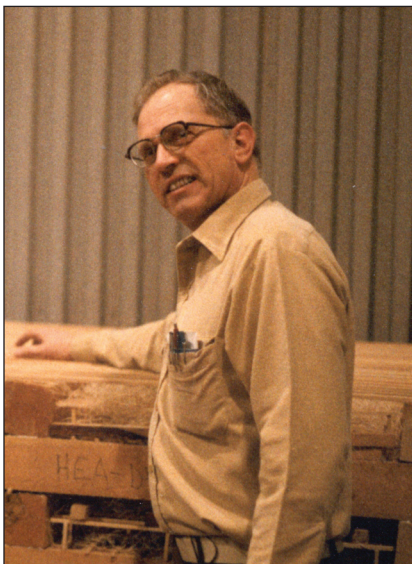


**Figure B.2**—Hal Anderson, 1985 (photo by Bill Frandsen).

Hal Anderson (fig. B.2) started work at the Fire Lab with Rothermel in 1961. He worked on the experimental basis for the fire model (Anderson 1969; Rothermel and Anderson 1966) and later on describing fuel models (Anderson 1982). Bill Frandsen's (fig. B.3) work provided a foundation for the basis of the spread model (Frandsen 1971). Frank Albini (fig. B.4) did an assessment of the fire model that led to some adjustments to the equations. He implemented the fire model as the FIREMOD computer program (Albini 1976a) and nomograms (Albini 1976b). Bob Burgan (fig. B.5) worked on implementing the fire model in the National Fire Danger Rating System (Deeming et al. 1977), made

the fire model available on a handheld calculator (Burgan 1979), and also worked with Rothermel on the fuel modeling portion of the BEHAVE system (Burgan 1987; Burgan and Rothermel 1984). Pat Andrews (fig. B.5) was the primary developer of the fire behavior prediction part of the BEHAVE fire behavior prediction and fuel modeling system (Andrews 1986) and later the BehavePlus fire modeling system (Andrews 2014).



**Figure B.3**—Bill Frandsen, 1992 (photo courtesy of USDA Forest Service).

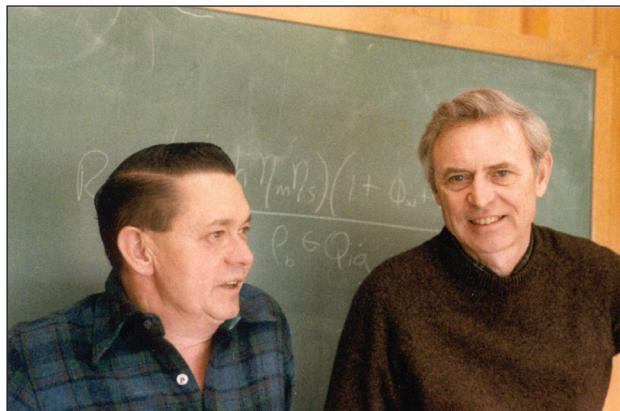


**Figure B.4**—Frank Albin and Dick Rothermel, 1985 (photo by Bill Frandsen).



**Figure B.5**—Frank Albin, Pat Andrews, and Bob Burgan, 1985 (photo by Bill Frandsen).

## References

- Albini, Frank A. 1976a. Computer-based models of wildland fire behavior: A user's manual. Ogden, UT: U.S. Department of Agriculture, Forest Service, Intermountain Forest and Range Experiment Station. 68 p.
- Albini, Frank A. 1976b. Estimating wildfire behavior and effects. Gen. Tech. Rep. INT-30. Ogden, UT: U.S. Department of Agriculture, Forest Service, Intermountain Forest and Range Experiment Station. 92 p.
- Anderson, Hal E. 1969. Heat transfer and fire spread. Res. Pap. INT-69. Ogden, UT: U.S. Department of Agriculture, Forest Service, Intermountain Forest and Range Experiment Station. 20 p.
- Anderson, Hal E. 1982. Aids to determining fuel models for estimating fire behavior. Gen. Tech. Rep. INT-122. Ogden, UT: U.S. Department of Agriculture, Forest Service, Intermountain Forest and Range Experiment Station. 22 p.
- Andrews, Patricia L. 1986. BEHAVE: Fire behavior prediction and fuel modeling system—BURN subsystem, part 1. Gen. Tech. Rep. INT-194. Ogden, UT: U.S. Department of Agriculture, Forest Service, Intermountain Forest and Range Experiment Station. 130 p.
- Andrews, Patricia L. 2014. Current status and future needs of the BehavePlus fire modeling system. *International Journal of Wildland Fire*. 23(1): 21–33.
- Burgan, Robert E. 1979. Fire danger/fire behavior computations with the Texas Instruments TI-59 calculator: User's manual. Gen. Tech. Rep. INT-61. Ogden, UT: U.S. Department of Agriculture, Forest Service, Intermountain Forest and Range Experiment Station. 25 p.
- Burgan, Robert E. 1987. Concepts and interpreted examples in advanced fuel modeling. Gen. Tech. Rep. INT-238. Ogden, UT: U.S. Department of Agriculture, Forest Service, Intermountain Research Station. 40 p.
- Burgan, Robert E.; Rothermel, Richard C. 1984. BEHAVE: Fire behavior prediction and fuel modeling system—FUEL subsystem. Gen. Tech. Rep. INT-167. Ogden, UT: U.S. Department of Agriculture, Forest Service, Intermountain Forest and Range Experiment Station. 110 p.
- Deeming, John E.; Burgan, Robert E.; Cohen, Jack D. 1977. The National Fire Danger Rating System—1978. Gen. Tech. Rep. INT-39. Ogden, UT: U.S. Department of Agriculture, Forest Service, Intermountain Forest and Range Experiment Station. 63 p.
- Frandsen, William H. 1971. Fire spread through porous fuels from the conservation of energy. *Combustion and Flame*. 16(1): 9–16.
- Rothermel, Richard C. 1983. How to predict the spread and intensity of forest and range fires. Gen. Tech. Rep. INT-143. Ogden, UT: U.S. Department of Agriculture, Forest Service, Intermountain Forest and Range Experiment Station. 161 p.
- Rothermel, Richard C.; Anderson, Hal E. 1966. Fire spread characteristics determined in the laboratory. Res. Pap. INT-30. Ogden, UT: U.S. Department of Agriculture, Forest Service, Intermountain Forest and Range Experiment Station. 34 p.





USDA is an equal opportunity provider and employer. To file a complaint of discrimination, write: USDA, Office of the Assistant Secretary for Civil Rights, Office of Adjudication, 1400 Independence Ave., SW, Washington, DC 20250-9410 or call (866) 632-9992 (Toll-free Customer Service), (800) 877-8339 (Local or Federal relay), (866) 377-8642 (Relay voice users).



To learn more about RMRS publications or search our online titles:

[www.fs.fed.us/rm/publications](http://www.fs.fed.us/rm/publications)

[www.treesearch.fs.fed.us](http://www.treesearch.fs.fed.us)